Identification and characterization of poplar ECERIFERUM2-LIKE, a clade II BAHD acyltransferase from hybrid poplar (*Populus alba* × *grandidentata*)

by

Michelle von Loessl

B.Sc., The University of British Columbia, 2013

A THESIS SUBMITTED IN PARTIAL FULFILLMENT OF

THE REQUIREMENTS FOR THE DEGREE OF

MASTER OF SCIENCE

in

THE FACULTY OF GRADUATE AND POSTDOCTORAL STUDIES

(Forestry)

THE UNIVERSITY OF BRITISH COLUMBIA

(Vancouver)

March 2017

Abstract

BAHD acyltransferases belong to a large family of enzymes that are involved in the biosynthesis of a wide variety of biologically diverse and important plant compounds. Poplar makes an assortment of different metabolites and therefore has a large number of putative BAHD-acyltransferases, of which only a few have been characterized to date. In this study, an uncharacterized BAHD acyltransferase, with a putative function in either non-canonical monolignol biosynthesis as the poplar *p*-hydroxybenzoate-CoA monolignol transferase (pHBMT), or in cuticular wax biosynthesis through very long chain fatty acid (VLCFA) elongation as a poplar ECERIFERUM2-LIKE (CER2-LIKE), was studied. To test the function of *Populus alba* × *grandidentata* acyltransferase-like (Pa×gACT-like), transgenic *Arabidopsis thaliana* and hybrid poplar plants mis-regulating the gene, were generated and subsequently analyzed for changes in both lignin *p*-hydroxybenzoylation and in the cuticular wax composition. No changes in lignin *p*-hydroxybenzoylation was observed, negating the possibility of Pa×gACT-like being a *p*-hydroxybenzoate-CoA monolignol transferase. The introduction of Pa×gACT-like into Arabidopsis caused the accumulation of aliphatic wax components 28 carbons in length (C_{28}), and a reduction in C_{30} wax components, likely due to competition with the native AtCER2 or slight differences in substrate specificity between Pa×gACT-like and AtCER2. In addition, RNAi-suppression of Pa×gACT-like in poplar resulted in a subtle phenotype showing a trend for accumulation of C_{28} wax components, suggesting an upstream "block" in VLCFA elongation. The shifts in cuticular wax chain length distribution detected in transgenics support a CER2-LIKE role for Pa×gACT-like. Consistent with this, heterologous gene expression in yeast (*Saccharomyces cerevisiae*) clearly demonstrated that Pa×gACT-like can participate in the elongation of very long chain fatty acids. Co-expression and tissue-specific

expression also support a role in cuticular wax biosynthesis, as 30% of genes co-expressed with Pa×gACT-like have predicted functions in lipid biosynthesis/metabolism. Finally, GUS histochemical staining of *Pa×gACT-like Prom::GUS* poplar transgenics revealed expression in the epidermis of leaf, petiole, and young stem tissue. This study reveals a function for a previously uncharacterized poplar BAHD acyl transferase as a CER2-LIKE protein that functions in the elongation of VLCFAs for cuticular wax production.

Preface

Targeted co-expression network analysis of *Pa×gACT-like* was performed by Dr. Oliver Corea (University of Victoria).

Heterologous expression of *Pa×gACT-like* in yeast, and yeast FAME analysis were performed by Tegan Haslam, (Ljerka Kunst lab, University of British Columbia).

All other work presented in this thesis represents original, unpublished and independent work conducted by the author, Michelle von Loessl.

Table of Contents

List of Tables

List of Figures

Acknowledgements

I would like to thank my supervisor, Dr. Shawn Mansfield for all of his support and scientific expertise, as well as for the opportunity he has given me to grow from a summer student in his lab, to conducting my own research and completing my degree. I would also like to thank my co-supervisor Dr. Lacey Samuels for her scientific expertise, as well as her mentorship, and relentless encouragement and support. I would like to thank my supervisory committee member Dr. Carl Douglas for his guidance. He passed away during the time of my research, on July 25, 2016 and I wish to honour his memory with this work.

I am also very thankful for the support and friendship of my fellow lab members, Mansfield and Samuels, past and present, of which, unfortunately, there are too many to name here. These members of my scientific family were not only important collaborators, but really good friends who made these past few years unforgettable. A special thank you goes to Eliana Gonzales-Vigil, Yaseen Mottiar, Faride Unda, and Letitia Da Ros, who were particularly generous with their time, scientific advice, and support.

I would also like to thank my collaborators Tegan Haslam and Ljerka Kunst who warmly welcomed me into the world of plant cuticular waxes. A thank you as well to collaborator Oliver Corea for his co-expression analysis.

I would also like extend my gratitude to the Forestry department staff, as well as the greenhouse staff, in particular Melina Biron, for her advice and for caring for my poplar trees.

Dedication

I would like to dedicate this work to my parents, Katrin and Hans. Without your continued love and support I would not be where I am today. To Stephanie, my sister, some-time roommate, and best friend. To my loving, supportive, and patiently waiting boyfriend, Riccardo Salton. And lastly to my grandmother Gudrun, who passed away June 7, 2016, who has inspired a fascination of the forest and its flora in me since I was a just a little girl.

Chapter 1: Introduction

Poplar is an important model system in plant biology and biotechnology, that has not only ecological, but also economical value. These trees make a wide variety of different metabolites, whose biosynthetic pathways are not fully understood. The study and characterization of genes with predicted functions in the biosynthesis of these metabolites is a key aspect in better understanding of their biosynthetic pathways. The objective of this research is to investigate the role of an uncharacterized BAHD acyltransferase, which has been postulated as functioning in one of two important biosynthetic pathways in poplar. Some evidence points to a functional role in non-canonical monolignol biosynthesis, whilst other evidence suggests a function in the biosynthesis of cuticular waxes. Elucidating the function of this gene will help gain a better understanding of the lignin and cuticular wax biosynthesis in poplar, as well as contribute to the growing body of knowledge on this large family of acyltransferases.

1.1 Acyltransferases

Plants are able to produce a wide variety of phenolics that include important compounds such as lignin, volatiles, pigments and toxins. This is made possible by an elaborate array of different enzymes that modify a few basic chemical structures to create a plethora of complex plant metabolites (Pichersky *et al.*, 2006). One such modification is acylation, which can affect stability, solubility, vacuolar uptake, as well as confer protection against enzymatic degradation (Nakayama *et al.*, 2003). Acylation involves an activated or energy-rich acyl donor which offers an acyl group to an acceptor substrate via an ester-bond. There are two described enzyme families that can use phenolic compounds as either donor or acceptor substrates; the Serine

CarboxyPeptidase-Like (SCPL) acyltransferases and the BAHD acyltransferases (BAHD-ATs), which differ in their use of activated acyl donor (Bontpart *et al.*, 2015).

1.1.1 BAHD acyltransferases

The BAHD-ATs are an acyl-Coenzyme A (CoA) dependent family of enzymes, named after the first four characterized members, **B**EAT, **A**HCT, **H**CBT, **D**AT; Benzylalcohol O-acetyltransferase from *Clarkia breweri,* Anthocyanin O-hydroxycinnamoyltransferases from *Petunia, Senecio, Gentiana, Perilla, and Lavandula,* Anthranilate N-hydroxycinnamoyl/benzoyltransferase from *Dianthus caryophyllus* and Deacetylvindoline 4-O-acetyltransferase from *Catharanthus roseus* respectively (St-Pierre & De Luca, 2000). These monomeric proteins are cytosolic, with molecular masses ranging from 48-55 kD (D'Auria, 2006). BAHD acyltransferases have relatively low protein sequence similarities (10 - 30%), but share two conserved motifs (St-Pierre & De Luca, 2000). The HXXXD motif containing the catalytic site, is highly conserved whilst the DFGWG motif is highly but not absolutely conserved and thought to play a structural role (Unno *et al.*, 2007). Acylation occurs via the histidine residue of the catalytic HXXXD motif, which acts as a base and deprotonates the oxygen or nitrogen atom of the acceptor substrate, thereby creating a nucleophile. The resulting nucleophile attacks the carbonyl carbon of the acyl-CoA donor substrate, forming an unstable tetrahedral intermediate. Reprotonation then frees the CoA, and an acylated substance is produced (St-Pierre & De Luca, 2000).

Originally, the family was organized into five separate clades (I-V) using 46 characterized members (D'Auria, 2006). A more recent phylogenetic study employing 69 characterized

enzymes along with several putative BAHD-ATs from *Arabidopsis, Medicago, Oryza, Populus, and Vitis*, expanded this phylogeny, further separating the clades into eight (Tuominen *et al.*, 2011). Characterized members of the BAHD-ATs have been found to catalyze steps in the biosynthesis of a variety of phenolics such as flavonoids and anthocyanins, whereas other members are responsible for the acylation of cell wall components such as hemicelluloses and lignins (D'Auria, 2006; Yu *et al.*, 2009). Some BAHD-ATs are involved in the biosynthesis of extracellular lipids such as cutin and suberin, acylating these lipidic polyesters with small amounts of phenolic acids such as *p*-coumaric and ferulic acid (Molina and Kosma, 2015). For an up-to-date list of these characterized BAHD-ATs and their functions refer to (Bontpart *et al.*, 2015).

Although the BAHD clades generally contain enzymes of similar biochemical activity, enzyme function can be clade independent and therefore acyl-donor or -acceptor substrate specificity can vary both between and within clades. For example, Clade I members modify flavonoids, whereas members of Clade V act upon a variety of acyl-acceptor substrates, from alcohols to monolignols (D'Auria, 2006). As for acyl-donors, enzymes from several clades have been reported to use hydroxycinnamoyl-CoA as a donor substrate, whereas benzoyl-CoA is used exclusively within Clade V (D'Auria, 2006). Therefore, though phylogenetics can be helpful in predicting possible gene functions of uncharacterized BAHD-ATs, clade placement is not always indicative of enzyme function.

1.1.2 BAHD acyltransferases in *Populus*

The updated phylogeny of the BAHD-ATs by Tuominen *et al*. (2011) includes 100 putative *Populus trichocarpa* BAHD-ATs, of which only five have been characterized to date, playing a role in three different biosynthetic pathways. Of the five characterized enzymes, PtSABT (benzoyl-CoA: salicyl alcohol O-benzoyltransferase), and PtBEBT (benzoyl-CoA: benzyl alcohol O-benzoyltransferase) are integral to the biosynthesis of salicinoids, important secondary metabolites in insect defense in the *Salicaceae* family (Chedgy *et al.*, 2015). Another enzyme, PtFHT1 (hydroxyacid/fatty alcohol hydroxycinnamoyltransferase 1), functions in the extracellular lipid biosynthesis pathway. This was illustrated by the ectopical expression of PtFHT1 in Arabidopsis, which caused the root and seed suberins to become acylated, which is not the case in wild-type Arabidopsis suberins (Cheng *et al.*, 2013). The final two enzymes were characterized in a large-scale enzyme kinetics study of *P. trichocarpa* monolignol biosynthetic enzymes. PtHCT1 and PtHCT6 are *p*-hydroxycinnamoyl-CoA:quinate shikimate *p*-hydroxycinnamoyltransferases, enzymes found in the lignin biosynthetic pathway that are known to be BAHD-ATs (Wang *et al.*, 2014).

Clearly BAHD-ATs are important in the synthesis of a range of metabolites, and we have only recently begun to characterize members of this important gene family in poplar. The following describes two areas of particular interest in which uncharacterized poplar BAHD-ATs are thought to be important biologically.

1.2 Lignin related BAHD acyltransferases

1.2.1 Functional importance of lignin

Lignin is one of the main components of the plant cell wall and the second most abundant polymer in the biosphere, surpassed only by cellulose (Boerjan *et al.*, 2003). This phenolic polymer is found mainly in plant secondary cell wall fibers and water conducting elements, where its incorporation lends the strength and stiffness necessary for whole plant structural support and erect growth (Barros *et al.*, 2015). Lignin is essential for long distance water transportation (Boyce *et al.*, 2004) and defense against various pathogens and herbivores, with its structural complexity, heterogeneity, and crosslinking with other cell wall components making it resilient to enzymatic digestion (Bhuiyan *et al.*, 2009). Lignin biosynthesis is an active area of research, not only because of its biological role, but also because it is a hindrance in the industrial processing of lignocellulosic materials (Mansfield *et al.*, 2012).

1.2.2 Lignin biosynthesis and plasticity of lignification

Lignin biosynthesis, polymerization, and deposition have been studied extensively (Boerjan *et al.*, 2003; Ralph *et al.*, 2004; Vanholme *et al.*, 2010; Liu, 2012). Lignin is a complex hydrophobic polymer produced through the oxidative polymerization of three main subunits, or monolignols that differ in their degree of methoxylation; *p*-coumaryl, coniferyl and sinapyl alcohol. Once incorporated into the lignin polymer, they form G (guaiacyl), H (p-hydroxyphenyl), and S (syringyl) lignin units, respectively. These lignin precursors are synthesized in the cytoplasm via the phenylpropanoid pathway, which has been rigorously studied (Boerjan *et al.*, 2003; Ralph *et al.*, 2004; Vanholme *et al.*, 2010). Monolignols are then transported across the plasma membrane to the secondary cell wall, in a temporally and spatially

regulated manner (Boerjan *et al.*, 2003; Liu, 2012). This is an active area of research, as the details of this process are not yet fully understood. Here, the monolignols polymerize via oxidative coupling reactions catalyzed by laccases and/or peroxidases to form the complex polyphenolic lignin (Ralph *et al.*, 2004).

Polymerization of lignin is stochastic, governed only by simple chemical combinatorial coupling reactions, making it a highly variable polymer (Ralph *et al.*, 2004). This complexity is further compounded by the variation in relative proportions of H, G, and S subunits, which vary with tissue and species. Furthermore, natural lignins have been found to incorporate a wide range of other monomers alongside these three canonical monolignols. studies misregulating key enzymes in the lignin biosynthetic pathway have produced plants with altered polymer composition, and lignins which incorporate wide range of pathway intermediates as monomers, demonstrating the plasticity of the lignin polymer (Franke *et al.*, 2002; Stewart *et al.*, 2009; Weng *et al.*, 2010; Chen *et al.*, 2012; Smith *et al.*, 2015; Wagner *et al.*, 2015; Mottiar *et al.*, 2016).

1.2.3 BAHD acylated lignins

Many natural lignins incorporate significant amounts of monolignols pre-acylated by BAHD-ATs with one of a variety acids, forming monolignol conjugates (Figure 1.1). Inclusion of these monolignol conjugates results in differentially acylated lignins. Acetylated lignin is found in kenaf (Ralph, 1996) and agave (Martínez *et al.*, 2008), while *p*-coumaroylated lignin is found in grasses (Shimada *et al.*, 1971; Hartley, 1972; Ralph *et al.*, 1994). Several plant species have *p*-hydroxybenzoylated lignins, such as poplars and aspens (*Populus spp.*) (Smith, 1955; Nakano *et al.*, 1961; Lu *et al.*, 2004; Morreel, 2004), willows (*Salix spp.*) (Landuccii *et al.*, 1992), *Aralia*

cordata (Hibino *et al.*, 1994) and palms (family *Arecaceae*) (Lu *et al.*, 2015). Native lignin feruylation occurs in many plant species, and has recently been found to be much more wide spread in plants than originally thought (Karlen *et al.*, 2016).

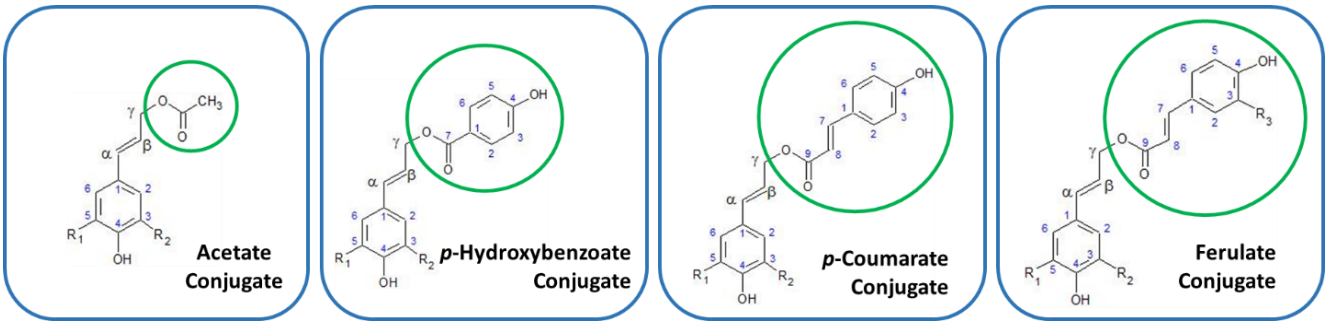

Figure 1.1 Schematic showing differentially acylated monolignols. These conjugates are non-canonical monolignols which are found to polymerize into the lignin of a variety of different plant species.

Several of the BAHD-ATs responsible for the acylation of monolignols have been characterized: the *p*-coumaroyl-CoA monolignol transferases from rice (OsPMT), *Brachypodium* (BdPMT) and *Zea mays* (p-coumaroyl CoA: hydroxycinnamyl alcohol transferase (pCAT) or ZmPMT) (Withers *et al.*, 2012; Marita *et al.*, 2014; Petrik *et al.*, 2014), as well as the feruloyl-CoA monolignol transferase from *Angelica sinensis* (AsFMT) and from rice (OsFMT) (Wilkerson *et al.*, 2014; Karlen *et al.*, 2016). These acyl-CoA monolignol transferases are another good example of clade independent function within the BAHD-ATs family. Where the BdPMT, OsPMT and OsFMT belong to clade V(a), the AsFMT belongs to clade IIIa (Petrik *et al.*, 2014; Karlen *et al.*, 2016). Acylation with acetates, *p*-coumarates, and *p*-hydroxybenzoates occurs at the γ-position of the lignin sidechain of primarily syringyl units as opposed to guaiacyl units (Lu *et al.*, 2015) and both *p*-coumarates and *p*-hydroxybenzoates exist as free phenolic appendages. These acyl groups do not incorporate integrally into the lignin backbone because of their

preference for radical transfer over radical coupling, and the resulting lignin polymer is adorned with pendant ester groups (Ralph, 2010; Lu *et al.*, 2015).

1.2.4 Poplar *p*-hydroxybenzoate-CoA monolignol transferase (pHBMT)

As mentioned, very little is known about BAHD-ATs in poplar, with only a few characterized. An example of a biosynthetic pathway in poplar where we are postulate that a BAHD-ATs is working, is the synthesis of *p*-hydroxybenzoate monolignol conjugates. Historically, *p*-hydroxybenzoate groups have been reported to account for as much as 7.5 - 10% of native lignin weight in some poplar vareities (Smith, 1955; Nakano *et al.*, 1961). A more recent study reports much lower amounts of *p*-hydroxybenzoylation, ranging between 0.56 - 0.76% of lignin weight (Smith *et al.*, 2015). The enzyme and associated gene responsible for *p*-hydroxybenzoylation of lignins are not known, but it is presumed that *p*-hydroxybenzoylation of poplar lignins is analogous to *p*-coumarylation of grasses. Therefore, a BAHD-AT that catalyzes the transesterification between a *p*-hydroxybenzoyl-CoA and a monolignol, most likely a syringyl unit, likely exists. The proposed reaction catalyzed by the hypothesized *p*-hydroxybenzoate-CoA monolignol transferase (pHBMT) is illustrated in Figure 1.2.

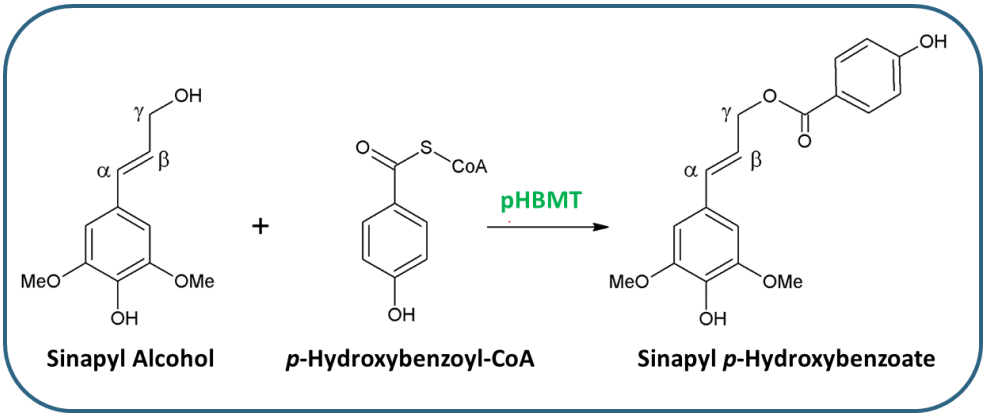

Figure 1.2 Monolignol acylation via a poplar pHBMT. Model shows the use of sinapyl alcohol as the acceptor substrate and *p*-hydroxybenzoyl-CoA as the donor substrate to form sinapyl *p*-hydroxybenzoate, an acylated S unit monolignol.

1.3 Cuticular wax related BAHD acyltransferase

In addition to a potential role in *p*-hydroxybenzoate monolignol production in poplar, another area in which uncharacterized poplar BAHD-ATs could be acting is cuticle biosynthesis.

1.3.1 The cuticle

The aerial portions of the primary growth of all land plants are covered by a thin hydrophobic layer called the cuticle. This interface between the plant and its environment functions mainly to minimize non-stomatal water loss, prevent organ fusion during plant development, and to protect against insect herbivores, as well as other biotic and abiotic stresses (Eigenbrode & Espelie, 1995; Riederer & Schreiber, 2001; Smirnova *et al.*, 2013).

The cuticle is mainly composed of two components; cutin and cuticular waxes. Cutin is the main structural polymeric component of the cuticle composed primarily of ester-cross linked C_{16} and C_{18} hydroxy fatty acids, and it forms a matrix that is partially integrated with and overlying the

epidermal cell wall (Yeats & Rose, 2013). Cuticular waxes are found embedded in the cutin matrix as intracuticular waxes, and can also accumulate as an overlying film or in crystalline form as epicuticular waxes (Samuels *et al.*, 2008). Cuticular waxes are composed primarily of very long chain fatty acids (VLCFAs) and their derivatives such as alkanes, aldehydes, primary and secondary alcohols, ketones and esters, but may also include smaller amounts of triterpenoids, flavonoids, and phenolic lipids. The composition of the cuticular wax varies depending on species, tissue, and age (Jetter *et al.*, 2006).

1.3.2 Cuticular wax biosynthesis

The *eceriferum* (cer) wax deficient Arabidopsis mutants, which are easily recognized by their shiny stems, have been crucial in advancing our understanding of wax biosynthesis (Jenks *et al.*, 1995). Wax biosynthesis begins with the production of C_{16} and C_{18} fatty acids in the plastid by the fatty acid synthase (FAS) complex. From here, the long chain fatty acids (FAs) are transported to the endoplasmic reticulum (ER) with activation with CoA via long-chain acyl-coenzyme A synthases. The long chain acyl-CoAs are further elongated by the ER-bound fatty acid elongation (FAE) complex, made of four core proteins that extend the long FAs to VLCFAs (longer than C_{18}). These can be sent to the cuticle to be used directly as cuticular wax components, or enter one of two pathways for further modification. The decarbonylation/alkane forming pathway, through which odd-chain-length alkanes, secondary alcohols and ketones are synthesized. The second pathway is the acyl-reduction/alcohol forming pathway, producing even-chain-length primary alcohols, and esters. (Kunst & Samuels, 2003; Samuels *et al.*, 2008; Yeats & Rose, 2013; Bernard & Joubès, 2013; Lee & Suh, 2015).

1.3.3 Fatty acid elongation

Elongation occurs in two-carbon increments, adding to the growing acyl-chain through rounds of four reactions within the FAE complex; condensation, carried out by β-ketoacyl CoA synthase (KCS); reduction, by β-ketoacyl-CoA reductase (KCS); dehydration, by β-hydroxyacyl-CoA dehydratase (HCD), followed by another reduction by enoyl-CoA reductase (ECR) (Figure 1.3). The KCS enzyme is of particular interest, for this first condensation reaction is rate limiting and substrate specific. In Arabidopsis there are 21 KCSs that work to elongate VLCFAs of specific chain lengths, while the other FAE complex enzymes are generalists. Therefore, many FAE complexes, incorporating different KCSs, are needed to elongate VLCFAs (Haslam & Kunst, 2013a). ECERIFERUM 6 (CER6) encodes a KCS involved in the biosynthesis of cuticular waxes in Arabidopsis, as shown by the significant decrease in all wax components longer than C_{24} in *cer6* mutants (Millar *et al.*, 1999; Hooker *et al.*, 2002). When expressed in yeast, CER6 elongates VLCFAs only up to C_{28} in length, (similar to its close homolog CER60), producing only trace amounts of C_{30} (Haslam *et al.*, 2015). No KCS has been found to elongate VLCFAs past this point. Given the bulk of Arabidopsis stem wax is made up of components derived from C_{30} VLCFAs, it seems logical that additional components are necessary to account for all the chain lengths apparent in cuticular wax.

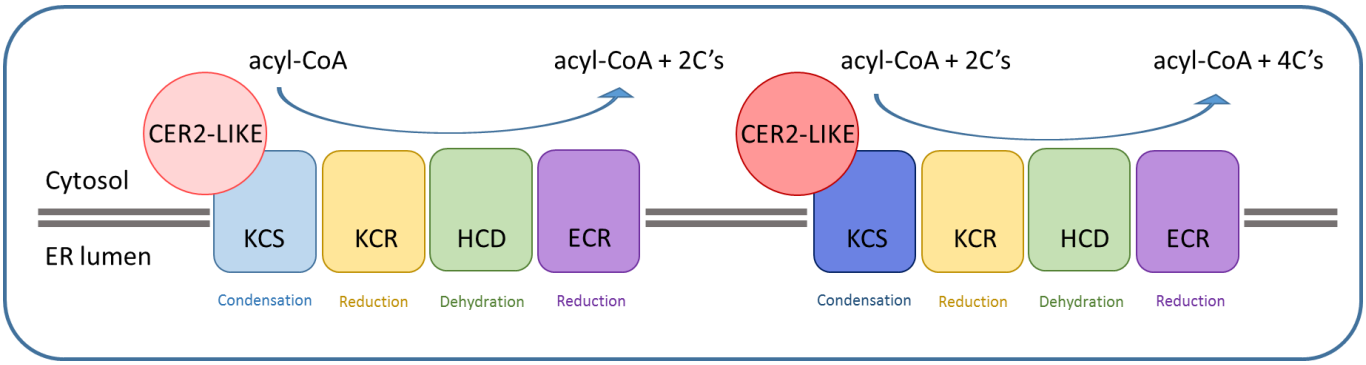

Figure 1.3: Two fatty acid elongation complexes consisting of different β-ketoacyl-CoA reductase**s (**KCSs) and ECERIFERUM 2-LIKEs (CER2-LIKEs) and similar β-hydroxyacyl-CoA dehydratase (HCDs) and enoyl-CoA reductases (ECRs). Each round of the four chemical reactions serves to elongate acyl-chains by two carbons. Two complexes are drawn to represent the necessity for multiple complexes containing different KCSs and CER2-LIKEs to elongate very long chain fatty acids.

1.3.4 ECERIFERUM2-LIKE (CER2-LIKE) BAHDs

In recent years, significant advances have been made in elucidating how VLCFAs are elongated past C_{28}. As it turns out, some of the first genes known to encode for BAHD-ATs, members of BAHD-ATs clade II including *ATCER2* (*Arabidopsis thaliana* ECERIFERUM 2) and *ZMGlossy2* (*Zea mays* Glossy 2), are required to work with the FAE complex in extension beyond C_{28}. The majority of the work on cuticular wax elongation has been done in Arabidopsis, researching ECERIFERUM 2-LIKE proteins (here, the term "CER2-LIKEs" includes CER2) and associated genes (Haslam *et al.*, 2012, 2015; Pascal *et al.*, 2013). The first gene to be characterized was CER2 (Jenks *et al.*, 1995; Xia *et al.*, 1996). The *cer2* Arabidopsis mutant is similar to the *cer6* mutant, in that the amount of all classes of wax compounds are reduced, causing a total wax reduction of 60 - 65% (Jenks *et al.*, 1995; Haslam *et al.*, 2012). In particular, all wax compounds longer than C_{28} are dramatically reduced, and accumulation of wax compounds C_{28} and shorter is observed, suggesting that CER2 acts in the elongation of VLCFAs

past C_{28}. The biochemical activity of CER2 is still unknown as it has no homology to the condensing enzymes, and has no effect on VLCFA elongation when expressed alone in yeast without a KCS. When expressed alongside CER6, C30 VLCFAs are formed, supporting its proposed function in elongation past C_{28} in cooperation with CER6 (Haslam *et al.*, 2012).

BAHD phylogenetic studies show that CER2 homologs exist in other taxa, such as *Populus*, *Medicago*, *Oryza*, and *Vitis* (Tuominen *et al.*, 2011). Published studies investigating CER2 homologs in Arabidopsis (CER2-LIKE1/CER26 and CER2-LIKE2/CER26-LIKE), revealed differential expression patterns and partially redundant activities(Haslam *et al.*, 2012, 2015; Pascal *et al.*, 2013). Yeast expression studies also show that all three enzymes can only work with two of five KCSs tested, i.e. CER6 and CER60, and co-expression of each of the CER2-LIKEs changed the acyl chain lengths of the products made by either CER6 or CER60 in the same manner (Haslam *et al.*, 2015). The composition of the cuticular wax is affected by the interplay of the CER2 family members with KCS components. The changes in chain length distribution of the wax components due to *CER2-LIKE* expression altered the epicuticular crystalline structure (Haslam *et al.*, 2015), highlighting the physiological importance of the CER2 family in the structure, of the cuticle.

Based on sequence homology, CER2 is classified as a BAHD-AT, clustering with the other CER2-like genes from Arabidopsis and *Zea mays Glossy2* in clade II (D'Auria, 2006). However, CER2 is different to other BAHD-ATs, as it has been shown to localize to the ER (Haslam & Kunst, 2013a), the site of wax biosynthesis, whereas BAHD-ATs are typically soluble cytosolic proteins (D'Auria, 2006). Second, CER2 possesses the highly conserved BAHD catalytic

HXXXD motif but is missing the second motif, as are all clade II members. Interestingly, CER2-LIKE1 is not considered in BAHD-AT phylogenies because it is missing the histidine of the highly conserved HXXXD motif, which led to the discovery that CER2-LIKE proteins do not require the catalytic histidine for activity as indicated by site-directed mutagenesis (Haslam *et al.*, 2012). These observations put into question whether clade II members should be considered BAHD-ATs at all (Tuominen *et al.*, 2011). It is not yet understood how the CER2-LIKES function to elongate cuticular waxes, but there is doubt that they work as acyltransferases.

1.3.5 Poplar CER2-LIKEs

Overall, very little is known about cuticular waxes in poplar. The few past studies looking at cuticular waxes of *Salix* and *Populus* species have all been descriptive, analyzing leaf cuticular wax composition and ultrastructure in different species, illustrating that cuticular waxes are dependent on species, leaf ontology, seasons, and a variety of different environmental factors (Hietala *et al.*, 1995; Cameron *et al.*, 2002; Maňkovská *et al.*, 2005). For example, most recently the cuticular waxes of desert poplar (P. euphratica) were described, and showed an increase in cuticular waxes and cuticle permeability in leaves from areas with lower soil water availability, relative to trees found in wetter regions (Xu *et al.*, 2016). This great variety is to be expected, as cuticular waxes are important in the adaptation of plants to different biotic and abiotic stresses (Joubès *et al.*, 2008). Only recently have genetic studies of wax related genes in *Populus* species been undertaken, characterizing a *P. trichocarpa* KCS (*PotriKCS1*), also representing another first, as the first gene characterized as being involved in alkene production in plants (Gonzales-Vigil *et al.* manuscript in preparation).

Cuticular wax elongation in poplar is an interesting pathway to investigate, because information on poplar CER2-LIKEs would not only add to the little information that is known about BAHD-ATs in poplar, but perhaps also aid in understanding how CER2-LIKEs function biochemically, and whether clade II members should be considered BAHD-ATs. No poplar *CER2-LIKE* genes have been characterized, but genes assigned to clade II in BAHD-ATs phylogenies are possible candidates (Tuominen *et al.*, 2011).

1.4 Rationale

Very few BAHD acyltransferases in *P. trichocarpa* have been biochemically characterized. In order to address this gap in our knowledge of poplar BAHDs, a candidate poplar BAHD-ATs was chosen to study. Originally, one of the 100 putative *P. trichocarpa* BAHD acyltransferases (Tuominen *et al.*, 2011) was selected as a putative poplar pHBMT gene. Transgenic hybrid poplar *Populus alba* × *grandidentata* (P39) overexpressing an *A.thaliana* galactinol synthase 3 gene (*AtGolS3*), were shown to be lacking lignin *p*-hydroxybenzoylation as compared to wild-type trees, (Figure 1.4) (Unda *et al.*, 2016). The transcriptome of these transgenic trees was analyzed under the assumption that a putative pHBMT would be downregulated in the xylem tissues of these trees. Using the RNA sequencing data, differential gene expression was calculated by comparing transcript FPKM values of transgenic and wild-type trees, and expressed as a log2fold value (Unda *et al.*, 2016). A list of candidate genes was assembled by selecting uncharacterized genes annotated as HXXXD-type BAHD-ATs, with significantly lower expression in the xylem of transgenic poplar trees relative to wild-type trees (Appendix Table A.1). Potri.005g052200 was the most highly down-regulated gene (-3.48 Log_2fold change) and

was therefore selected for further investigation as an interesting *Populus alba* × *grandidentata* acyltransferase-like gene (Pa×gACT-like).

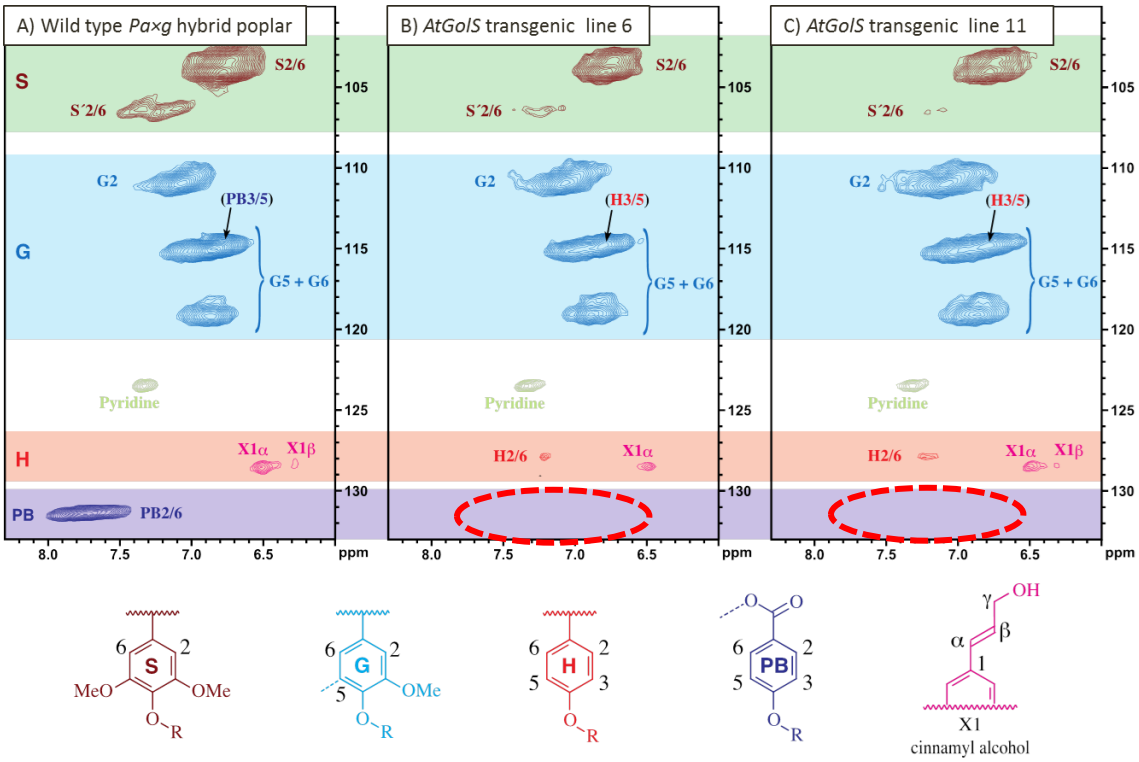

Figure 1.4: 2D-NMR from whole cell wall of wild-type *Populus alba* × *grandidentata* (P39) and AtGolS3 transgenic poplar samples. The image is adapted from (Unda, 2012; Unda *et al.*, 2016) with red ovals to highlight the missing *p*-hydroxybenzoate groups.

Interestingly, previous phylogenetic analysis of BAHD-ATs placed Pa×gACT-like within clade II, alongside the cuticular wax elongation CER2-LIKE enzymes (Tuominen *et al.*, 2011) (Figure 1.5). Though transcriptome analysis of the trees with abnormal lignin support a function for Pa×gACT-like in lignin acylation, the phylogenetics provide evidence to suggest a function in cuticular wax elongation. Though proteins belonging to the same clade of the BAHD acyltransferase family often have similar functions, there are exceptions. As described earlier,

the monolignol transferases characterized to date are found spread across different clades (Figure 1.5). Taking all of this evidence into consideration, a function as either a pHBMT or a CER2-LIKE seemed plausible for Pa×gACT-like.

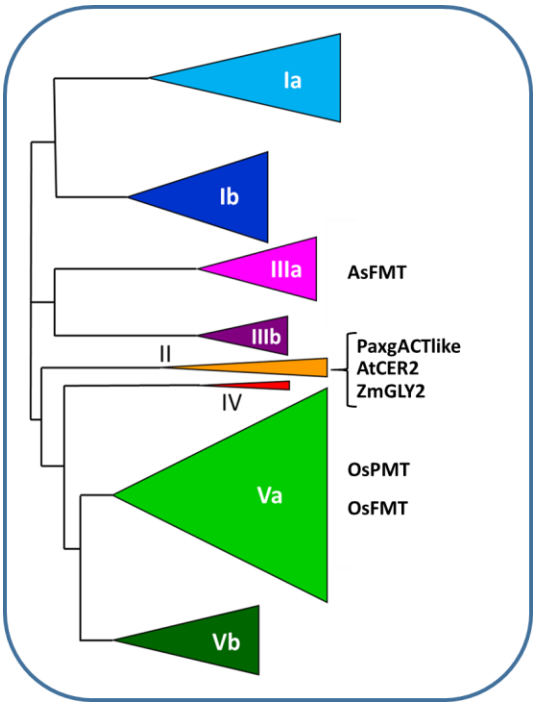

Figure 1.5. The BAHD phylogeny modified from Tuominen *et al.* (2011) to show the placement of characterized monolignol transferases and CER2-LIKEs. The clade placement of genes characterized after 2011 is derived from the more the recent BAHD phylogenetic analysis by Karlen *et al.* (2016). The BdPMT placement is described in terms of the clades as described by D'Auria (2006), placing it in clade V, which is split into two sub-clades in the above phylogeny.

1.5 Objectives/Scope

Assigning gene function to an undescribed BAHD-AT, such as the Pa×gACT-like, based on sequence information alone is difficult because members within a clade do not always have similar biochemical function. BAHD-ATs have low sequence identities, and participate in a wide range of biosynthetic pathways. Therefore, it is not surprising that there is conflicting evidence

for the putative function of Pa×gACT-like. Some evidence supports a likely function in the lignin biosynthetic pathway and as a potential candidate for the elusive pHBMT. In contrast, other evidence, points to a role in the cuticular wax biosynthesis as a CER2-LIKE.

The objective of this research is therefore, to investigate the function of the putative BAHD-ATs Pa×gACT-like, encoded by Potri.005g052200. Two main hypotheses were tested:
Hypothesis 1: Pa×gACT-like is a *p*-hydroxybenzoate-CoA monolignol transferase (pHBMT) involved in lignin modification.
Hypothesis 2: Pa×gACT-like is an ECERIFERUM2-LIKE (CER2-LIKE) involved in VLCFA elongation for cuticular wax biosynthesis.

The first part of this work examines the first hypothesis through the generation and analysis of gain-of-function and loss-of-function transgenic plants with altered expression of *Pa×gACT-like*. The gene was expressed in *A.thaliana* under the control of the cauliflower mosaic virus (CaMV) *35S* constitutive promoter to investigate the effects of the exogenous gene overexpression. A *Pa×gACT-like-RNAi* construct was expressed in hybrid P39 poplar to study the effects of gene downregulation. These transgenic plants were analyzed for changes in lignin *p*-hydroxybenzoylation through the saponification of extractive-free ground stem tissue and subsequent analysis via high-performance liquid chromatography (HPLC). In the second part of this project, transgenic poplar harbouring a *Pa×gACT-like Prom:GUS* fusion construct were generated in order to examine tissue scale expression of *Pa×gACT-like* to test a potential function of the BAHD-AT in either lignin or cuticular wax synthesis. Lastly, to test the second hypothesis, wax extractions and subsequent analysis via gas chromatography and flame

ionization detection (GC-FID) were performed to investigate changes in the wax profiles of the same transgenic plants mis-regulating Pa×gACT-like. Whether Pa×gACT-like functions as a pHBMT or a CER2LIKE, understanding the function of this putative BAHD-AT can fill in the gaps in our understanding of this gene family in poplar.

Chapter 2: Materials and Methods

2.1 Phylogenetic analysis

Homologs of Pa×gACT-like were identified using Phytozome V11 (Goodstein *et al.*, 2012). The closest protein homologs were Potri.013G039700 and Potri.013G039900. They share 99% similarity with one another and are likely a result of a tandem repeat, and are 91% similar to Pa×gACT-like. A close homolog was also found in willow, SapurV1A.0635s0150 with 88% similarity. The closest two Arabidopsis homologs, AT4G29250 and AT4G24510 (AtCER2), only share 50% and 43.8% similarity, respectively.

In order to help visualize the relationships between Pa×gACT-like, and its poplar and Arabidopsis homologs, as well as all CER2-LIKE genes, phylogenetic analysis was performed on clade II poplar and Arabidopsis BAHD-ATs as defined by Tuominen *et al.* (2011) with the addition of AtCER2-LIKE1 and Potri.013G039700. All amino acid sequences were obtained using Phytozome V11 (Goodstein *et al.*, 2012) and aligned using MUSCLE multiple sequence alignment. Protein similarity and identity were calculated using BioEdit (Ibis Biosciences, Carlsbad, CA, USA). An un-rooted Neighbour-Joining phylogenetic tree was constructed in MEGA6 (Tamura *et al.*, 2013) using the p-distance method and 10,000 replicates for bootstraps, eliminating positions containing gaps and missing data, using the pairwise deletion method.

2.2 Expression analysis

2.2.1 *In silico* gene expression analysis

Available gene expression data for the clade II poplar and Arabidopsis members was collected from several sources, including Phytozome v. 11 (Goodstein *et al.*, 2012) and the Arabidopsis eFB browser (Winter *et al.*, 2007). Expression data, based on transcriptome sequencing data

from hybrid P39 tissues (Unda *et al.*, 2016) and *P. trichocarpa* tissues (Hefer *et al.*, 2015), were also examined to determine tissues level gene expression patterns of clade II poplar genes.

2.2.2 Targeted co-expression network analysis

Corea *et al.* (manuscript in preparation) developed an RNAseq co-expression network of leaf and xylem tissues of *P. trichocapra* using tissues from nearly 200 poplar accessions. These 200 genotypes represent a subset of a collection of accessions sampled from across the natural range of *P. trichocarpa,* and grown in a common garden experiment at the University of British Columbia (McKown *et al.*, 2014). Using the leaf co-expression network, a co-expression analysis was performed targeting *Pa×gACT-like* to identify genes with correlating expression above a Pearson Correlation Coefficient threshold of 0.7 (Corea, personal communication).

2.3 Construct development

2.3.1 Over-expression construct

The full length coding sequence of *Pa×gACT-like* was isolated from hybrid poplar *Populus alba x grandidentata* (P39) leaf cDNA using primers # 3 and 4 (Table 2.1), and cloned into the entry vector pENTR/D-TOPO (Invitrogen Canada Inc., Burlington, ON). See Appendix Figure A.2 for differences in the nucleotide and amino acid sequence of the coding sequence of Potri.005g052200 in hybrid P39 vs. *P. trichocarpa*. A *Prom-35S::Pa×gACT-like* construct was generated by sub-cloning the coding sequence of *Pa×gACT-like* from pENTR into an overexpression vector pK2GW7 (Karimi *et al.*, 2002), via the LR reaction using Gateway LR Clonase II Enzyme Mix (Life Technologies Inc., Burlington ON). After transformation into chemically competent DH5α *E. coli* and sequencing (NAPS Unit, UBC) to confirm appropriate

insertion, the final construct was transformed into *Agrobacterium tumefaciencs* strain GV3101and used to transform wild-type *A. thaliana* (ecotype Columbia-0).

2.3.2 RNAi constructs

Two RNAi constructs, *Pa×gACT-like-RNAi S1* (suppression 1) and *Pa×gACT-like-RNAi S2* (suppression 2), were generated using the pHELLSGATE12 GATEWAY cloning system (Helliwell & Waterhouse, 2005). Both constructs were generated with the intention of targeting and suppressing the expression levels of Potri.005g052200 and homologs Potri.013g039900 and Potri.013g039700 simultaneously due to high level of sequence homology. Two constructs were generated to increase the likelihood of creating successful knock-down lines. A gene fragment of 324bp located at 81bp – 404bp, and another of 347bp located at 513bp - 859bp, were selected as target sequences for hairpin construction to suppress *Pa×gACT-like-RNAi* S1 and *Pa×gACT-like-RNAi* S2, respectively. To ensure the RNAi constructs would target all three genes, the sequence regions for the hairpin generation were chosen based on having high similarity between all three genes containing many conserved regions of up to 20bp. See Appendix Figure A.3 for a nucleotide alignment of the target regions. Target regions were cloned using primer pairs #19 and 20 and #21 and 22 for *Pa×gACT-like-RNAi S1* and *Pa×gACT-like-RNAi S2*, respectively (Table 2.1). These primers add attB sites to facilitate cloning into vector pDONR221 through a BP reaction using Gateway BP Clonase II Enzyme Mix (Life Technologies Inc., Burlington, ON). These vectors were transformed into chemically competent *E.coli*, and positive colonies sequence confirmed (NAPS Unit, UBC). Gene target sequences were sub-cloned from the entry vector pDONR221 into the destination vector pHELLSGATE12 by way of LR Clonase II Enzyme Mix Kit (Life Technologies Inc., Burlington, ON) to create *Pa×gACT-like-RNAi S1* and

Pa×gACT-like-RNAi S2 suppression constructs. These resulting RNAi constructs were sequenced to confirm identity and correct orientation of gene target regions needed for successful hairpin formation, then transformed into *Agrobacterium tumefasciens* strain EHA105 to be used for hybrid poplar transformation.

2.3.3 Promoter::GUS construct

A 2.3 kb promoter region upstream of *Pa×gACT-like* was cloned from genomic DNA isolated from hybrid poplar P39 leaf tissue, into entry vector pENTR/D-TOPO (Invitrogen Canada Inc., Burlington, ON), using primer set #7 and 10 (Table 2.1). The *Pa×gACT-like* promoter was sub-cloned from the resulting vector using primers #23 and 24, adding attB sites to facilitate cloning into vector pDONR/Zeo through a BP reaction using Gateway BP Clonase II Enzyme Mix (Life Technologies Inc., Burlington, ON) (Table 2.1). Correct insertion of the fragment into pDONR/Zeo was confirmed by sequencing. Then, LR Clonase II Enzyme Mix Kit (Life Technologies Inc., Burlington, ON) was used for GATEWAY directional cloning of the *Pa×gACT-like* promoter fragment into promoter-GUS reporter vector pMDC162 (Curtis, 2003). Following sequence verification for the correct insertion of the promoter into pMDC162, the *Pa×gACT-like Prom::GUS* vector was transformed into *Agrobacterium tumefasciens* strain EHA105 to be used for hybrid poplar transformation.

Table 2.1 A list of primers and their uses

#	*PRIMER ID*	*TYPE*	*SEQUENCE (5' TO 3')*
3	Pa×gACT-like_CDS_fw	Cloning	CACCATGGCGAACA AA C
4	Pa×gACT-like_CDS_rv	Cloning	CTATCTACCACTGATCAGCATTG
19	S1_attB_fw	Cloning	GGGGACAAGTTTGTACAAAAAAGCAGGCTCCATCCATTATCAGCGCTTG
20	S1_attB_rv	Cloning/Genotyping	GGGGACCACTTTGTACAAGAAAGCTGGGTCATGTACTAGGATCCTCAGGC
21	S2_attB_fw	Cloning	GGGGACAAGTTTGTACAAAAAAGCAGGCTATCCTGGATTGAGAGTCACCG
22	S2_attB_rv	Cloning/Genotyping	GGGGACCACTTTGTACAAGAAAGCTGGGTGCACGAGCCTTCTAAAGTCT
7	Prom_CACC_fw	Cloning	CACCCATCGTTGGCTGACATTAAG
10	Prom_rv	Cloning	CACTCCAAGCTGTATGTGTGTGATTTG
23	attB_Prom_fw	Cloning	GGGGACAAGTTTGTACAAAAAAGCAGGCTCATCGTTGGCTGACATTAAG
24	attB_Prom_rv	Cloning	GGGGACCACTTTGTACAAGAAAGCTGGGTTTTTCACTCCAAGCTGTATGTG
29	Pa×gACT-like_gen_fw	Genotyping	CCTTTCGTATCCAGGTAAATGA
30	Pa×gACT-like_gen_rv	Genotyping	AGGTTAGCTCAGGACCATAC
26	35S_fw	Genotyping	CTATCCTTCGCAAGACCCTTC
	35S_rv	Genotyping	

#	PRIMER ID	TYPE	SEQUENCE (5' TO 3')
27	Prom_mid_fw	Genotyping	CTACTTGCCACCGCCTCTTA
14	Prom_midseq_rv	Genotyping	CCTCGTGATCCAGAAATGGTG
28	GUS_rv	Genotyping	GGAACTGTTCGCCCTTCACT
17	Pa×gACT-like_qPCR_fw	qPCR	CACGGTTTGGGAGGAAATGC
18	Pa×gACT-like_qPCR_rv	qPCR	GGGTCTGCATTCATGTGTGT
35	AtEF1a_fw	qPCR	AGTTCTCGATTGCCACACCTC
36	AtEF1a_rv	qPCR	ACCATACCAGCGTCACCATTCTTC
31	PtTif_qPCR_fw	qPCR	GACGGTATTTTAGCTATGGAATTG
32	PtTif_qPCR_rv	qPCR	CTGATAACACAAGTTCCCTGC
33	M13_fw	Sequencing	GTAAAACGACGGCCAG
34	M13_rv	Sequencing	CAGGAAACAGCTATGAC
13	Prom_midseq_fw	Sequencing	CTGTGAAGCATTATTCTCGGG

2.4 *Agrobacterium* transformation

Transformation of *Agrobacterium tumefaciens* strain GV3101 was used to facilitate Arabidopsis transformation with the *35S::Pa×gACT-like* construct, while strain EHA105 was used to transform hybrid poplar with the hairpin RNAi constructs, and the *Pa×gACT-like Prom::GUS* construct. In all cases, Agrobacterium was transformed using a freeze-thaw method, where 1 µg of plasmid DNA was added to a carefully thawed 50 µl aliquot of the corresponding Agrobacterial strain and incubated on ice for 30 minutes. Cells were heat-shocked in a 37 °C water bath for 5 minutes. After this, 1 ml of YEP medium was added, and the cells were incubated at 28 °C for 2-4 hours in a gyratory shaker at 200 rpm. After this recovery period, cells were centrifuged at 13000 rpm for 1 minute in a bench top centrifuge. The supernatant was discarded and the cells carefully resuspended in 100 µl of fresh YEP medium and spread onto YEP-agar plates containing either 50 mg/L rifampicin and spectinomycin for *35S::Pa×gACT-like* and *Pa×gACT-like-RNAi* S1/ *Pa×gACT-like-RNAi* S2 constructs, or 50 mg/L rifampicin and kanamycin for the *Pa×gACT-like Prom::GUS* construct. Colonies were grown on plates incubated at 28 °C for 2 days, after which potential positive colonies were screened for the presence of the construct by PCR. To confirm the constructs presence in Agrobacterium, primers #33 and 14 were used for detecting the *35S::Pa×gACT-like* construct, primers #26 and 20 and #26 and 22 were used for detecting constructs *Pa×gACT-like-RNAi* S1 and S2, and primers #33 and 14 were used for detecting the *Pa×gACT-like Prom::GUS* construct (Table 2.1). Positive colonies were stored as glycerol stocks at -80 °C.

2.5 Agrobacterium-mediated transformation

2.5.1 Arabidopsis

Overexpression construct *35S::Pa×gACT-like* was transferred into Arabidopsis via Agrobacterium-mediated transformation using a modified floral dip method (Zhang *et al.*, 2006). In short, sterilized Arabidopsis wild-type Col-0 seeds were stored in the dark at 4 °C for 3 days to break dormancy. After stratification, seeds were spread onto autoclaved potting soil (Westcreek Farms Ltd., Fort Langely, BC), and grown covered in a growth chamber under long-day 16/8-h light/dark cycle at 21 °C. After germination, they were uncovered and thinned to 9 plants per pot. A 250 ml liquid Agrobacterium culture was grown overnight at 28 °C at 200 rpm in YEP media containing 50 mg/L rifampicin and spectinomycin. Cultures were concentrated and resuspended in a 5% sucrose solution containing 0.02% Silguard309 Norac. The optical density (OD) was measured and sucrose solution added to adjust the OD_{600} = 1-1.5. One by one, pots of Arabidopsis were inverted, the aerial portion of the plants dipped directly into the Agrobacterium mixture. Inoculated plants were laid on their sides and covered in black bags for approximately 24 hours. After 6-7 days, the transformation procedure was repeated. Once inflorescences matured, T1 seeds were collected in bulk. To screen for potential transformants, sterilized T1 seeds were plated on half MS medium (Murashige & Skoog, 1962) with no added sucrose, containing 50 mg/L of kanamycin as the selection antibiotic and allowed to grow for 10-14 days. Potential transformants were transferred onto autoclaved soil and genotyped for the presence of the exogenous poplar gene, *Pa×gACT-like*. PCR-positive plants were screened, using primers #29 and 30, and allowed to grow to maturity (Table 2.1). Each positive transformant was treated as a separate line, from which five individuals were chosen for further study.

2.5.2 Hybrid poplar

The Agrobacterium-mediated transformation procedure of wild-type hybrid P39 poplar used, was the same for the generation of *Pa×gACT-like-RNAi* S1 and *Pa×gACT-like-RNAi* S2 as well as *Pa×gACT-like Prom::GUS* lines. Large volume Agrobacterium cultures (3 x 90 ml) containing the vector of interest, were grown in McCown's Woody Plant Media (WPM) liquid media each containing 900 µl acetosyringone, overnight at 28 °C at 200 rpm. The next day, cultures were mixed and diluted to OD_{600} = 0.2 with additional liquid WPM. Using a 7 mm^2 cork borer under sterile conditions, around 600 leaf discs were cut from leaves of 4 week old P39 tissue culture grown plantlets. 500 leaf discs were separated into 25 leaf discs batches, suspended in 20-30 ml of Agrobacterium in 50 ml falcon tubes, and left to co-cultivate in the dark at 28 °C at 100 rpm in a gyratory shaker for 30-60 minutes. The other 100 leaf discs were used as a control, and co-cultivated in liquid WPM without Agrobacterium. After co-cultivation, batches of leaf discs were blotted with sterile paper towel to remove excess Agrobacterium, and transferred, abaxial side up, onto petri plates containing WPM 0.1/0.1/0.1 (0.1 µM NAA, BA, TDZ) and cultured in the dark at room temperature for 2 days. Leaf discs were then moved onto Agrobacterium-kill media containing 250 mg/L cefotoxine and 500 mg/L carbenicillin (WPM 0.1/0.1/0.1 $carb^{500}$ cef^{250}), leaving two plates of control leaf discs on the previous media as a positive control. After another three days, plates were removed from the dark, and leaf discs were transferred onto selection media containing 50 mg/L kanamycin for Pa×gACT-like-RNAi S1 and Pa×gACT-like-RNAi S2 or containing 20 mg/L hygromycin (WPM 0.1/0.1/0.1 $carb^{500}$ cef^{250} kan^{50}/hyg^{20}). Plated leaf discs were left to develop calli, and checked for Agrobacterium contamination regularly. After 4 weeks, leaf discs had good amounts of calli, and some shoots

began to appear. These calli were moved onto shooting media (WPM 0/0.01/0 carb^{500} cef^{250} kan^{50}/hyg^{20}) for another 4 weeks, or until the generation of elongated shoots. To avoid the generation of poplar lines with the same insertional event, one shoot per calli was excised and moved onto rooting media (WPM 0.01/0/0 carb^{500} cef^{250} kan^{50}/hyg^{20}) for another 3-4 weeks. Shoot tips were excised from shoots with established roots, so as to be taken off of the antibiotic rich media and transferred onto WPM 0.01/0/0 kan^{50}/hyg^{20} to promote growth. After one more round of growth on selection media, these plants were taken off all antibiotics and grown in tissue culture. Plants were confirmed to be transgenic by genomic DNA screening using primers #26 and 20 for *Pa×gACT-like-RNAi* S1 lines, #26 and 22 for *Pa×gACT-like-RNAi* S2 lines, and #27 and 28 for *Pa×gACT-like Prom::GUS* lines (Table 2.1). Each positive transformant was numbered and treated as a separate line to be subcultured and multiplied for planting in the greenhouse.

2.6 DNA screening

PCR screening of isolated genomic DNA was used to confirm the presence of the constructs in all transformed poplar and Arabidopsis lines, using appropriate primers and isolated genomic DNA as the template. Genomic DNA was isolated from Arabidopsis and poplar tissues to facilitate PCR screening for positive transformants. In short, 1-2 very small Arabidopsis or tissue cultured poplar leaves were ground in 400 µl of DNA extraction buffer (25 mM NaEDTA, 250 mM NaCl, 200 mM Tris HCl, 0.5% SDS). This mixture was centrifuged in a bench-top centrifuge at 13000 rpm for 3 minutes and the supernatant transferred to a new tube. To precipitate the DNA, 300 µl of isopropanol was added and incubated at room temperature for 5 minutes. Following centrifugation at 13000 rpm for 5 minutes, the supernatant was discarded and

the pellet washed by adding 500 µl of 70% ethanol and subsequently centrifuged at 13000 rpm for 2 minutes. After the ethanol wash was removed, the pellet was left to dry for 10-20 minutes before resuspension in double distilled water. All PCR screening reaction were performed using Taq DNA Polymerase and Buffer mix from New England BioLabs (Whitby, ON) following the manufacturer's instructions.

2.7 Transcript abundance analysis

2.7.1 RNA isolation/cDNA production

Total RNA isolation was performed identically for the various poplar and Arabidopsis tissues. First, the tissue was removed from -80 °C storage and ground to a fine powder in liquid nitrogen using mortar and pestle. Between 50-100 mg of the ground tissue was partitioned into a tube and kept chilled in liquid nitrogen until all tissues were processed, and any remaining tissue was stored separately as backup a at -80 °C. Total RNA was extracted using TRIzol Reagent (Life Technologies Inc., Burlington, ON) following the manufacturer's protocol. RNA extraction from poplar tissues resulted in a much larger pellet, probably due, in large part, to a higher amount of residual polysaccharides, and was therefore resuspended in 150 µl of nuclease-free water, whereas Arabidopsis RNA was resuspended in 30 ul. To remove any DNA contamination, RNA was treated with TURBA DNAase (Ambion, Burlington, ON), following manufacturer's instructions. Concentration and purity (A260/280) of DNA-free RNA was measured using a Nanodrop 1000 (Thermo-Fischer Scientific Inc., Wilmington, DE, USA). First strand cDNA was synthesized using iScript Select cDNA Synthesis Kit (Bio-Rad Laboratories Ltd., Mississauga, ON). Manufacturer's instructions were followed, using 1µg of total RNA, and 2 µl of both Oligo(dT) and random primers in the reactions.

2.7.2 Quantitative RT-PCR

Quantitative real-time PCR was used to assess transcript levels of *Pa×gACT-like* in both the PCR positive Arabidopsis over-expression lines, and hybrid poplar RNAi lines, using a Bio-Rad CFX96 Touch Real-Time PCR Detection System and Bio-Rad SsoFast EvaGreen Supermix (Bio-Rad Laboratories Ltd., Mississauga, ON) according to manufacturers' instructions. Analyses were performed separately on Arabidopsis and poplar cDNA, following the same general work flow. In order to calculate primer efficiency, and determine optimal RNA concentration, a five-point dilution series, using pooled cDNA from all transgenic lines and wild-types, was used in all qRT-PCR. These cDNA dilution samples were run in triplicates, using gene-specific qRT-PCR primers #17 and 18 paired with reference gene specific primers; PtTIF specific primers #31 and 32 for poplar, and AtEF1α specific primers #35 and 36 for Arabidopsis (Table 2.1). A 16x working dilution of cDNA and an annealing temperature of 56.5 °C was used for qRT-PCR analysis of both Arabidopsis and poplar cDNA. Relative gene expression levels were determined using the formula: $2^{-(Cq_{sample} - Cq_{reference})}$.

2.8 Lignin analysis

2.8.1 Tissue growth/collection

2.8.1.1 Arabidopsis

Transgenic *35S::Pa×gACT-like* lines and wild-type Arabidopsis seeds were sterilized and stored in the dark at 4 °C for 3 days to break dormancy. After stratification, seeds were spread onto half MS medium (Murashige & Skoog, 1962) plates without sucrose, containing 50 mg/L of kanamycin as the selection antibiotic for transgenic seeds, and allowed to grow for 10-14 days.

Putative transformed germinants were planted, six plants per pot, on autoclaved potting soil (Westcreek Farms Ltd., Fort Langely, BC) and grown (covered for a week to retain high humidity) in a growth chamber under long-day conditions 16/8-h light/dark cycle at 21 °C. Plants were screened by PCR to verify the presence of the transgene using primers #29 and 30 (Table 2.1), and non-transformants removed from the pots. Plants were watered approximately every 3 days with tap water for approximately 6 weeks. When the plants bolted, they were staked to promote upright growth and reduce tangling. After 6 weeks, watering ceased and plants were removed from the chamber to dry out and set seed. Seeds were collected, and the bottom 10 cm of the main inflourescence of each plant was harvested and pooled by line in order to have enough tissue for saponification. Stem tissue was then ground using a Wiley mill, to pass through a 40-mesh (0.4 mm) screen. Samples were acetone extracted overnight (about 16 hours) using a soxhlet apparatus, and stored at room temperature until needed.

2.8.1.2 Poplar

A small subset of positively transformed *Pa×gACT-like-RNAi* S2 lines, were selected for an initial screen. Three plantlets representing separate lines (S2.1, S2.2, S2.3) along with a wild-type P39 control, were transferred to 2 gallon pots of perennial mix (Westcreek Farms Ltd., Fort Langley, BC) and kept under clear plastic cups and closely monitored for signs of desiccation for 2 weeks. Plants were grown with supplemental lighting (18 hours) at temperatures ranging between 20-26 °C with fertilization and daily watering. After 3 months of growth, stem tissue was harvested from the trees by cutting 40 cm above soil level, and the leaves and bark stripped off of the harvested stem portion. The scrapings of debarked stems were collected and flash frozen in liquid nitrogen at -80 °C for subsequent qRT-PCR. The pith was removed from the

already debarked stems and this tissue was cut into smaller matchstick sized pieces. These specimens were then ground using a Wiley mill, to pass through a 40-mesh (0.4 mm) screen and acetone extracted overnight (about 16 hours) using a soxhlet apparatus, and stored at room temperature until needed. Extractive free ground wood samples of a variety of other *Salicaceae* species were also saponified, both as positive controls for the experiment, as well as to survey the natural variation in lignin *p*-hydroxybenzoylation. These wood samples were pre-existing in the lab from other finished and ongoing projects.

2.8.2 Saponification

In order to quantify the amount of lignin *p*-hydroxybenzoylation of different wood samples, a slightly modified version of a saponification protocol developed in house was used (Johnson, 2015). Saponification is a nucleophilic acyl substitution, where an ester and a strong base yield an alcohol and a salt, which, when a source of protons is added, forms a carboxylic acid. Approximately 30 mg of extractive free ground tissue was weighed out into a screw top tube and exact weights recorded. To the wood meal, 1.5 ml of 0.2 M NaOH was added to each sample, and these were incubated at 60 °C for 75 minutes in a shaker set to 500 rpm. Afterwards, the samples were acidified by adding 15 µl of 72% (w/w) H_2SO_4, and allowed to cool for 5 minutes on ice. Tubes were then centrifuged at 13000 rpm for 2 minutes, and the supernatant collected and filtered through a 0.45 µm filter into HPLC vials. A *p*-hydroxybenzoic acid (pHBA) standard was also prepared to be run along with samples on the HPLC.

2.8.3 Analysis via HPLC

The pHBA content was quantified by high pressure liquid chromatography (HPLC) on a Summit HPLC (Dionex, USA) fit with a Symmetry C18 column (Waters) and a PDA-100 Photodiode Array Detector (Dionex, USA). Components were eluted from the column at a flow rate of 0.7 mL/minute using a gradient from 95% A (100% water:0.1% trifluoroacetic acid (TFA)) to 45% B (75% acetonitrile:25% methanol: 0.1% TFA) over 50 minutes, followed by a 10-minute wash with 75% B and re-acclimation of the column with 95% A for 10 minutes. The pHBA peak was identified based on comparison to the retention time and UV spectra of the known standard. Peaks were manually integrated and pHBA concentrations were calculated using standard curves created from external pHBA standards.

2.9 Prom::GUS analysis

2.9.1 Tissue collection

Three clones of four positive *Pa×gACT-like Prom::GUS* lines were grown in the greenhouse under the same conditions as described above for the poplar RNAi lines. Fresh tissues were collected from greenhouse-grown plants for same day sectioning and subsequent GUS staining. Leaves were collected using leaf plastochron index, where PI=4 was defined as the first fully unfolded leaf, measuring greater than 5 cm in length, where PI=3 and PI=5 are the leaves directly above and below it, respectively (Appendix Figure A.4). Using a sliding benchtop microtome (American optical, Model #860), 60 µm thick cross-sections were cut from younger (leaf 4) and more mature (leaf 15) tissues (leaf blade, petiole and above internode) as well as from young (primary growth) and mature (secondary growth) roots.

2.9.2 GUS staining

Histochemical GUS analysis was performed as described by Jefferson *et al.,* (1987) with some alterations and considerations taken from Vitha *et al.,* (1995). Sections were fixed in 90% cold acetone and incubated on ice for 10-15 minutes. The acetone was subsequently replaced with a washing solution (0.1 M $NaPO_4$, 0.1% Triton X-100, 10 mM EDTA, 1 mM K_3FeCN, 1 mM K_4FeCN). The wash solution was removed and replaced with X-gluc staining solution (00.1 M $NaPO_4$, 0.1% Triton X-100, 10 mM EDTA, 1 mM K_3FeCN, 1 mM K_4FeCN, 1mM 5-brommo-4-chloro-3-indolyl-beta-D-glucuronide), and placed under vacuum infiltration for 10-15 minutes, to aid stain penetration into sections, and then incubated for 2-3 hours at 37 °C. Samples were then washed with 70% ethanol to clear the sections, and were visualized using Leica DMR light microscope (Leica Microsystems Inc.). Images were captured with a QImaging Qicam camera (QImaging) using OpenLab software (PerkinElmer Inc.)

2.10 Wax profile analysis

2.10.1 Fatty acid methyl ester (FAME) analysis

Yeast assays were performed by Tegan Haslam, in Ljerka Kunst's lab as described in Haslam *et al.,* (2012). In short, *AtCER6*, *AtCER2* and *Pa×gACT-like* were expressed in *Saccharomyces cerevisiae* strain W3031a. Assays were run, where AtCER6, AtCER2, Pa×gACT-like, AtCER6 + AtCER2, and AtCER6 + Pa×gACT-like were expressed independently and together, using 4-8 technical replicates. FAME analyses were conducted using GC-FID, identifying peaks based on comparison to standards with known retention times.

2.10.2 Wax profile analysis of transgenic plant tissues

2.10.2.1 Tissue growth/collection

2.10.2.1.1 Arabidopsis stems

Transgenic *35S::Pa×gACT-like* lines and wild-type Arabidopsis were grown similarly as described above for plants grown for lignin analysis, with a few minor changes. Two plants were grown per pot, and the main inflorescence stems were harvested 6-8 weeks after seedlings were transferred to soil. The experiment was run three independent times, and subsequently stem tissue collection was conducted for wax analysis.

The main inflorescence was cut at base of the plant and the tissue was handled carefully using forceps and gloves to avoid perturbing the stem waxy layer. Cauline leaves and siliques were removed from the stem, and the top 10 cm were harvested for wax analysis. The stem tissue was placed into a 50 ml beaker which had previously been washed twice with chloroform, and to which 10 µl of 10 mg/mL of n-tetracosane (Sigma-Aldrich) had been added as an internal standard. At this time, 4-5 leaves were collected in screw-cap tubes and flash frozen in liquid nitrogen to be stored at -80 °C for RNA isolation.

2.10.2.1.2 Poplar leaves

Transgenic *Pa×gACT-like-RNAi* S1 and *Pa×gACT-like-RNAi* S2 lines were clonally multiplied and grown for 5 weeks in tissue culture before being planted in the greenhouse. Six clones of each of three *Pa×gACT-like-RNAi* S1 lines, two *Pa×gACT-like-RNAi* S2 lines, and wild-type P39, were transferred from tissue culture containers into two gallon pots of perennial mix soil (Westcreek Farms Ltd., Fort Langley, BC). For the first two weeks, plantlets were kept under

clear plastic cups and closely monitored for signs of desiccation. Plants were grown in the UBC Greenhouse (Vancouver, BC) with supplemental lighting (18 hours) at temperatures ranging between 20-26 °C with fertilization and daily watering. Based on RT q-PCR results, Leaf tissue collection for wax analysis was conducted only on *Pa×gACT-like-RNAi* S1 lines, three separate times from the same plants (Table 2.2).

To collect a uniform amount of tissue for wax analysis, two leaf discs were cut from the leaf tissue of interest, using a 13 mm cork borer, avoiding the midvein. To prevent perturbing the cuticular waxes, leaf discs were handled using forceps, placed into 50 ml beakers which had previously been rinsed twice with chloroform, and to which 10 µl of n-tetracosane (Sigma-Aldrich) had been added as an internal standard. Four leaf discs were placed in a screw-cap tube and flash frozen in liquid nitrogen to be stored at -80 °C for RNA isolation.

Table 2.2: Poplar tissue collections for wax extraction.

Trial	Leaf PI #	Tree age (Weeks after planting)
1	7	9
2	7	20
3	4 and 5	26

2.10.2.2 Wax extraction

Analyses were performed separately on Arabidopsis and poplar tissues. The method used were slightly altered from those previously described for Arabidopsis (Haslam *et al.*, 2012; Haslam & Kunst, 2013b) and poplar (Gonzales-Vigil *et al.* manuscript in preparation). In order to extract waxes, 10 ml of HPLC-grade chloroform was added to a beaker, fully submerging the tissue for

30 seconds after which the tissue was removed and disposed of. For surface area determination, the Arabidopsis stem was laid out straight and photographed before disposal. After all samples were extracted, chloroform was allowed to evaporate at room temperature in a fume hood. Samples were resuspended in 300 µl of chloroform and transferred into 2 mL glass vials containing 200 µL inserts. The samples were also derivatized by first evaporating the chloroform under a gentle stream of nitrogen gas, after which 10 µL of both pyridine and N,O-bis(trimethylsilyl) trifluoroacetamide (Sigma-Aldrich) were added to the remaining wax sample and incubated at 75 °C for 60 min. Derivatization reagents were then evaporated, again using nitrogen gas, and samples were resuspended in 200 µl of chloroform for GC-FID analysis.

2.10.2.3 Analysis via GC-FID

The wax profile was analyzed by running samples on a HP 5890 Series II GC system fitted with a 30 m x 320 µm x 1 µm HP-1 column and an FID detector (Agilent), programmed with an oven temperature of 50 °C for 2 minutes, then increased at 40 °C/min to 200 °C, and held for 1 minute, then raised at 3 °C/min to 320 °C, and held for 15 minutes.

To calculate the amount of each wax component present in a sample, the peak area was normalized to the amount of internal standard and expressed per surface area of tissue. For Arabidopsis stems, the surface area was determined using ImageJ software (Schindelin *et al.*, 2012, 2015) to measure the two-dimensional stem area from digital photographs and multiplying it by π. For poplar leaf discs, surface area was determined by multiplying the area of one side of a leaf disc, by four (two leaf discs, two sides each) giving the equation $4\pi r^2$ where r = 6.5 mm. Since Arabidopsis waxes have been thoroughly studied, determining the chemical identity of

GC-FID chromatograph peaks from stem samples could be accomplished by comparing to annotated wax GC-FID profiles (Jetter *et al.*, 2006). Determining the chemical identity of the poplar leaf wax peaks was more difficult, as relatively little is known about poplar cuticular waxes. Wild-type Arabidopsis stem, and poplar leaf waxes were run in tandem on the GC-FID and their chromatograms used to compare retentions times between identified Arabidopsis peaks (Jetter *et al.*, 2006), and unknown poplar peaks (Figure 2.1).

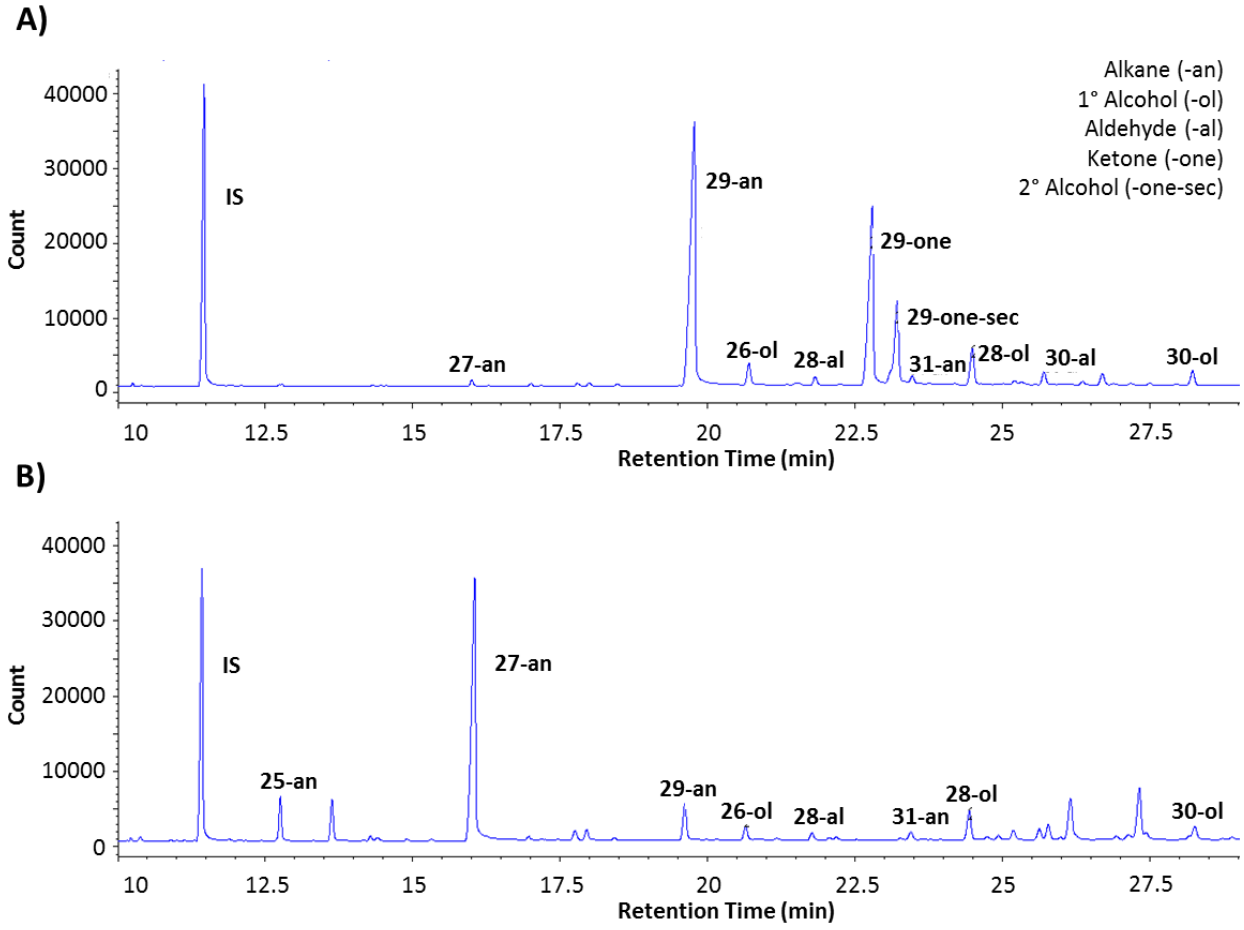

Figure 2.1. GC Chromatographs showing the identified peaks from cuticular wax profile of wild-type A) Arabidopsis stem and B) P39 leaf (PI-7) tissue.

2.11 Statistical analysis

Statistical analysis of the differences in cuticular wax components between wild-type and transgenic plant lines, was performed using R version 3.3.1 (R Core Team, 2016). Data sets of poplar and Arabidopsis, and yeast wax analyses were imported separately and analyzed using a generalized linear model (glm) and an analysis of variance at a significance level of $P < 0.05$ from the statistical packages *car* v.2.1-4 (Fox & Weisberg, 2011) and *stats v.3.3.2*, respectively (R Core Team, 2016). Differences between means were tested by calculating the least squares means using the package *lsmeans* v.2.25 (Lenth, 2016) and the resulting values were used to perform paired t-tests at a significance level of $p < 0.05$. The Tukey method for p-value adjustment was used due to the multiple comparisons made. An example of the code run can be found in Appendix Figure A.5.

Chapter 3: Results

3.1 Phylogenetic analysis

To characterize Pa×gACT-like, an updated phylogenetic analysis was required, as new information about this clade of BAHD acyltransferases has emerged. The thorough phylogenetic analysis of BAHD acyltransferases by Tuominen *et al.* (2011), places Pa×gACT-like in clade II, along with its poplar and Arabidopsis homologs. The clade II enzymes characterized thus far are CER2-LIKEs, which function in VLCFA elongation, however not all BAHD-ATs were included in this previous phylogenetic analysis, as an additional CER2-LIKE (CER2-LIKE1) has since been identified. This protein however, lacks the HXXXD motif characteristic of BAHD-ATs. All other clade II members contain the highly conserved HXXXD motif, however, they lack the second BAHD-ATs motif (some variation of DFGWG), as illustrated by a protein alignment to OsPMT, a previously characterized BAHD-AT from clade Va (Figure 3.1). To account for the recently identified CER2-LIKE1, a slightly modified phylogenetic tree was generated, assessing the relationship of poplar and Arabidopsis clade II BAHD-ATs, as described by Tuominen *et al.* (2011).

To this end, the deduced amino acid sequences were aligned, and an unrooted Neighbor-Joining tree was constructed, which illustrates the assembly into two main groups (Figure 3.2). The first includes Pa×gACT-like and its closest poplar and Arabidopsis homologs, where Pa×gACT-like clusters with its two close poplar homologs as expected, considering their 91% amino acid similarities (Figure 3.2). Also in this group is the Pa×gACT-like closest Arabidopsis homolog AT4G29250 (CER2-LIKE3) (46.4% similarity), which clusters with Potri.018g032700. The other main group includes two poplar genes and the three characterized Arabidopsis CER2-

LIKEs; Potri.005g153600 clusters with CER2, and Potri.001g319200 clusters with CER2-LIKE1 and CER2-LIKE2. This tree shows that although Pa×gACT-like falls into clade II, there are other poplar BAHD-ATs that are more similar to the characterized Arabidopsis CER2-LIKEs.

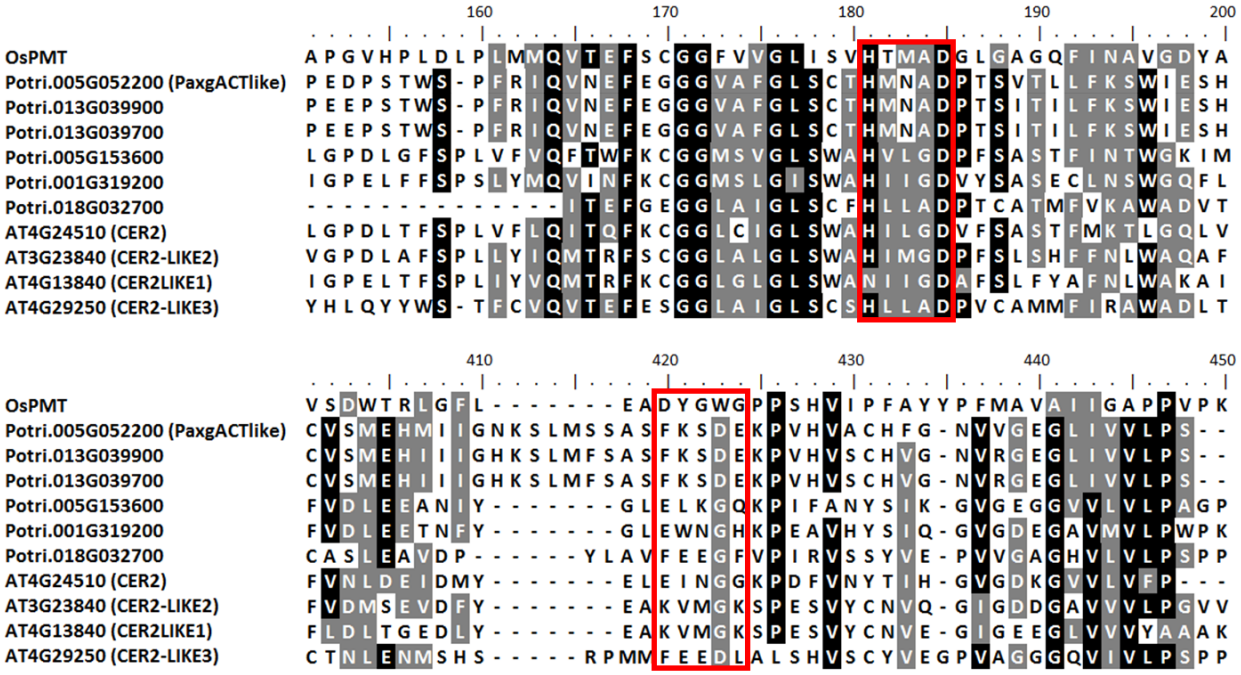

Figure 3.1. Amino acid sequence alignment of all poplar and Arabidopsis clade II BAHD-ATs with the addition of CER2-LIKE1 as compared to clade V BAHD-ATs member, OsPMT. Red rectangles highlight the two characteristic BAHD motifs; HXXXD, and DFGWG (present as DYGWG in OsPMT). Identical amino acids are shaded in black and similar residues in grey.

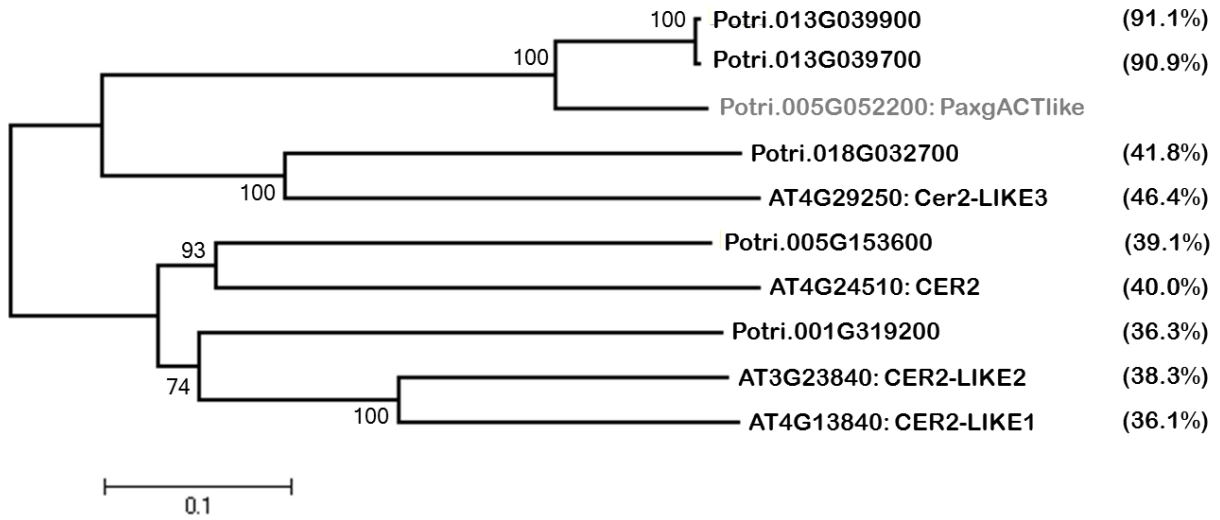

Figure 3.2. Unrooted Neighbour-Joining tree of all poplar and Arabidopsis clade II BAHD-ATs as defined by Tuominen *et al.* (2011), plus CER2-LIKE1 to include all functionally characterized Arabidopsis CER2-LIKEs. Bootstrap values are based on 10,000 replicates. Bars, 0.1 amino acid substitutions per site. Percentages in brackets represent similarity of Arabidopsis and poplar clade II BAHD-ATs to Pa×gACT-like.

3.2 Expression analysis

3.2.1 *In silico* gene expression analysis

There is evidence to support a functional role for the BAHD-ATs of interest, Pa×gACT-like, in either lignin biosynthesis as a poplar pHBMT, or in cuticular wax biosynthesis as a poplar CER2-LIKE. To gain more insight into the putative function of Pa×gACT-like, available gene expression data, based on transcriptome sequencing data from hybrid P39 tissues (Unda *et al.*, 2016) and *P. trichocarpa* tissues (Hefer *et al.*, 2015), were examined to determine tissue-level gene expression patterns.

As demonstrated by *Populus alba* × *grandidentata* (P39) expression data, *Pa×gACT-like* has very low expression in the cambium/bark, and is expressed at similar levels in xylem and in source leaves, and in *P. trichocarpa* the expression is higher in sink leaves than in xylem (Table

3.1). The other poplar clade II BAHD-ATs are also expressed in these tissues, except Potri.018G032700, which is expressed mainly in male catkins (Phytozome v. 11), similar to the closest Arabidopsis homolog AT4G29250 (CER2-LIKE3), which, based on the Arabidopsis eFB browser, is expressed solely in flowers (Winter *et al.*, 2007). The two very close poplar homologs Potri.013G039700 and Potri.013G039900, are expressed at much lower levels in all tissues than *Pa×gACT-like*, in both species. Potri.005G153600 is mainly expressed in sink leaves, while Potri.001G319200 is expressed at lower levels in source and sink leaf tissues. Taken alone, the *P. trichocarpa* expression data would suggest a putative wax function is more likely, but as in the hybrid P39, *Pa×gACT-like* is expressed in both leaf and xylem tissues, a role in lignin biosynthesis cannot be discounted. The other poplar clade II members are, in some cases, expressed in similar tissues, and may display redundant functionality to *Pa×gACT-like*.

Table 3.1. Transcript abundance of *Pa×gACT-like* and poplar clade II BAHD-ATs in different tissues of hybrid P39 and *P. trichocarpa*. P39 and *P. trichocarpa* expression (FPKM) based on transcriptome sequencing data from Unda *et al.* (2016) and Hefer *et al.* (2015) respectively. Leaf expression data based on sink leaves (PI 4-5) for *P. trichocarpa*, and source leaves (PI 9).

	P. trichocarpa		**Hybrid P39**		
Gene ID	*Xylem*	*Sink Leaf*	*Xylem*	*Source Leaf*	*Cam/bark*
Potri.005G052200 (PaxgACTlike)	0.746	4.970	6.937	6.989	0.150
Potri.013G039700	0.021	0.111	0	0.805	0
Potri.013G039900	0.165	0.072	0	0.184	0.015
Potri.001G319200	0.073	0.754	0.067	1.598	0.045
Potri.005G153600	0	11.071	0.093	0.024	0.025
Potri.018G032700	0	0	0	0	0

3.2.2 Co-expression network analysis

To identify genes displaying similar expression patterns to *Pa×gACT-like*, co-expression analysis was performed by Oliver Corea on a *P. trichocarpa* leaf transcripts, targeting *Pa×gACT-like* and using a Pearsons Correlation Coefficient threshold of 0.7 (Corea *et al.*, manuscript in preparation). The resulting list of genes was surveyed for genes related to lignin or wax biosynthesis. A breakdown of the putative GO-enrichment-terms of the co-expressed genes revealed that a considerable number (~ 30%) of the genes are involved in lipid/fatty acid biosynthesis and metabolism (Figure 3.3). A closer look revealed a list of 28 co-expressed genes, annotated as homologs of a variety of different characterized Arabidopsis genes involved in wax and fatty acid biosynthesis, as well as lipases and lipid transfer proteins (Table 3.2).

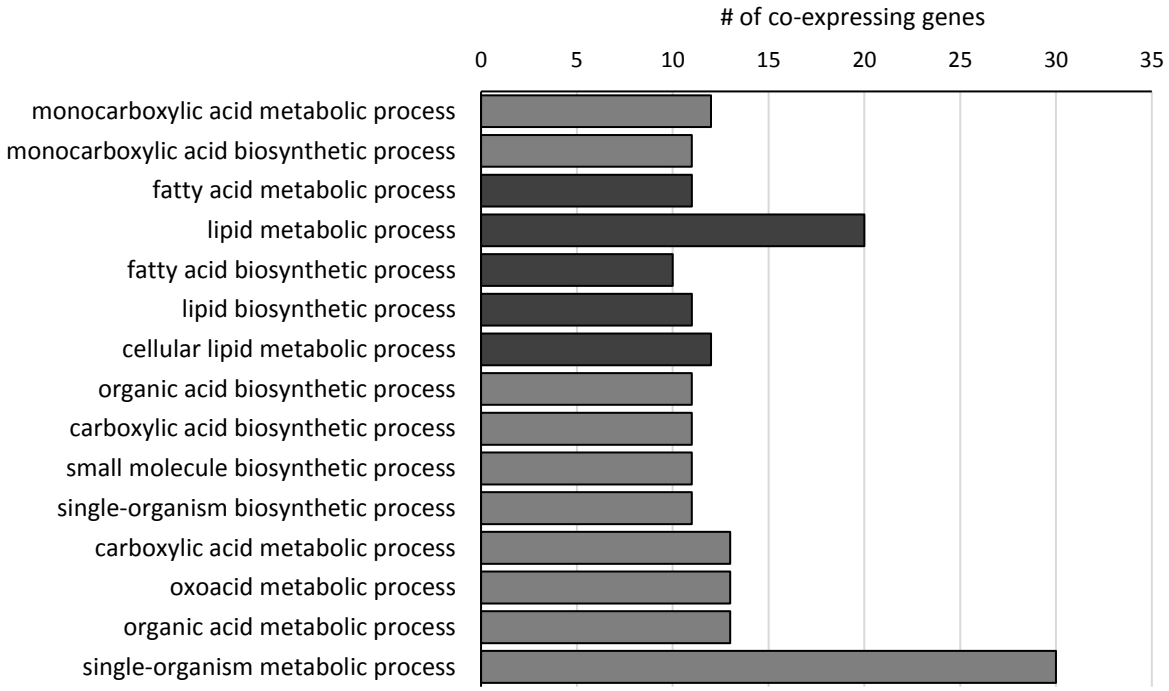

Figure 3.3. GO-enrichment-terms for biological processes. Darker bars represent fatty acid/lipid related genes.

Table 3.2. List of lipid biosynthesis related genes co-expressed with *Pa×gACT-like* as defined by a Pearsons Correlation Coefficient (PCC) of 0.7.

Gene ID	PPC	Annotation of Arabidopsis Homologs
Potri.003G129100	0.855	MAH1 (midchain alkane hydroxylase) Cyp86A7
Potri.014G180300	0.851	CER1 (Eceriferum 1); Octadecanal Decarbonylase
Potri.009G144900	0.832	CER4 (Eceriferum 4); Fatty Acyl-CoA Reductase
Potri.015G089700	0.829	GDSL-Motif Lipase/Hydrolase Family Protein
Potri.019G024800	0.825	GDSL-Motif Lipase/Hydrolase Family Protein
Potri.006G095800	0.821	a-CT (Acetyl-CoA Carboxylase)
Potri.019G024700	0.816	GDSL-Motif Lipase/Hydrolase Family Protein
Potri.003G142000	0.815	KAS I (3-Ketoacyl-Acyl Carrier Protein Synthase I)
Potri.010G179400	0.812	SAD (Stearoyl-ACP Desaturase) Putative
Potri.008G181700	0.806	KCR (β-Keto Acyl Reductase)
Potri.013G102400	0.797	GDSL-Motif Lipase/Hydrolase Family Protein
Potri.013G136000	0.797	LIP1-like (Lipoic Acid Synthase Family Protein)
Potri.014G085800	0.795	MAH1 Like Similar to Cytochrome P450
Potri.017G092500	0.788	BCCP1 (Biotin Carboxyl Carrier Protein)
Potri.009G109900	0.783	LACS2 (Long-Chain Acyl-CoA Synthetase 2)
Potri.013G031300	0.776	ACP1 (Acyl Carrier Protein 1)
Potri.005G044800	0.772	ACP1 (Acyl Carrier Protein 1)
Potri.007G139600	0.746	Wax Ester Synthase-Like Acyl-CoA Acyltransferase Domain
Potri.016G113100	0.743	GPAT6 (Glycerol-3-Phosphate Acyltransferase 6)
Potri.010G189300	0.738	GDSL-Motif Lipase/Hydrolase Family Protein
Potri.001G120900	0.736	KAS III (3-Ketoacyl-Acyl Carrier Protein Synthase III)
Potri.016G110500	0.734	α-CT (Acetyl-CoA Carboxylase)
Potri.008G068000	0.734	GDSL-Motif Lipase/Hydrolase Family Protein
Potri.008G178700	0.725	KAR (3-Ketoacyl-Acyl Carrier Protein Reductase)
Potri.019G024400	0.723	GDSL-Motif Lipase/Hydrolase Family Protein
Potri.010G052300	0.709	KCR (B-Keto Acyl Reductase)
Potri.010G204400	0.706	CER10 (Eceriferum 10)/ECR (Enoyl-CoA Reductase)
Potri.001G056200	0.703	LTPG1 (Glycosylphosphatidylinositol-Anchored Lipid Transfer Protein 1)

3.2.3 Relative expression of *Pa×gACT-like* in transgenics

3.2.3.1 Heterologous expression of *Pa×gACT-like* in Arabidopsis

To assess if the expression of the exogenous poplar gene could affect lignin or cuticular wax biosynthesis, gain-of-function Arabidopsis plants were generated through *Agrobacterium*-mediated transformation with a *35S::Pa×gACT-like* construct. This yielded 14 PCR positive transformants, which were grown for 6 weeks after which RNA was extracted from leaf tissue for real-time qRT-PCR. Five lines with the highest transcript abundance, lines 37, 38, 32, 12, 7 were then chosen for further study (Figure 3.4). Transgenic lines overexpressing the construct did not have any noticeable differences in bolting time, height or rosette diameter as compared to concurrently grown wild-type Arabidopsis plants (data not shown).

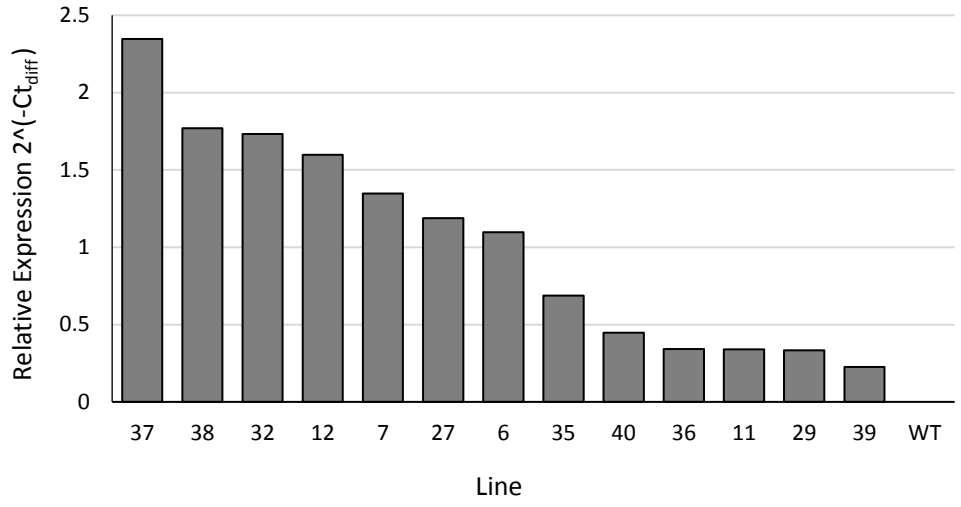

Figure 3.4. Relative expression of *Pa×gACT-like* in *35S::Pa×gACT-like* Arabidopsis over-expression lines relative to wild-type. Expression normalized to Arabidopsis elongation factor 1 alpha (AtEF1α). n=1

3.2.3.2 Downregulation of *Pa×gACT-like* through RNA silencing

To assess if the suppression of the endogenous gene would affect lignin or cuticular wax biosynthesis, RNAi-poplar lines were generated via *Agrobacterium*-mediated transformation of

hybrid poplar with constructs that targeted different regions of the gene for downregulation, *Pa×gACT-like-RNAi* S1 (suppression 1) and *Pa×gACT-like-RNAi* S2 (suppression 2). PCR screening of genomic DNA for transformants identified several positive lines for each construct. Leaves of tissue culture grown plants of S1 and S2 RNAi-lines, were used to determine transcript abundance by real-time qRT-PCR, which revealed that the lines created using the *Pa×gACT-like-RNAi* S1 construct, down-regulate *Pa×gACT-like* more, relative to the S2 construct (data not shown). Therefore, only S1 lines were further considered. To continue with, three lines (S1.15, S1.10, S1.14) possessing the lowest transcript levels compared to native expression levels were selected and transferred to the UBC greenhouse. Gene suppression in greenhouse grown trees was confirmed through analysis of the relative expression of *Pa×gACT-like*, via real-time qRT-PCR using RNA extracted from leaf PI-4. All lines were found to have significantly reduced *Pa×gACT-like* expression, where lines S1.10, and S1.15 appeared to have the lowest transcript abundance (Figure 3.5). No morphological phenotypes were apparent relative to concurrently grown wild-type trees (data not shown).

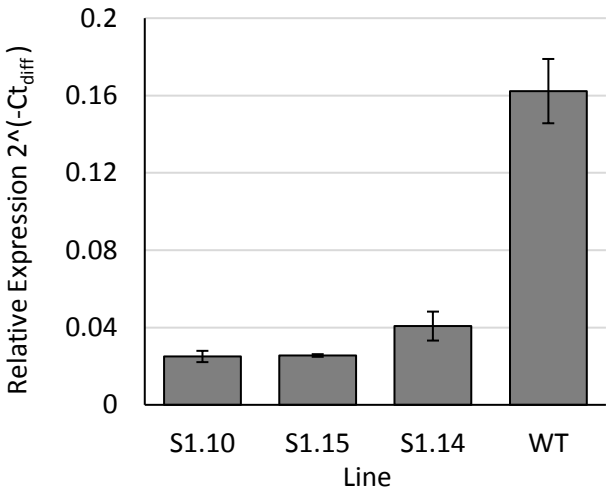

Figure 3.5. Transcript abundance of *Pa×gACT-like* in leaf PI-4 tissue of greenhouse grown *Pa×gACT-like-RNAi* lines. Expression relative to the Translation Initiation Factor 5A (PtTIF5A). Error bars represent standard error of the mean (n=3).

3.3 Pa×gACT-like as a poplar pHBMT

Originally, Pa×gACT-like was selected as the BAHD-ATs of interest due to the evidence which supported the gene as a candidate for the elusive poplar pHBMT. In earlier studies of transgenic hybrid poplar trees with lignin devoid of the usual pendant *p*-hydroxybenzoate groups, the expression of this uncharacterized gene was reduced, suggesting that the putative BAHD member may be responsible for catalyzing the reaction forming *p*-hydroxybenzoate monolignol conjugates (Unda, 2012; Unda *et al.*, 2016). In order to test this hypothesis, lignin *p*-hydroxybenzoylation in transgenic Arabidopsis and poplar plants misregulating Pa×gACT-like were quantified. This was accomplished by saponifying extractive-free ground wood samples and subsequently analyzing the extracts using HPLC to quantify the amount of released *p*-hydroxybenzoic acid (pHBA). Assuming that pHBA groups are terminal, free-phenolic pendant groups, decorating only the lignin polymer and not, for example, cell wall polysaccharides, the amount of released pHBA following saponification is considered to be representative of the amount of lignin *p*-hydroxybenzoylation in the original sample. These values are represented as the amount of pHBA released as a function of the weight of the extractive-free ground wood sample used also known as the whole cell wall (WCW) weight (mg g^{-1}WCW).

3.3.1 Natural variations of lignin *p*-hydroxybenzoylation

The saponification protocol was originally developed to analyze wood acetylation and therefore quantify acetyl groups released by saponification (Johnson, 2015). Saponification strips lignin of its pendant *p*-hydroxybenzoate groups by cleaving the ester bonds by which they are attached,

leaving the ether bonds common to the lignin polymer intact, thereby allowing quantification of the released pHBA via HPLC.

In order to test the suitability of this method for the quantification of *p*-hydroxybenzoate groups, it was performed on a series of different species known to have or lack *p*-hydroxybenzoylated lignins, to serve as positive and negative controls. The resulting HPLC chromatograph of the poplar (wild-type hybrid P39 poplar, *Populus balsamifera*, *P. trichocarpa*) and willow (*Salix dasyclados*, *Salix eriocephala*) positive controls, illustrate the method's suitability to detect pHBA, as well as demonstrate the natural variability of lignin *p*-hydroxybenzoylation found in these species (Figure 3.6). The highest level of lignin *p*-hydroxybenzoylation was observed in hybrid P39 poplar, which contains around 1.07-1.65 mg g^{-1}WCW, followed by *P. balsamifera* (0.58-1.05 mg g^{-1}WCW). *P. trichocarpa* has very low levels of pHBA when compared to the other poplars, 0.16 mg g^{-1}WCW, an amount comparable to that found in *S. eriocephala*, whereas *S. dasyclados* has an intermediate level of pHBA of 0.34 mg g^{-1}WCW.

As expected, both wild-type Arabidopsis and Eucalyptus, which served as negative controls, showed no detectable amounts of pHBA (Figure 3.6), indicating that this method is suitable for specific identification of pHBA. Results from the hybrid poplar AtGolS3 transgenics, used to identified Pa×gACT-like as a candidate in *p*-hydroxybenzoylation, surprisingly showed low levels of pHBA release at 0.16 mg g^{-1}WCW, though much lower than wild-type P39, even though the original NMR analysis did not detect any lignin *p*-hydroxybenzoylation.

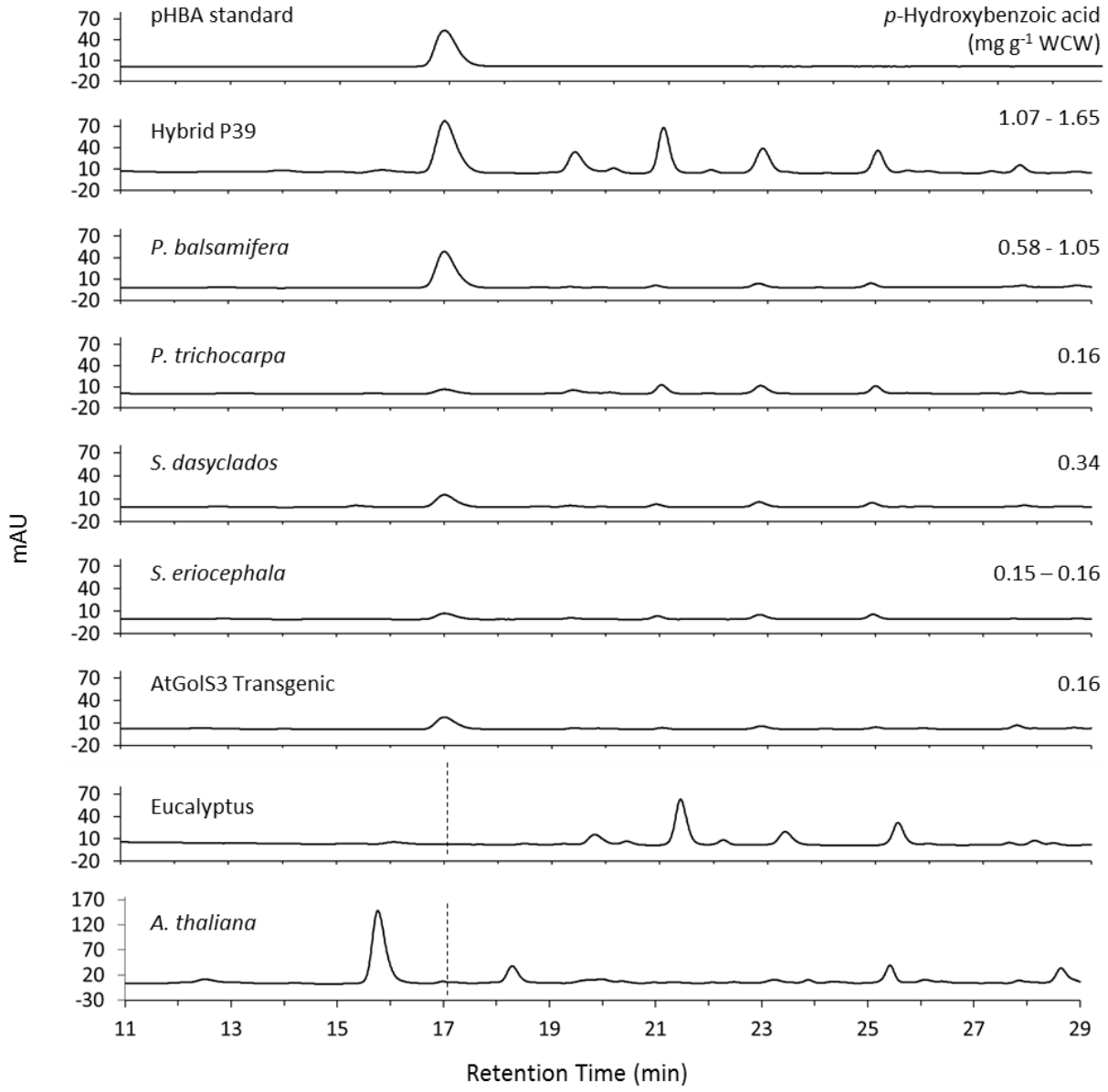

Figure 3.6. HPLC traces quantifying *p*-hydroxybenzoic acid (pHBA) release from saponified xylem tissue. Levels of pHBA released on right hand side are averages of two technical replicates expressed as released pHBA (mg) per extractive free whole cell wall (WCW) weight (g). The values indicate the range of pHBA levels released between two biological replicates.

3.3.2 Quantification of lignin *p*-hydroxybenzoylation in transgenic plants

Arabidopsis lignin is not *p*-hydroxybenzoylated and consequently it is unlikely a pHBMT is naturally present. To test Pa×gACT-like's role as a pHBMT, it was introduced into Arabidopsis

under the control of the constitutive 35S promoter to see if this would induce lignin *p*-hydroxybenzoylation. The reverse was done in hybrid poplar, which naturally possesses *p*-hydroxybenzoylated lignin. Here, Pa×gACT-like was suppressed to test if this resulted in the reduction or loss of lignin *p*-hydroxybenzoylation. To this end, ground extractive-free tissues of transgenic Arabidopsis and poplar were saponified alongside the appropriate wild-type tissues after which the released pHBA was quantified by HPLC.

Interestingly, there seems to be no difference in lignin *p*-hydroxybenzoylation between wild-type and transgenic plants. As seen from the HPLC chromatographs for the Arabidopsis samples, there is no detectable pHBA released from saponification of transgenic Arabidopsis plants (Figure 3.7). Levels of pHBA from transgenic RNAi-poplar lines were also not significantly different than in wild type (Figure 3.8). Clearly, neither the down-regulation of Pa×gACT-like in poplar, nor its heterologous expression in Arabidopsis was sufficient to elicit a change in lignin *p*-hydroxybenzoylation, and therefore these results do not support Pa×gACT-like as a pHBMT.

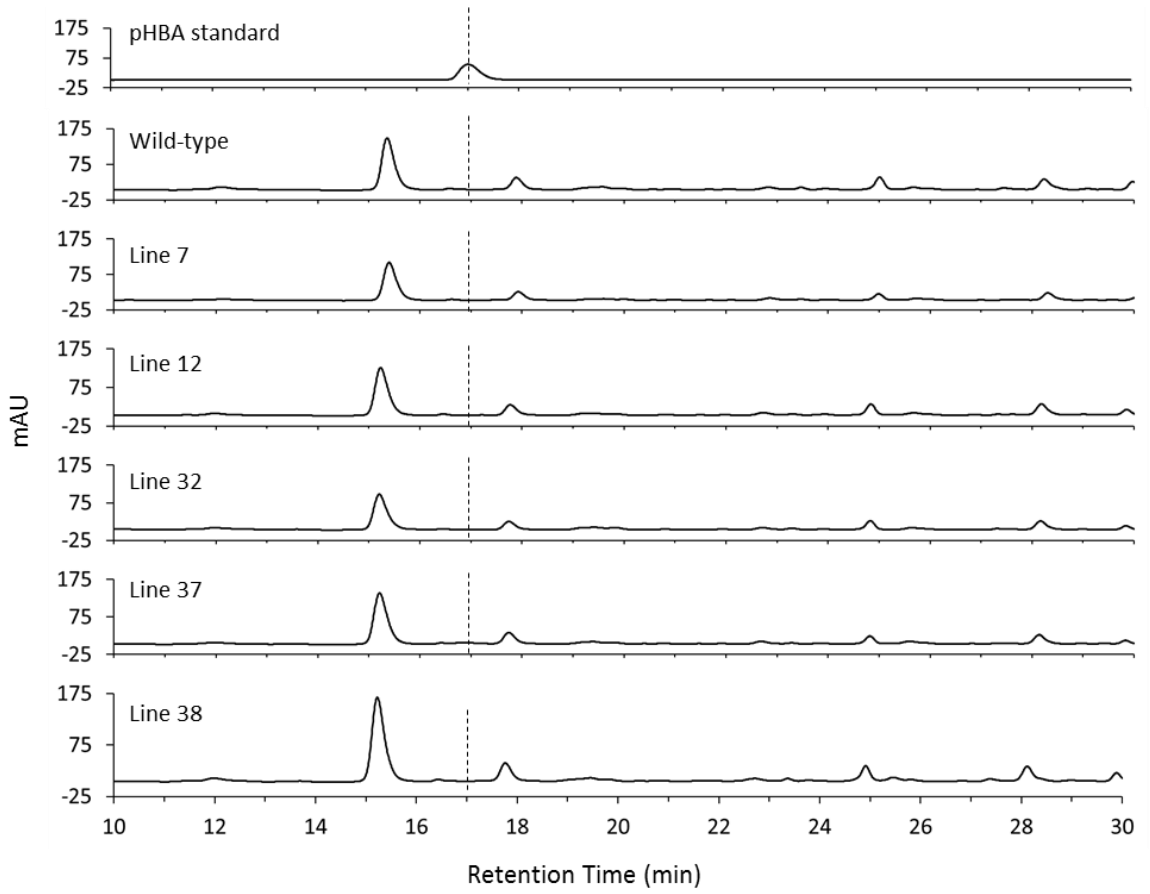

Figure 3.7. HPLC traces of saponified stem tissues of Arabidopsis *35S::Pa×gACT-like* lines.

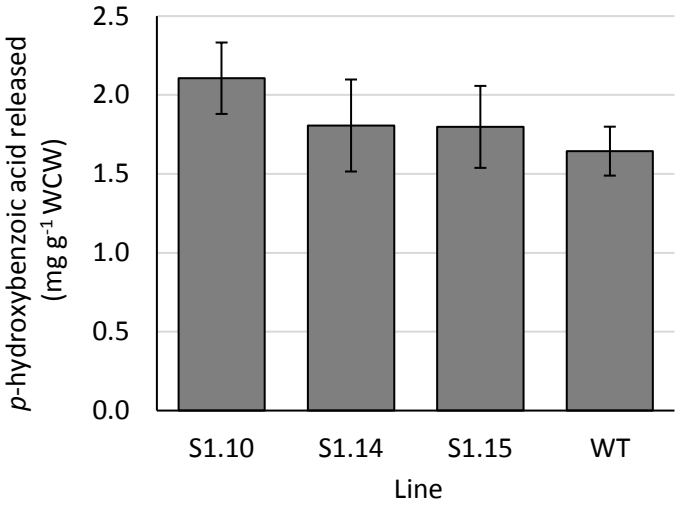

Figure 3.8. Levels of pHBA released by saponification of extractive free whole cell wall tissues from *Pa×gACT-like-RNAi* S1 lines expressed as released pHBA (mg) per extractive free whole cell wall (WCW) weight (g). Error bars represent mean standard error. (n=3).

3.4 *Pa×gACT-like Prom::GUS* visualization

To understand where the *Pa×gACT-like* is expressed, promoter activity was investigated using transgenics expressing *Pa×gACT-like* promoter fused to the *β-Glucuronidase* (GUS) reporter gene. These results could aid in ascertaining whether Pa×gACT-like is a pHBMT or CER2-LIKE, since lignin and wax related genes generally have different expression patterns-both spatially and temporally. Wax genes are commonly expressed in the epidermis, while lignin genes are expressed in xylem and sclerenchyma tissues. Several PCR positive *Pa×gACT-like Prom::GUS* lines were generated using *Agrobacterium*-mediated transformation of P39, and lines 2, 3 and 19 were randomly selected to be grown in the greenhouse. Subsequent histochemical analysis of cross-sections of young and mature leaf blades, petiole, stem and root transgenic tissues was performed by histochemical GUS staining. Wild-type cross-sections stained with toluidine blue were used to aid in cell type identification (Figure 3.11).

Strong GUS staining was consistently observed in the epidermal layer of all transgenic leaf and petiole tissues (Figure 3.9). Young stem tissues also showed epidermal GUS activity, but in cross-sections of mature stem tissue, where the epidermis has been replaced with the periderm, staining is very faint, or completely absent (Figure 3.10 B, C vs E, F). Root staining was seen only in line 2, where in young root cross-sections GUS staining was observed in the pericycle (Figure 3.10 I), and in mature root cross-sections it was observed in the parenchymous xylem rays, and diffusely in the phloem (Figure 3.10, L, Appendix Figure B.1 B). GUS staining was also observed around emerging lateral roots (Appendix Figure B.1 E).

In line 3 leaf, petiole, and young stem tissues, staining was restricted mainly to the epidermal layer, with very faint staining of the underlying parenchymous cortex cells (Figure 3.11 B). For line 2, in addition to the strong GUS staining of epidermal cells, there was similar more wide-spread staining pattern throughout leaf, petiole, and stem, which was stronger in younger tissues (Figure 9, 10). Using a higher magnification, it became clear that this staining pattern seemed to be limited to living cell types including phloem, pith, and cortex cells, parenchymous cells of interfascicular regions, and xylem/phloem ray cells, whilst lignifying cells such as xylem and phloem-fibre cells remained unstained (Figure 3.11, Appendix Figure B.2). Results of histochemical analysis of *Pa×gACT-like Prom::GUS* line 19 show a similar expression pattern to that described for line 2, at more intermediate levels in all tissues (Appendix Figure B.3).

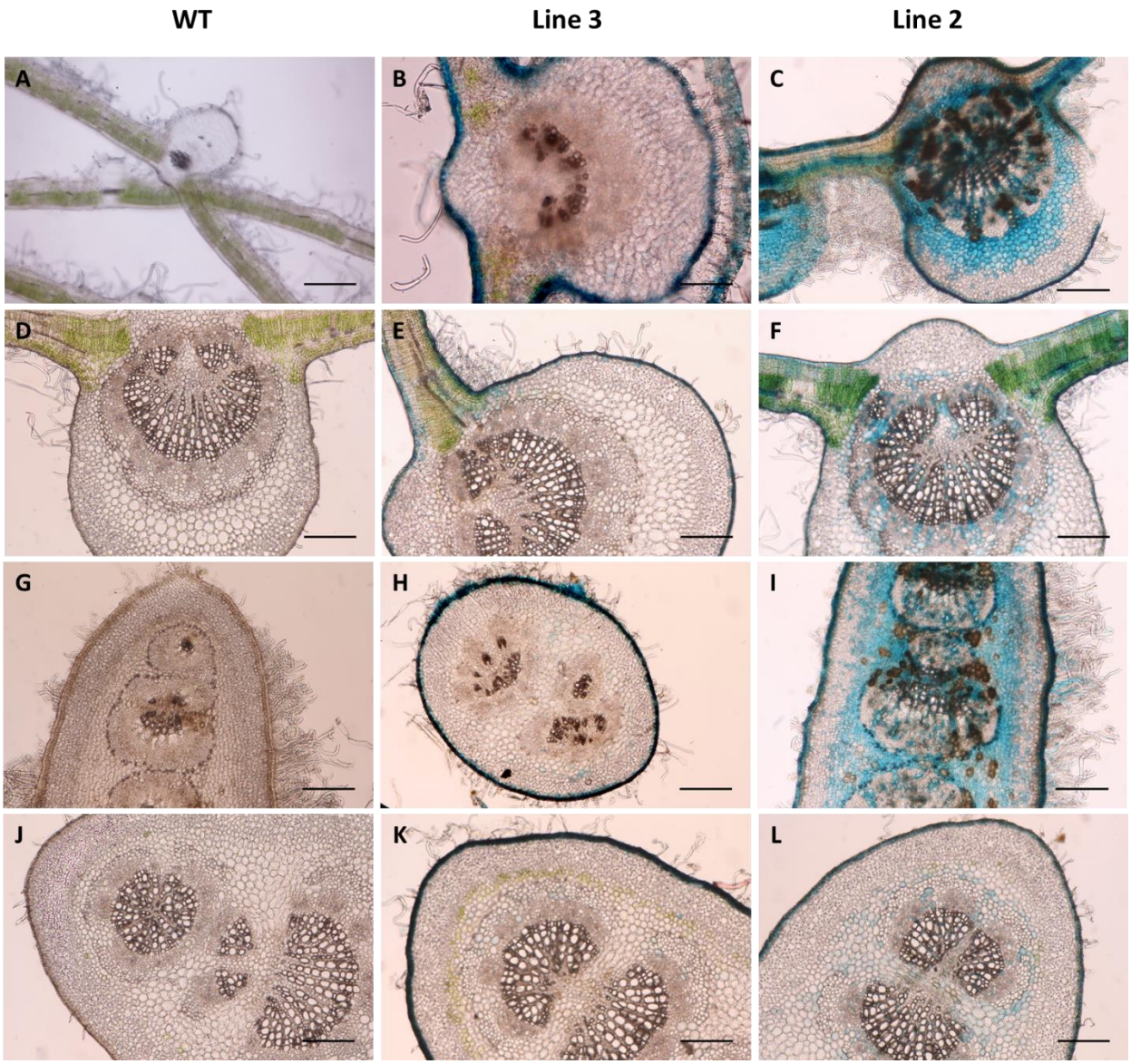

Figure 3.9. β-Glucuronidase (GUS) staining of *Pa×gACT-like Prom::GUS* transgenic hybrid poplar leaf and petiole cross-sections. Comparing expression patterns in wild-type control (A,D,G,J), *Pa×gACT-like Prom::GUS* line 3 (B,E,H,K) and *Pa×gACT-like Prom::GUS* line 2 (C,F,I,L) tissues. Cross-sections of young leaf (A-C), mature leaf (D-F), young petiole (G-I), and mature petiole (J-L) tissue. Scale bar: 200 µm except in (B, C) where scale bar: 100 µm.

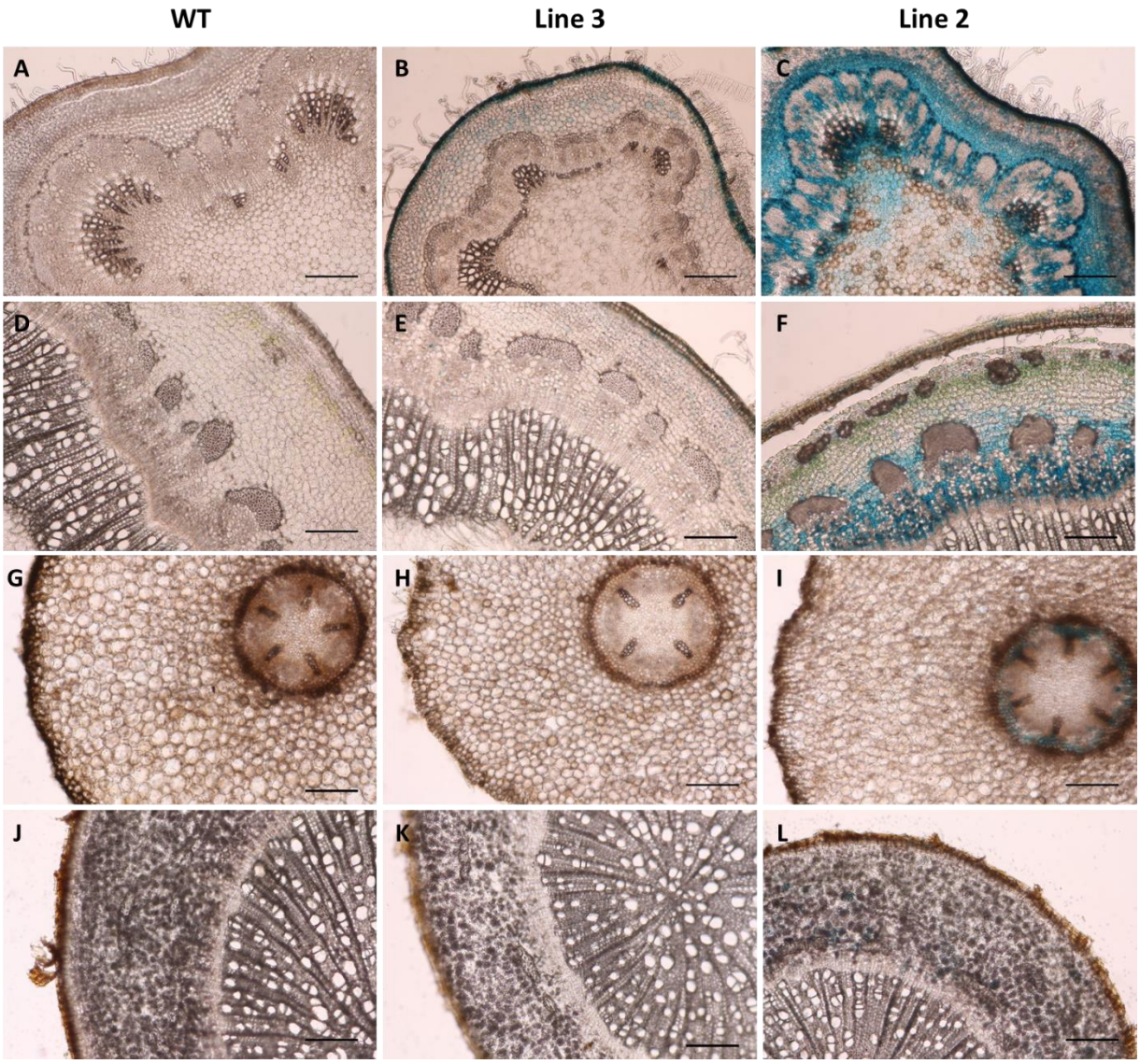

Figure 3.10. β-Glucuronidase (GUS) staining of of *Pa×gACT-like Prom::GUS* transgenic hybrid poplar stem and root cross-sections. Comparing expression patterns in wild-type control (A,D,G,J), *Pa×gACT-like Prom::GUS* line 3 (B,E,H,K) and *Pa×gACT-like Prom::GUS* line 2 (C,F,I,L) tissues. Cross-sections of young stem (A-C), mature stem (D-F), young root (G-I), and mature root (J-L) tissue. Scale bar: 200 µm.

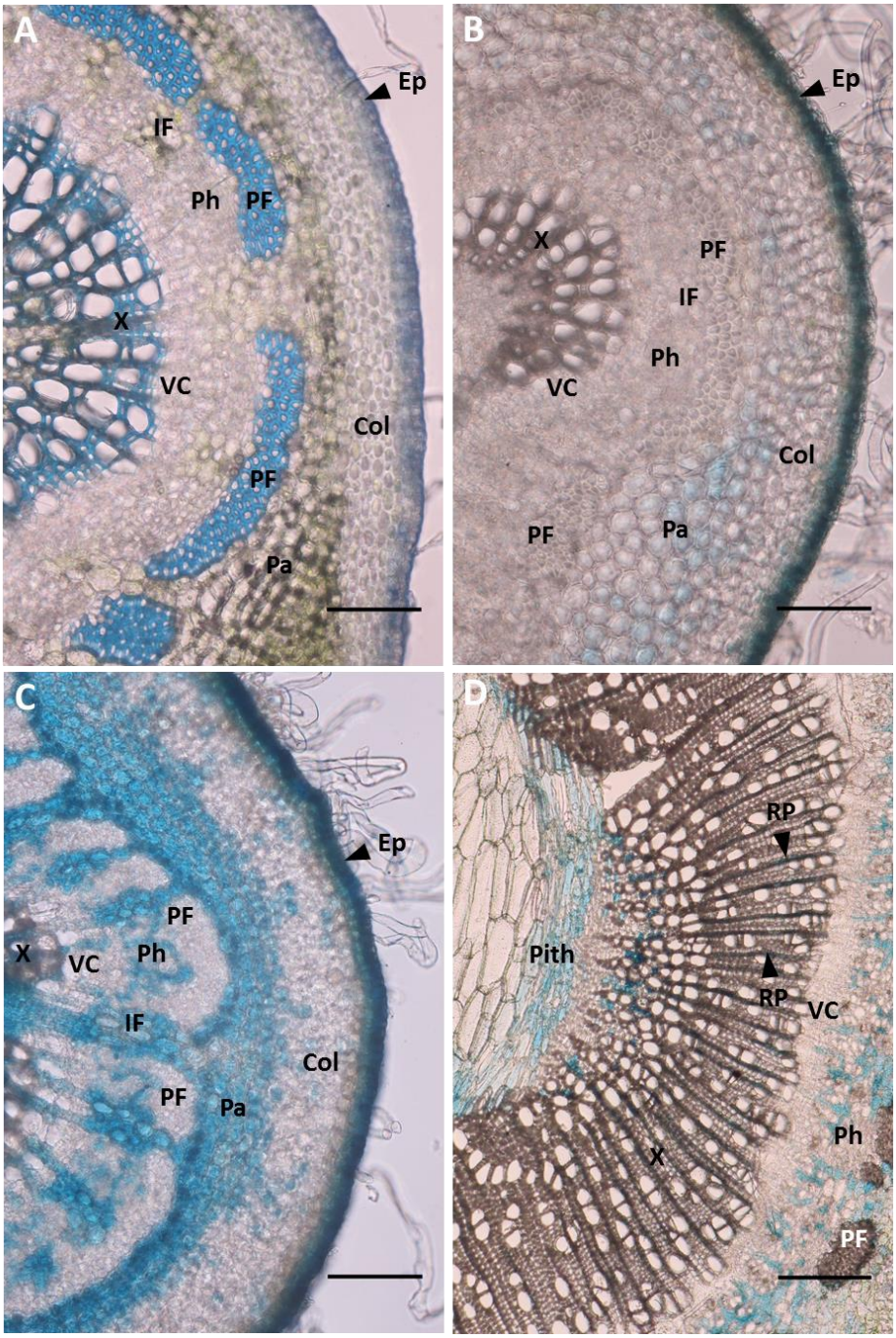

Figure 3.11. Histochemical localization of GUS activity in of *Pa×gACT-like Prom::GUS* transgenic hybrid poplar stem tissues. (A) Wild-type poplar stem cross-section stained with 0.05% Toluidine Blue. (B) *Pa×gACT-like Prom::GUS* line 3 young stem tissue. (C) *Pa×gACT-like Prom::GUS* line 2 young stem tissue. (D) *Pa×gACT-like Prom::GUS* line 2 mature stem tissue. Ep = Epidermis, Col = Collenchyma, Pa = Parenchyma, PF = Phloem Fibre, IF = Interfascicular region, Ph = Phloem, VC = Vascular cambium, X = Xylem, RP = Ray Parenchyma. Scale bar: 100 µm except for (D) where scale bar: 200 µm.

3.5 Pa×gACT-like as a poplar CER2-LIKE

Although originally selected as a putative BAHD-AT involved in generating the *p*-hydroxybenzoate conjugate that could participate in lignification, substantial evidence supports an alternative putative function for *Pa×gACT-like* in VLCFA elongation as a poplar CER2-LIKE. In order to test this alternate hypothesis, two different approaches were taken. One approach was to use heterologous gene expression of *Pa×gACT-like* in yeast, while the other was to analyze the wax profile of the transgenic Arabidopsis *Pa×gACT-like* over-expression plants, as well as the hybrid poplar RNAi suppression lines as compared to the appropriate wild-type controls.

3.5.1 Expression of Pa×gACT-like in yeast with CER6 KCS

The further elongation of VLCFAs past C_{28} in length, requires the interaction of the KCS of the fatty acid elongase complex with AtCER2 or a CER2-LIKE (Haslam *et al.*, 2012). In order to establish whether Pa×gACT-like could work with a KCS to elongate yeast fatty acids, the gene was expressed in yeast strain w3031a alongside the KCS AtCER6, and the resulting fatty acid profile was assessed by fatty acid methyl ester (FAME) analysis. This was achieved by transmethylating yeast cultures to their fatty acid methyl esters after which the lipids were extracted and analyzed by GC-FID. As a positive control, the previously characterized AtCER2, which is known to modify the activity of AtCER6, was included. The FAME analysis results showing the fatty acid products of different chain lengths (C_{26}, C_{28}, and C_{30}) as percentages of total yeast VLC-FAMEs are shown in Figure 3.12.

As previously reported (Haslam *et al.*, 2012, 2015), wild-type w3031a yeast produces C_{26} and low levels of C_{28} FAs, but with the addition of AtCER6 elongation of C_{26} to C_{28} occurs resulting in increased C_{28} concentrations. When AtCER2 is expressed on its own, there is no change in elongation relative to wild-type but, when both AtCER6 and AtCER2 are expressed together, elongation to C_{30} FAs results. Interestingly, FAME analysis revealed a similar result when expressing *Pa×gACT-like*. When expressed on its own, there was no elongation past C_{28}, but when expressed alongside AtCER6, C_{30} fatty acids were detected. When compared to AtCER6 co-expressed with AtCER2, expressing Pa×gACT-like with AtCER6 results in higher levels of C_{28} (1.16% vs 0.46% FAMEs), and lower levels of C_{30} (0.42% vs 0.75%). These results strongly support the function of Pa×gACT-like as a CER2-LIKE.

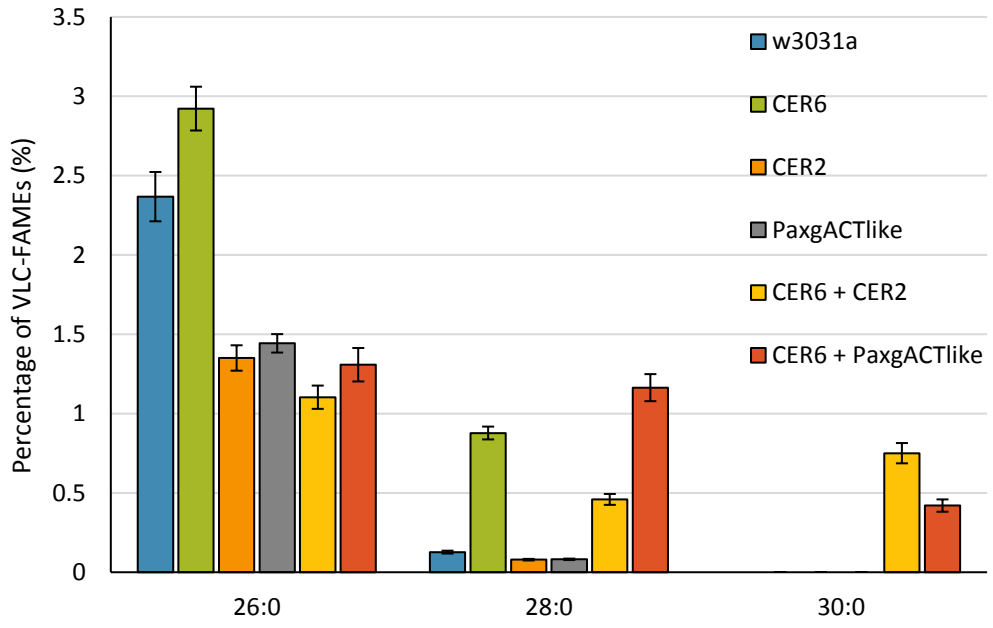

Figure 3.12. VLC-FAME profiles resulting from heterologous expression of *Pa×gACT-like* and *AtCER2-LIKE* alongside *AtCER6* in yeast strain w3031a. Bars represent the mean relative abundance as a percentage of VLCF-FAMEs. Error bars represent mean standard error. (n=4-8)

3.5.2 Wax profile analysis via GC-FID

The wax profile of the transgenic plants generated to misregulate *Pa×gACT-like* were analyzed to assess if the altered gene expression would result in changes in the chain length distribution of the individual compound classes that make up the cuticular wax profile. To this end, waxes extracted from Arabidopsis stems and poplar leaves were analyzed by GC-FID, and their relative abundance expressed as a percentage of the total wax load.

3.5.2.1 Testing the role of Pa×gACT-like in Arabidopsis transgenics

If Pa×gACT-like does, in fact, have CER2-LIKE activity, overexpression in Arabidopsis could cause a shift in the chain length distribution of VLCFA precursors that would be reflected in a similar shift in the resulting cuticular wax components. To test this, the two *35S::Pa×gACT-like* lines with the highest transcript abundance (Line 37 and 38) were tested for changes in the cuticular wax profile relative to the wild-type.

The total wax load of the *35S::Pa×gACT-like* Arabidopsis stems was not significantly different than that of wild-type stems, at around 16 µg/cm^2 (Appendix Table C.1). Arabidopsis stem waxes were predominantly made up of compounds derived from VLCFA precursors of 30 carbons in length (C_{30}), the three compounds with highest abundance being C_{29} alkane (47%), C_{29} ketone (24%) and C_{29} secondary alcohol (14%) (Figure 3.13). The other stem components analyzed included the homologous series of alcohols (C_{26}-C_{30}), aldehydes (C_{28}-C_{30}), and the C_{31} alkane (Figure 3.13). The changes in wax profile relative to wild-type were all relatively subtle. Significant increases were seen in C_{28} alcohol from 4.35 ± 0.15% in WT to 5.11 ± 0.14% and 4.97 ± 0.14%, in lines 37 and 38, respectively; as well as in C_{28} aldehyde with an increase from

1.02 ± 0.08% to 1.20 ± 0.03% in line 38 (Figure 3.13). For an overview of the changes in chain length distribution, the relative abundance values of the wax components were pooled by the chain length of their precursors. As all odd numbered compounds are derived from even numbered VLCFAs through the alkane biosynthetic pathway, they were placed in the group with the chain length plus one carbon. This analysis reveals a significant increase in C_{28}-derived components in both line 37 (6.26 ± 0.16%) and line 38 (6.17 ± 0.15%), relative to wild-type (5.37 ± 0.20%), and a significant decrease in C_{30}-derived components in both line 37 (88.66 ± 0.20%) and line 38 (88.89 ± 0.20%), relative to wild-type (89.70 ± 0.26%) (Figure 3.14). As suggested by these results, the heterologous over-expression of Pa×gACT-like in Arabidopsis influences the stem wax profile, causing a shift in chain length distribution with increased accumulation of C_{28}-derived compounds, and reduction in C_{30}-derived compounds.

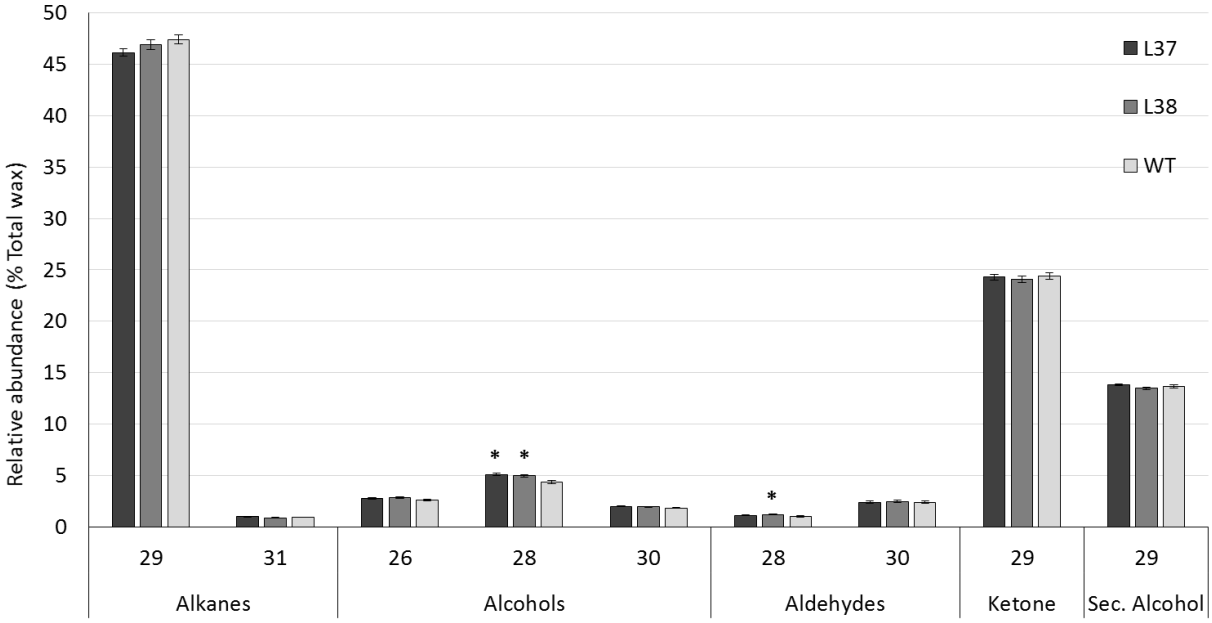

Figure 3.13. Wax profile of *35S::Pa×gACT-like* Arabidopsis stem tissue relative to wild-type. Relative abundance values expressed as the percentage of the total wax, separated by individual chemical compound class where numbers represent chain length. Asterisks represent a significant difference from wild-type at $p < 0.05$. Error bars represent mean standard error. (n = 22-32)

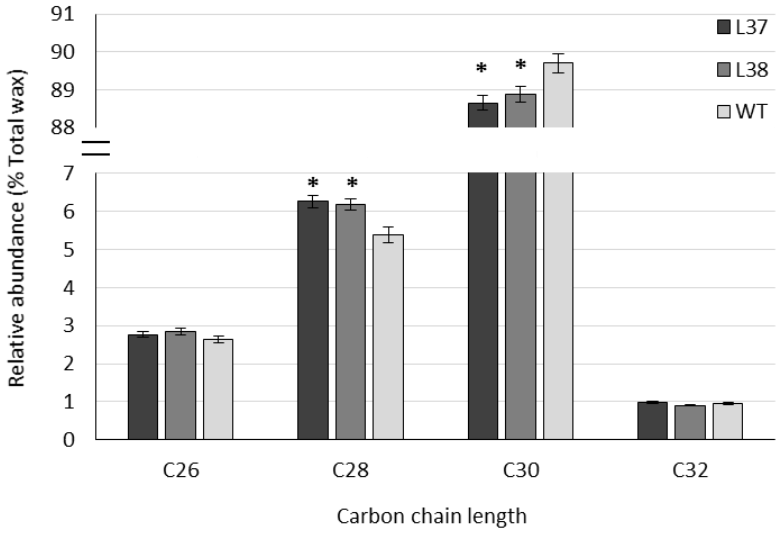

Figure 3.14. Carbon chain length distribution of cuticular wax compounds from *35S::Pa×gACT-like* Arabidopsis stem tissue**.** All wax components relative abundance pooled by chain length of precursors, where odd numbered compounds such as alkanes are derived from even numbered VLCFAs with an added carbon. Asterisks represent a significant difference from wild-type at $p < 0.05$. Error bars represent mean standard error. n=22-32.

3.5.2.2 Testing the role of Pa×gACT-like in poplar transgenics

To examine the role of Pa×gACT-like an assessment of the cuticular wax profile of *Pa×gACT-like-RNAi S1* lines was performed to test if the suppression of this putative CER2-LIKE gene would alter the leaf wax profile relative to wild-type P39. If Pa×gACT-like has CER2-LIKE activity, knocking-down the production of this enzyme could inhibit further elongation of VLCFAs via the FAE complex past a certain chain length, possibly causing an accumulation of shorter VLCFA-derived wax components, and a reduction in longer VLCFAs.

Although not much work has been done on cuticular waxes of poplar, a recent study screening natural accessions of *P. trichocarpa* (Gonzales-Vigil, manuscript in preparation) clearly shows that leaf ontogeny has a very strong influence on the cuticular wax profile with cuticular wax

profiles of same age leaves from different *P. trichocarpa* accessions being more similar than younger and older leaves from the same tree. Therefore, wax profile comparisons should be made only between same aged poplar leaves. Transcriptome data from a developmental series of *P. trichocarpa* leaves was used to select leaf stages with the highest expression of *Pa×gACT-like* to optimize phenotyping. Assuming similar expression patterns between P39 and *P. trichocarpa* leaves, *Pa×gACT-like* has the highest expression in leaf PI-4 making it a suitable choice for analysis (Table 3.3). The other putative poplar CER2-LIKEs are also expressed in PI-4 leaves, Potri.005G153600 being the most highly expressed, and Potri.001G319200 having lower expression than *Pa×gACT-like* (Table 3.3). Additionally, leaves of PI-5 and 7 were also analyzed to test if the differences were maintained in older leaves.

Table 3.3. Expression levels of *Pa×gACT-like* and Poplar clade II BAHD-ATs in a developmental series of leaf tissue from *P. trichocarpa* accession HALS30_0. Expression data based on transcriptome sequencing data from and expressed in FPKM. Potri.018G032700 is not included, as it is not expressed in leaves.

Gene ID	Leaf PI-1	Leaf PI-2	Leaf PI-3	Leaf PI-4	Leaf PI-5
Potri.005G052200 (PaxgACTlike)	10.602	23.825	26.987	29.114	25.845
Potri.013G039700	0.205	0.242	0.316	0.172	0.201
Potri.013G039900	0.307	0.208	0.274	0.059	0.029
Potri.001G319200	0.603	0.661	1.269	2.755	1.171
Potri.005G153600	16.013	34.969	39.631	42.389	51.322

Gonzales-Vigil *et al.* found that the total wax load also varied with leaf ontogeny in *P. trichocarpa* (manuscript in preparation). This held true in P39, where total leaf wax load decreased significantly with leaf age from 9.39 ± 0.36 μg/cm^2 in leaf PI-4, to 7.08 ± 0.3 μg/cm^2

in leaf PI-5, to 6.27 ± 0.12 μg/cm^2 in leaf PI-7 (Figure 3.15 A). Between leaves of the same age, the total wax load from transgenic lines was not significantly different from wild-type (Figure 3.15 B). The P39 leaf cuticular wax components that were identified and analyzed, included the homologous series of alkanes (C_{25}-C_{31}), alcohols (C_{26}-C_{30}), and the C_{28} aldehyde (Figure 3.16). Odd-numbered alkanes make up the largest portion of the cuticular wax profiles of leaves of PI 4, 5, and 7. For P39, C_{27} alkane is the most abundant compound comprising 41-46.5% of the total wax load, depending on leaf age (Figure 3.16, Appendix Table C.4).

Differences in cuticular wax profile between *Pa×gACT-like-RNAi* S1 lines and wild-type were very minor and not consistent across all lines. Very minor changes were detected in leaf PI-5 or PI-7 (Appendix C3, C4), and therefore the focus of the analysis was directed to leaf PI-4, where the gene is most highly expressed. One of the most down-regulated lines (S1.10) showed significant changes in the cuticular wax profile, where the relative abundance of C_{27} alkane was almost 7% higher than wild-type levels, the relative abundance of C_{29} alkane was also increased, while the relative abundance of C_{30} alcohol decreased (Figure 3.16, Table 3.4). Although not many of the shifts in cuticular wax components were significant, overall there seemed to be a general trend for an increase in the abundance of shorter wax components $\leq C_{28}$ and a decrease in the abundance in longer wax components $\geq C_{30}$, with the exception of C_{29} alkane (Figure 3.16, Table 3.4). Similar to the Arabidopsis cuticular wax analysis, an overview of the changes in chain length distribution was gleaned by pooling the relative abundance values of the wax components by the chain length of their precursors. This analysis showed an accumulation in the C_{26} and C_{28}-derived components, where the increase in C_{28}-derived compounds was statistically significant, and no change in C_{30} and C_{32}-derived components (Figure 3.17). These results do not

show a very clear trend, and there is no very strong reduction in any of the naturally occurring wax components, which would be expected by a reduction in the activity of a gene involved in VLCFA elongation like Pa×gACT-like. However, given that the other poplar CER2-LIKEs; Potri.005g153600 and Potri.001g319200 are also expressed in leaves, the lack of a clear phenotype may be due to functional redundancies between members of this clade.

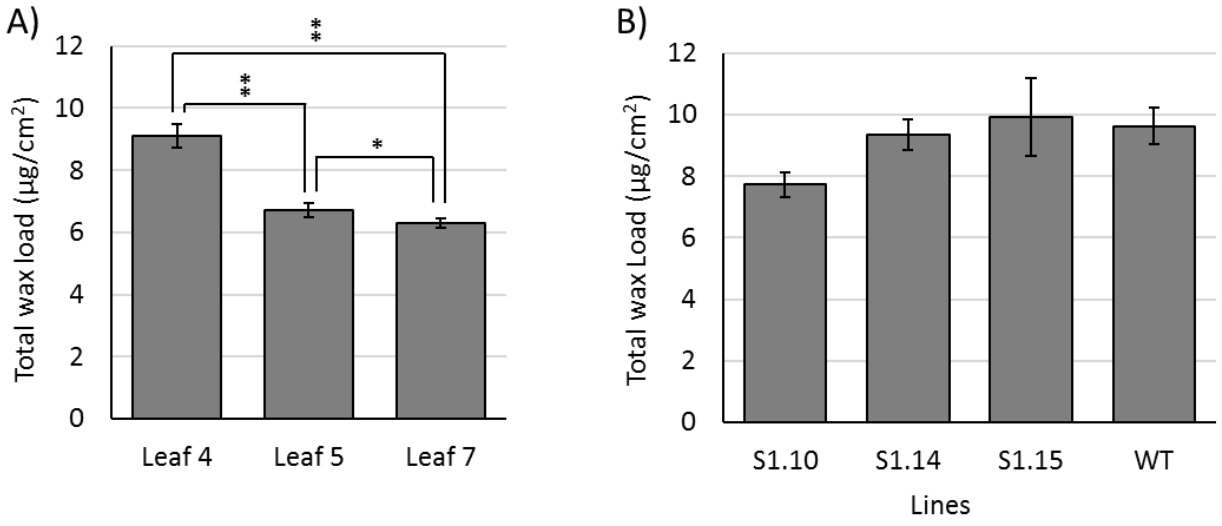

Figure 3.15. Average total cuticular wax load of P39 leaf tissue A) Comparing the total wax load of leaves of varying ages B) Comparing the total wax load of leaf PI-4 between separate transgenic *Pa×gACT-like-RNAi* lines relative to wild-type. Asterisks represents a significant difference from wild-type following a one-way ANOVA and comparison of means by a student t-test where * = $p < 0.05$, ** = $p < 0.0001$. Error bars represent mean standard error. n = 33-77 in A, n = 5-6 in B.

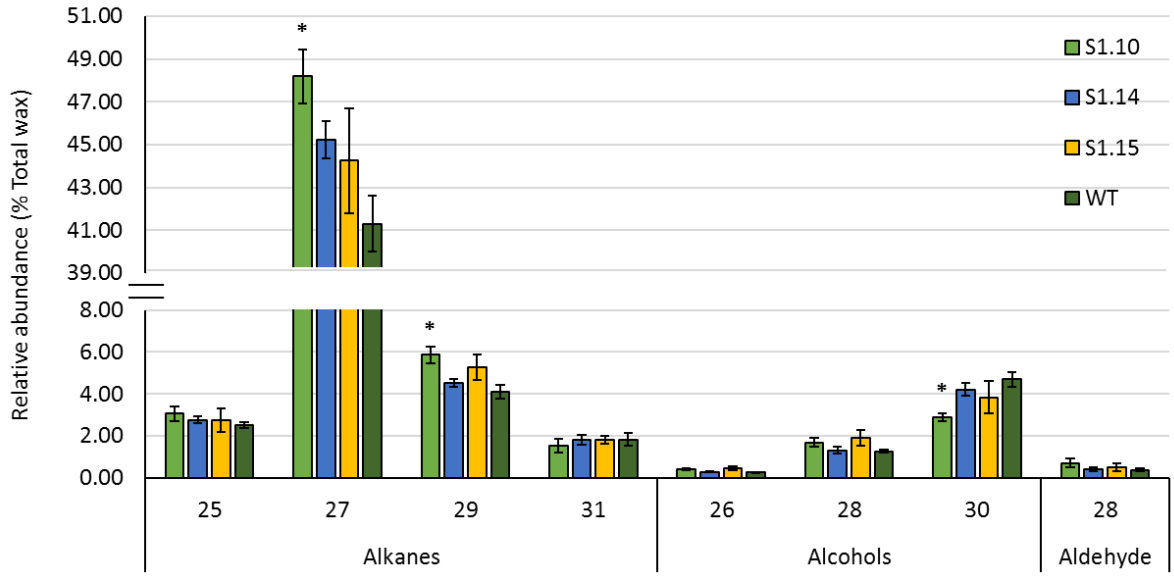

Figure 3.16. Cuticular wax profile of RNAi-poplar leaf (PI-4) tissue relative to wild-type. Relative abundance values are expressed as the percentage of the total wax, separated by individual chemical compound class where numbers represent chain lengths. Asterisks represent a significant difference from wild-type following a one-way ANOVA and comparison of means by a student t-test where $p < 0.05$. Error bars represent mean standard error. (n = 5-6).

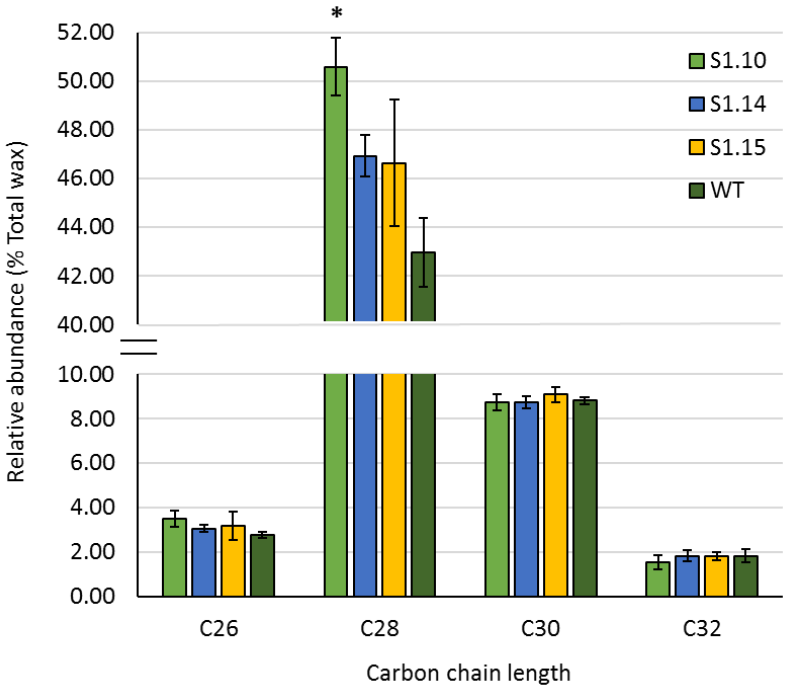

Figure 3.17. Carbon chain length distribution of cuticular wax compounds from RNAi-poplar leaf (PI-4) tissue**.** All wax components relative abundances are pooled by chain length of precursors, where odd numbered compounds such as alkanes are derived from even numbered VLCFAs with an added carbon. Asterisks represent a significant difference from wild-type following a one-way ANOVA and comparison of means by a student t-test where $p < 0.05$. Error bars represent mean standard error. (n = 5-6)

Table 3.4. Wax profile of RNAi poplar leaf (PI-4) tissue relative to wild-type trees. Separated by individual chemical compound class where numbers represent chain length. Values represent the mean relative abundance as a percentage of the total wax load. Standard error of the mean in parenthesis. Bold values indicate a significant difference from wild-type following a one-way ANOVA and comparison of means by a student t-test where $p < 0.05$. (n = 5-6)

Lines	Alkanes				Alcohols			Aldehyde
	25	***27***	***29***	***31***	***26***	***28***	***30***	***28***
S1.10	3.07 (0.35)	**48.20 (1.26)**	**5.86 (0.39)**	1.53 (0.33)	0.42 (0.04)	1.69 (0.20)	**2.89 (0.19)**	0.7 (0.20)
S1.14	2.76 (0.15)	45.21 (0.87)	4.53 (0.19)	1.82 (0.24)	0.29 (0.03)	1.31 (0.15)	4.21 (0.30)	0.41 (0.07)
S1.15	2.73 (0.56)	44.25 (2.46)	5.26 (0.61)	1.80 (0.19)	0.45 (0.10)	1.89 (0.37)	3.83 (0.78)	0.49 (0.19)
WT	2.49 (0.14)	41.31 (1.30)	4.11 (0.32)	1.82 (0.30)	0.27 (0.02)	1.26 (0.06)	4.70 (0.35)	0.38 (0.06)

Table 3.5. Carbon chain length distribution of cuticular wax compounds, and total wax concentrations of RNAi poplar leaf (PI-4) tissue. All wax components relative abundance are pooled by length of VLCFA from which they were derived. Values represent the mean relative abundance as a percentage of the total wax load as a function of area (μg/cm^2). Standard error of the mean in parenthesis. Bold values indicate a significant difference from wild-type following a one-way ANOVA and comparison of means by a student t-test where $p < 0.05$. (n = 5-6)

Line	C26	C28	C30	C32	Total wax
S1.10	3.49 (0.37)	**50.59 (1.19)**	8.75 (0.35)	1.53 (0.33)	7.73 (0.39)
S1.14	3.05 (0.16)	46.93 (0.86)	8.74 (0.26)	1.82 (0.24)	9.35 (0.51)
S1.15	3.18 (0.64)	46.63 (2.60)	9.09 (0.33)	1.80 (0.19)	9.92 (1.27)
WT	2.76 (0.15)	42.96 (1.40)	8.81 (0.16)	1.82 (0.30)	9.63 (0.60)

Chapter 4: Discussion

BAHD acyltransferases have received considerable attention because the members of this large family are integral to the biosynthesis of a variety of biologically important compounds, including phenolics. In poplar, which synthesizes a variety of phenolics, there are more than 100 putative poplar BAHD-ATs, of which only few have recently been characterized (Tuominen *et al.*, 2011).

The primary objective of this work was to investigate the functional role of *Pa×gACT-like*, an uncharacterized poplar BAHD-ATs, which was initially selected as a putative candidate for a monolignol transferase (pHBMT). However, as the research progressed, it became apparent that this gene might be involved in cuticular wax biosynthesis, and carry out a CER2-LIKE function. There has been significant advancements in lignin and cuticular wax research in the last 5 years. In lignin research, the PMTs (homologous to the pHBMT in poplar) of different grass species have been characterized, and differentially/heterologously expressed (Withers *et al.*, 2012; Marita *et al.*, 2014; Petrik *et al.*, 2014; Smith *et al.*, 2015; M. Marita *et al.*, 2016; Sibout *et al.*, 2016). A large portion of the research on CER2-LIKEs has been accomplished in Arabidopsis in this same time frame (Haslam *et al.*, 2012, 2015; Pascal *et al.*, 2013), as well as a seminal study discovering a gene involved in poplar cuticular wax synthesis (Gonzales-Vigil *et al.* manuscript in preparation). Gathering evidence to support *Pa×gACT-like* activity in either pathway would therefore serve to expand our knowledge in either of two very active fields of research. Furthermore, as there has been much debate as to whether the members of clade II are true BAHD-ATs, and most of the research has been done in Arabidopsis. Therefore, the use of a poplar clade II gene member may provide valuable insights to support or refute this claim.

The three main research goals of this thesis were: i) to analyze the gene expression pattern of *Pa×gACT-like* in poplar by mining published *in silico* expression data, and using a *Pa×gACT-like Prom::GUS* construct in poplar to determine the tissue specific localization of protein; ii) to test for a changes in the degree of lignin p-hydroxybenzoylation in *Pa×gACT-like-RNAi* poplar and *35S::Pa×gACT-like* Arabidopsis; and iii) to test for changes in the cuticular wax profile of tissue from the same *Pa×gACT-like-RNAi* poplar and *35S::Pa×gACT-like* Arabidopsis lines.

4.1 Pa×gACT-like is one of five poplar clade II BAHD-ATs

Previous phylogenetic analysis placed *Pa×gACT-like* into the small clade II of the BAHD-ATs alongside four other uncharacterized poplar genes (Potri.013G039700 was removed, as a tandem repeat of Potri.013g039900) (Tuominen *et al.*, 2011). The characterized Arabidopsis genes assigned to this clade are known to function in VLCFA elongation and therefore are important in cuticular wax synthesis. The placement of Pa×gACT-like into this clade, suggests a role in wax instead of lignin synthesis. However, BAHD-ATs function is not always clade specific, and the monolignol transferases characterized thus far do not all group in one clade, therefore a function in lignin biosynthesis cannot be ruled out by phylogenetics alone.

Pa×gACT-like has two very close homologs, which most likely arose from the Salicoid duplication event, as chromosomes V and XIII share homologous regions where these genes are located (Tuskan *et al.*, 2012). From the perspective of Pa×gACT-like as a putative pHBMT, as originally selected, the lack of a close Arabidopsis homolog and the existence of a close willow homolog seem logical, as Arabidopsis lacks *p*-hydroybenzoylated lignin and willow inherently possess these pendant groups. The low similarity of Pa×gACT-like to Arabidopsis clade II

members could also be explained by the character of BAHD-ATs, which are documented as having low protein sequence similarities (D'Auria, 2006). The fact that Pa×gACT-like is missing the second structural motif, DFGWG, which is highly conserved in all characterized monolignol transferases, makes it less likely to be lignin-related. Although the evidence weighs more towards a CER2-like identity for Pa×gACT-like, there are clearly other poplar genes that are more closely related to the characterized Arabidopsis CER2-LIKEs that are strong candidates to function as poplar CER2-LIKEs, such as Potri.005G153600 which is the most similar to AtCER2 and is highly expressed in young leaves (Phytozome v.11).

4.1.1 Pa×gACT-like is co-expressed with cuticular wax genes

For the identification of grass PMTs, researchers used co-expression network analyses to identify putative BAHD-AT genes that were co-regulated along with genes involved in lignin biosynthesis. For example, Withers *et al.* (2012) found that the OsPMT co-expressed with the three rice 4-coumarate:CoA ligase (4CL) genes, as well as other lignin genes including caffeic acid 3-*O*-methyltransferase (COMT), caffeoyl-CoA *O*-methyltransferase (CCoAOMT), and phenylalanine ammonia-lyase (PAL). The BdPMT was also found to be co-expressed with predicted *Brachypodium* lignin biosynthetic genes including PAL, COMT, and cinnamoyl-CoA reductase (CCR) (Petrik *et al.*, 2014).

The results of this study demonstrate that Pa×gACT-like is not co-expressed with any lignin related genes, and therefore does not support for a pHBMT role. Instead, the co-expression data suggests a lipid function, as many of the co-expressed genes are involved in lipid synthesis. Moreover, the most highly co-regulated genes are integral to the cuticular wax biosynthesis

pathway. The top two are annotated as mid-chain alkane hydroxylase 1 (MAH1) (Greer *et al.*, 2007) and ECERIFERUM 1 (CER1) (Bernard *et al.*, 2012), which are part of the alkane-forming pathway in Arabidopsis; and, the third highest co-expressed gene is annotated as ECERIFERUM 4 (CER4) encoding a fatty acyl-coenzyme A reductase (FAR), which is part of the alcohol-forming pathway in the same species (Rowland *et al.*, 2006). These co-expression results clearly support Pa×gACT-like as a CER2-LIKE over that of a pHBMT.

4.2 Mis-regulation of Pa×gACT-like does not affect lignin pHBA levels.

For a long time, scientists have known of the existence of pendent pHBA groups on poplar lignins, but few studies have quantified these, with reported levels of pHBA ranging from 7.5% in *P. maximowiczii* (Nakano *et al.*, 1961) and 10% in *P. tremula* (Smith, 1955) of native lignin weight. This study has added to what little has been described, by reporting additional inherent levels of variation in the quantity of pHBA in lignin of other poplar and willow species, where the highest level of lignin *p*-hydroxybenzoylation was found in the hybrid poplar P39 (1.07-1.65 mg g^{-1}WCW) at levels consistent with the 1.2 mg g^{-1}WCW recently reported by Smith *et al.* (2015).

To test the function of other BAHD-ATs thought to acylate lignins, several studies have manipulated gene expression in native plants and used heterologous expression in plants that do not normally synthesize these specialized functionalities. For example, RNAi-mediated suppression of the endogenous PMT in *Brachypodium* (BdPMT) and in *Zea mays* (p-coumaroyl CoA: hydroxycinnamyl alcohol transferase, pCAT; or ZmPMT) resulted in decreased levels of lignin *p*-coumaroylation, as expected (Marita *et al.*, 2014; Petrik *et al.*, 2014). PMTs have also

been introduced into plants that do not naturally incorporate monolignol-*p*-coumarate conjugates. For example, OsPMT was introduced into Arabidopsis and P39 poplar, which resulted in the incorporation of monolignol-*p*-coumarate conjugates, and therefore *p*-coumaroylated lignin (Smith *et al.*, 2015). Similarly, in another study, the introduction of BdPMTs into Arabidopsis also caused lignin *p*-coumaroylation (Sibout *et al.*, 2016). Assuming the *p*-hydroxybenzoylation of poplar lignins is analogous to *p*-coumarylation of grasses, similar results would be expected with the endogenous suppression and heterologous expression of a poplar pHBMT. To test this hypothesis, Pa×gACT-like gene expression was downregulated in poplar using RNAi-mediated suppression, and Pa×gACT-like was introduced into Arabidopsis. Interestingly, the results of this study show neither the appearance of *p*-hydroxybenzoylated lignin in *35S::Pa×gACT-like* Arabidopsis, nor the reduction in lignin *p*-hydroxybenzoylation in *Pa×gACT-like-RNAi* poplar, therefore again indicating that Pa×gACT-like does not act as a pHBMT.

4.3 Pa×gACT-like is strongly expressed in the epidermis of aerial tissues.

As determined by real-time PCR, as well as through the use of the GUS reporter system, AtCER2, AtCER2LIKE1 (CER26), and AtCER2LIKE2 (CER26-like) generally follow an expression pattern typical of wax-related genes, being expressed in all above ground tissue and reproductive organs, but absent in roots (Pascal *et al.*, 2013). Though similar in this regard, the three genes are differentially expressed in these tissues; AtCER2 and AtCER2-LIKE1 are both highly expressed in leaves, but only AtCER2 is significantly expressed in the inflorescence, while AtCER2-LIKE2 is mainly expressed in flowers (Pascal *et al.*, 2013). Furthermore, GFP (green fluorescent protein) labelling of AtCER2 shows its expression to be confined to epidermal cells of young, expanding stem tissue, developing siliques, young rosette and cauline leaves,

where wax biosynthesis is predominant (Haslam *et al.*, 2012). Similar expression patterns were found for other Arabidopsis FAE complex members, KCS1, KCS6 and KCS20, ECR and KCR using the GUS reporter gene (Joubès *et al.*, 2008). These genes are all expressed strongly in aerial tissues, especially young leaves, with GUS activity decreasing with leaf maturation. In addition, there was also epidermis-specific expression in stems. Unlike the CER2-LIKEs, in most cases GUS expression was also detected in roots, where VLCFA's precursors for suberin are synthesized (Joubès *et al.*, 2008).

The expression pattern of Pa×gACT-like is consistent with that of a typical wax gene, showing strong expression in the epidermis of all aerial parts of the plant, and very little expression in the roots. The expression pattern of line 3 especially, is similar to that of AtCER2, being epidermis-specific, with strong GUS staining in young tissues, and absent in mature stems and roots, supporting the hypothesis that Pa×gACT-like may be a poplar CER2-LIKE. Although GUS expression in lines 2 and 19 was not confined to the epidermis, the overall expression was stronger in younger tissues, with decreasing GUS activity in more mature tissues, a pattern consistent with those observed by Joubès *et al.* (2008). The elevated expression of wax related genes in younger tissues is consistent with the finding that the cuticular wax load of Arabidopsis stems and leaves remains constant during growth, as the high rate of surface expansion is matched with high levels of wax biosynthesis (Suh *et al.*, 2005; Busta *et al.*, 2016).

VLCFAs are not only important components of cuticular waxes, but are also essential precursors of other lipids such as aliphatic suberins found in roots, sphingolipids and phospholipids that are important membrane components, and triacylglycerols which are major lipid storage compounds

in seeds (Samuels *et al.*, 2008; Bach & Faure, 2010). The need for VCLFA biosynthesis for these additional specialized compounds perhaps accounts for the more wide-spread GUS expression of Pa×gACT-like relative to AtCER2-LIKEs. The Arabidopsis KCS (*AtKCS9*) has been shown to be involved in the synthesis of VLCFA precursors of cuticular wax as well as suberins, sphingolipids and phospholipids, and GUS expression revealed it was not only isolated to the epidermal cells (Kim *et al.*, 2013). Expression of wax related genes in the root pericycle, as seen for Pa×gACT-like in line 2, has also been reported in a wax related gene, an ABC transporter required for cuticular lipid secretion (ABCG11/WBC11) (Bird *et al.*, 2007). As there are no other studies reporting on the expression pattern of poplar wax related genes, it is not currently possible to discern and/or compare the nature of the typical expression pattern of poplar wax related genes.

The *in silico* expression data of Pa×gACT-like in P39 corroborates the GUS line 2 expression results, as Pa×gACT-like is expressed in both xylem and leaf tissues. Similarly, the *P. trichocarpa* expression data is consistent with GUS line 3 staining results, in that expression is higher in leaf tissue than in the xylem, and the leaf developmental series shows that expression is much higher in younger leaf tissues. Taken together, all of the expression data supports the functional role of Pa×gACT-like as a poplar CER2-LIKE.

4.4 Pa×gACT-like is necessary for elongation of VLCFAs

4.4.1 Pa×gACT-like shows VLCFA elongation activity with CER6 in yeast

In Arabidopsis, the KCSs of the FAE complex work together with a AtCER2-LIKE, through a yet unknown biochemical mechanism, for the elongation of VLCFAs past an acyl chain length of

C_{28} (Haslam *et al.*, 2012, 2015). As shown by heterologous expression in yeast, AtCER6 can synthesize VLCFAs up to C_{28}, but with the addition of AtCER2, VLCFAs up to C_{30} is possible; while expression of AtCER2 alone in yeast does not result in any VLCFA elongation (Haslam & Kunst, 2013a). Consistent with Pa×gACT-like's role as a poplar CER2-LIKE, very similar findings were observed when introducing Pa×gACT-like alongside AtCER6 in yeast.

Similar experiments have been done with AtCER2-LIKE1 and AtCER2-LIKE2, and it was found that all three characterized AtCER2-LIKEs can work with the same KCSs (AtCER6/AtCER60), but impart different substrate specificities upon these (Haslam *et al.*, 2015). None of the AtCER2-LIKEs have activity on their own, but when expressed with AtCER6, AtCER2-LIKE1 produces C_{28}, C_{30}, C_{32} and C_{34} VLCFAs, and AtCER2-LIKE2 produces C_{28}, C_{30} and traces of C_{32} VLCFAs. When expressed with AtCER6 in yeast, both Pa×gACT-like and AtCER2 elongate up to C_{30}, but synthesized different levels of C_{28} and C_{30}, which could suggest a difference in substrate specificity (Figure 4.1). Although Pa×gACT-like can function biochemically with the Arabidopsis KCS to elongate VLCFAs to C_{30} in yeast, it is unknown whether it would have the same substrate specificity when coupled with its native poplar KCS. Even so, the existence of poplar leaf wax components longer than C_{30} could indicate that other poplar CER2-LIKEs are responsible to partner with poplar KCSs to synthesize even longer VLCFAs.

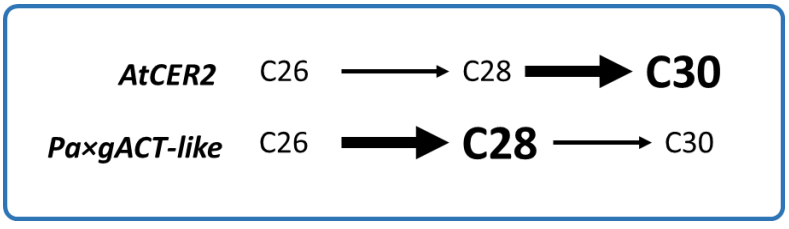

Figure 4.1 Differential substrate specificity of the CER2's; AtCER2 and Pa×gACT-like as seen in yeast assays.

4.4.2 Pa×gACT-like expression in Arabidopsis causes a shift in the chain length distribution of wax components towards shorter VLCFAs.

Research on CER2-LIKEs has predominantly been carried out in Arabidopsis, and this is the first time an exogenous CER2-LIKE gene has been expressed in wild-type Arabidopsis. It could be expected that the introduction of this PaxgACTlike would further drive the synthesis of longer VLCFAs, resulting in a reduction in shorter VLCFAs relative to wild-type levels, as it seems to be able to function biochemically with the predominant Arabidopsis KCS in yeast. However, the shift in cuticular wax component chain length distribution in *35S::Pa×gACT-like* Arabidopsis lines observed was the opposite, showing a significant increase in C_{28} compounds, and a reduction in C_{30} compounds. This phenotype is in some ways similar to, but much less severe than, the Arabidopsis *cer2* mutant phenotype, which, along with a 65% reduction in total wax load, shows a drastic reduction in all stem wax components longer than C_{28}, and an accumulation of wax compounds shorter than C_{28} (Jenks *et al.*, 1995). In the transgenic Arabidopsis created here, however, there was no significant decrease in total wax load of *35S::Pa×gACT-like* plants relative to wild-type plants. Although perhaps counter-intuitive, this phenotype could be explained by one of two mechanisms, or more likely could be the result of the action of both. First, the ubiquitous expression of Pa×gACT-like in Arabidopsis may be causing competition with the native AtCER2 for AtCER6 (AtCER2-LIKE1 and AtCER2-LIKE2 are not expressed highly in stems), and therefore blocking its ability to elongate VLCFAs from C_{28} to C_{30} (Figure 4.2.A). Though Pa×gACT-like is able to function with AtCER6 in yeast, this is an optimized system and Pa×gACT-like may not be functional in Arabidopsis. Second, even if Pa×gACT-like is able to function with AtCER6 in Arabidopsis, heterologous expression in yeast suggests a difference in substrate specificity between AtCER2 and Pa×gACT-like, as described earlier

(Figure 4.1) which may explain the increased C28/C30 ratio. If both mechanisms are acting simultaneously, Pa×gACT-like is outcompeting AtCER2 in the *35S::Pa×gACT-like* plants, causing AtCER6 to partner with Pa×gACT-like more often than with AtCER2, the difference in elongation efficiencies would manifest in an increased C_{28}/C_{30} wax components ratio, relative to wild-type Arabidopsis (Figure 4.2.B).

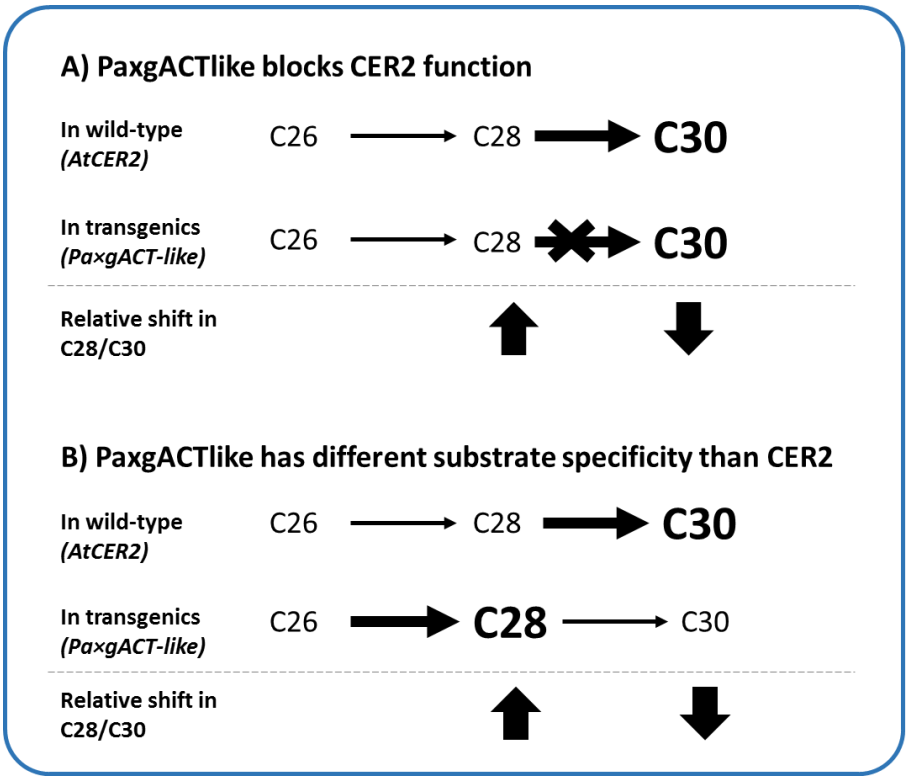

Figure 4.2. Two possible mechanisms affecting the observed shift in stem cuticular wax compound lengths in *35S::Pa×gACT-like* Arabidopsis plants relative to wild type. In A) the poplar CER2-LIKE Pa×gACT-like competes with the native CER2, blocking the ability to elongate VLCFAs past C_{28}, while in B) the poplar CER2-LIKE Pa×gACT-like competes with the native CER2, and functions in VLCFA elongation, but with a different substrate specificity to the native CER2.

4.4.3 Downregulation Pa×gACT-like in poplar causes a subtle wax phenotype, and an accumulation of C_{28} wax components.

The wax phenotypes of *cer2, cer2-like1* and *cer2-like2* Arabidopsis mutants make evident that knocking out CER2-LIKE genes generally results in a reduction in longer VLCFAs and the accumulation of shorter VLCFAs, although the phenotypes are different depending on the particular CER2-LIKEs preferred substrates (Haslam *et al.*, 2015). Similarly, the suppression of Pa×gACT-like in the poplar-RNAi lines causes and accumulation of C_{28} wax components relative to wild-type, reflected by the accumulation of the major wax constituent C_{27} alkane, which is consistent with Pa×gACT-likes functional role as a poplar CER2-LIKE.

Arabidopsis *cer2* mutants have a drastic phenotype in the stem cuticular waxes, interestingly there is no leaf wax phenotype. The reason is likely that, although *CER2* is the only family member expressed in stem tissue, *CER2, CER2-LIKE1* and *CER2-LIKE 2* are all expressed in rosette leaves, and have semi-redundant functions in VLCFA elongation (Haslam *et al.*, 2015). The *P. trichocarpa* leaf developmental series expression data suggests that the situation in poplar leaves may be similar, as other poplar clade II members are expressed in young leaves. The expression of other putative poplar CER2-LIKEs in leaves alongside Pa×gACT-like, in particular Potri.005G153600 which is more highly expressed, and more similar to *AtCER2*, could explain why the suppression of PaxgACT-like alone does not cause a very drastic wax phenotype, given the possibility for functional redundancy in poplar CER2-LIKEs.

In the acyl reduction pathway, the increase in C_{26} and C_{28} alcohols with a significant reduction in C_{30} alcohols suggests a blockage of VLCFA elongation past C_{28}. In the alkane-forming pathway,

the accumulation of C_{27} and C_{29} alkanes would suggest a block of VLCFAs after elongation of VLCFAs to C_{30}. The substrate specificity of PaxgACT-like seen in transgenic yeast, or in Arabidopsis, may not be the same in poplar, as it is working with a yet unknown native KCS. The suppression of Pa×gACT-like does not completely block the synthesis of any particular wax components, and therefore, given that like in Arabidopsis, poplar KCSs require CER2-LIKEs for the further elongation of VLCFAs after a certain length, it is likely that other poplar CER2-LIKEs are required, likely the other clade II BAHD-ATs members.

Chapter 5: Conclusion

5.1 Proposed biological function of Pa×gACT-like

This thesis presents the characterization of Pa×gACT-like, a previously uncharacterized clade II BAHD acyltransferase that was initially thought to have a functional role in lignin biosynthesis. However, the results of this thesis are consistent with Pa×gACT-like acting as a CER2-LIKE, involved in VLCFA elongation for cuticular wax biosynthesis.

In the initial stages of this thesis, it became clear that mis-regulation of *Pa×gACT-like* in Arabidopsis and poplar did not cause a significant difference in the levels of *p*-hydroxybenzoylation of lignin. More specifically, there was no decreased level of lignin *p*-hydroxybenzoylation in *Pa×gACT-like-RNAi* lines relative to wild-type levels, and the expression of Pa×gACT-like in Arabidopsis did not lead to the introduction of non-native *p*-hydroxybenzoate monolignol conjugates. These findings clearly suggested that Pa×gACT-like is not the elusive poplar pHMBT. Moreover, these findings were further supported by co-expression data, which revealed that *Pa×gACT-like* is not co-expressed with any lignin related genes, instead 30% of the genes who share expression patterns highly coordinated with *Pa×gACT-like* are annotated as functioning in lipid biosynthesis/metabolism.

In the second portion of this study, the expression pattern of *Pa×gACT-like* was studied through the use of the GUS reporter gene driven by the *Pa×gACT-like* promoter. Histochemical staining of *Pa×gACT-like Prom::GUS* transgenics clearly showed staining in the epidermis of leaves, petioles, and young stems, the location of active cuticular wax biosynthesis. Expression was stronger in younger tissues, which is consistent with the expression patterns reported for other

wax-related genes, probably due to the fact that younger tissues exhibit higher levels of cuticular wax biosynthesis to maintain an intact cuticle during expansion. In some lines, expression was also seen in other parenchymous cells as well as in the root pericycle, which could indicate that Pa×gACT-like elongates VLCFAs that are used as precursors for non-cuticular lipids. The expression pattern observed is indeed consistent with *in silico* expression data.

Through collaboration with Tegan Haslam and Ljerka Kunst, *Pa×gACT-like* was heterologously expressed in yeast, alongside AtCER6, to test for CER2-LIKE function. These results demonstrate that Pa×gACT-like has similar biological function to AtCER2, and can work with a KCS in the elongation complex to elongate VLCFAs past C_{28}. To further test the hypothesis that Pa×gACT-like is a poplar CER2-LIKE, the cuticular wax profile of the *35S::Pa×gACT-like* Arabidopsis lines, and the *Pa×gACT-like-RNAi* poplar lines were analyzed to see if the mis-regulation of the gene would manifest in a shift in the cuticular wax component chain length distribution relative to wild-type plants. In Arabidopsis *35S::Pa×gACT-like* lines, a shift towards an accumulation of C_{28} derived wax components was observed, as well as a reduction in C_{30} derived components. This could be explained by competition of the ubiquitously expressed Pa×gACT-like with the native AtCER2 for partnering with AtCER6, which may cause a block in VLCFA elongation. Or perhaps Pa×gACT-like outcompeting AtCER2 for AtCER6 caused the observed shift in the cuticular wax component chain length due to slight differences in substrate specificity compared to AtCER2. The suppression of Pa×gACT-like in poplar resulted in a more subtle phenotype, showing a trend for the accumulation of C_{28} wax components, suggesting an upstream block in VLCFA elongation. The subtle phenotype of the RNAi-poplar suggests that other CER2-LIKEs might be present in leaves and function redundantly. The other members of

the clade II BAHD-ATs, in particular Potri.005G153600 and Potri.001g319200, which are more closely related to AtCER2 and are also expressed in leaf tissue, and therefore are strong candidates to interact with the poplar KCS in the elongation complex. Functional redundancy between Arabidopsis CER2-LIKEs has been reported, and it is likely that this is also the case with poplar CER2-LIKEs. While the knock-down phenotypes are complex to interpret, overall, the characterization of Pa×gACT-like is consistent with its role as a partner to KCSs, and therefore an accessory of the fatty acid elongation complex, based on the co-expression data, heterologous yeast expression data, and *35S::Pa×gACT-like* Arabidopsis cuticular wax data, presented here.

5.2 Relevance

Much of what we currently know about cuticular waxes comes from studies done in Arabidopsis, Barley and Maize. This study expands the field into another model system, poplar, an ecologically and economically importance species. In all species, it is still unknown how exactly CER2-LIKEs work with KCSs to elongate VLCFAs, and future research will focus on understanding the biochemical mechanisms of these enzymes. However, this study confirms that other clade II members of the BAHD-AT family have a similar function to those in Arabidopsis, and supports the dogma that this clade does not have acyltransferase activity.

This is also, to the best of our knowledge, the first paper describing the cuticular waxes of poplar, and one of only two studies examining the genetics behind cuticular wax formation in *Populus*. The cuticle is the interface at which the plant interacts with its environment, and it plays essential role in plant-pathogen and water relations. Alterations in the wax components

chain length distribution can have an effects on the physical properties of the cuticle (Haslam *et al.*, 2015). Differences in the composition of cuticular waxes, such as the alkene rich *P. trichocarpa* accessions described by Gonzales Vigil *et al.* (manuscript in preparation), can affect the plants ability to deal with pathogens or limited water resources, thereby directly affecting their fitness. Ergo, having a better understanding of the genetic underpinnings of cuticular wax biosynthesis in poplar could aid in breeding for or engineering these economically important species for better growth and resilience to a changing climate.

5.3 Future Research

This study revealed a wide range and diversity of lignin *p*-hydroxybezoylation in *Populus* species. Consequently, in the future, a comparison of the xylem transcriptomes of disparate poplar individuals (species) could be used to mine for other putative BAHD-ATs candidates that are responsible for this unique biochemical function. Using RNAseq, the transcript abundance of the 100 plus poplar BAHD-ATs could be assessed simultaneously. To identify the potential candidate genes, expression levels should be correlating with the abundance of *p*-hydroxybenzoylation. Additionally, one could generate RNAseq data from different tissues to narrow down the initial list of candidate genes. Once a putative pHBMT gene(s) has been identified, its functional role could be tested through mis-regulation *in planta*, as has been described in this study, followed by saponification of extractive free ground wood samples in order to test for a change in the level of lignin *p*-hydroxybenzoylation. Another follow-up experiment that is warranted is to test the functional role of putative pHBMTs by screening their recombinant enzyme activity. In this case, the candidate genes should be expressed in *Escherichia coli* or another suitable expression system, followed by protein purification, and

tested for its ability to use *p*-hydroxybenzoate-CoA and sinapyl alcohol as substrates to produce of *p*-hydroxybenzoate monolignol conjugates.

Based on the results presented in this thesis, it is possible that the wax phenotype observed in the Arabidopsis transgenics was obscured by the presence of native CER2s, or possibly due to the fact that the native CER2s could not work as efficiently while concurrently competing with Pa×gACT-like. To investigate this disparity further and to conclusively demonstrate Pa×gACT-like's role in cuticular wax biosynthesis, one should complement the Arabidopsis *cer2* mutant with Pa×gACT-like. For this, we would introduce Pa×gACT-like driven by the native AtCER2 promoter into an Arabidopsis *cer2* mutant background, to test if the poplar CER2-LIKE would rescue the wax deficient mutant phenotype. These plants should initially be screened visually, as Arabidopsis *cer2* mutants have a glossy stem phenotype due to the reduced wax load, so transgenics with a rescued wax function would have a glaucous wild-type stem. As for the wax profile, one would expect to see complementation of the deficiency in waxes derived from VLCFAs longer than C_{28}, which is characteristic of Arabidopsis *cer2* mutants. Adding a GFP tag to the introduced *AtCER2pro::Pa×gACT-like* construct would also allow for the intracellular localization of the protein, which would be interesting since most BAHD-ATs are cytosolic, and CER2-LIKEs are recruited to the ER through their interactions with KCSs (Pascal *et al.*, 2013).

Additionally, it would be interesting to mutate the catalytic Histidine residue of the characteristic BAHD HxxxD motif in Pa×gACT-like, and introduce the mutant allele for expression in yeast, and subsequent conduct FAME analysis. This would test if the poplar clade II members require the His residue to aid in the elongation of VLCFA, and therefore have the same catalytic

mechanism as other characterized BAHD-ATs, or if they do not require the residue for normal VLCFA elongation function, as is the case for Arabidopsis CER2-LIKEs (Haslam *et al.*, 2012).

Further research should also focus on studying the additional poplar clade II members, in particular Potri.005G153600, which is the closest AtCER2 homolog and has the highest expression in leaf tissue of *P. trichocarpa*. These other poplar CER2-LIKEs could be cloned for use in overexpression, or RNAi suppression in poplar, followed by the wax profile analysis of transgenic lines, using the same methods described in this work. Heterologous expression of these other poplar CER2-LIKEs in yeast alongside AtCER6, should also be used to test their functional role in VLCFA elongation, and study which chain lengths they preferentially elongate. In tandem with this proposed work, putative poplar KCS partners should be identified, and cloned for expression in yeast alongside Pa×gACT-like and the other poplar CER2-LIKEs. This permits the formulation of realistic model for how each CER2-LIKE elongates VLCFAs with native KCSs in poplar during cuticular wax biosynthesis.

References

Bach L, Faure J-D. **2010**. Role of very-long-chain fatty acids in plant development, when chain length does matter. *Comptes Rendus Biologies* **333**: 361–370.

Barros J, Serk H, Granlund I, Pesquet E. **2015**. The cell biology of lignification in higher plants. *Annals of Botany* **115**: 1053–1074.

Bernard A, Domergue F, Pascal S, Jetter R, Renne C, Faure J-D, Haslam RP, Napier J a., Lessire R, Joubes J. **2012**. Reconstitution of Plant Alkane Biosynthesis in Yeast Demonstrates That Arabidopsis ECERIFERUM1 and ECERIFERUM3 Are Core Components of a Very-Long-Chain Alkane Synthesis Complex. *The Plant Cell* **24**: 3106–3118.

Bernard A, Joubès J. **2013**. Arabidopsis cuticular waxes: Advances in synthesis, export and regulation. *Progress in Lipid Research* **52**: 110–129.

Bhuiyan NH, Selvaraj G, Wei Y, King J. **2009**. Role of lignification in plant defense. *Plant Signaling & Behavior* **4**: 158–159.

Bird D, Beisson F, Brigham A, Shin J, Greer S, Jetter R, Kunst L, Wu X, Yephremov A, Samuels L. **2007**. Characterization of Arabidopsis ABCG11/WBC11, an ATP binding cassette (ABC) transporter that is required for cuticular lipid secretion†. *The Plant Journal* **52**: 485–498.

Boerjan W, Ralph J, Baucher M. **2003**. Lignin Biosynthesis. *Annual Review of Plant Biology* **54**: 519–546.

Bontpart T, Cheynier V, Ageorges A, Terrier N. **2015**. BAHD or SCPL acyltransferase? What a dilemma for acylation in the world of plant phenolic compounds. *New Phytologist* **208**: 695–707.

Boyce CK, Zwieniecki MA, Cody GD, Jacobsen C, Wirick S, Knoll AH, Holbrook NM. **2004**. Evolution of xylem lignification and hydrogel transport regulation. *Proceedings of the National Academy of Sciences* **101**: 17555–17558.

Busta L, Hegebarth D, Kroc E, Jetter R. **2016**. Changes in cuticular wax coverage and composition on developing Arabidopsis leaves are influenced by wax biosynthesis gene expression levels and trichome density. *Planta*.

Cameron KD, Teece M a., Bevilacqua E, Smart LB. **2002**. Diversity of cuticular wax among Salix species and Populus species hybrids. *Phytochemistry* **60**: 715–725.

Chedgy RJ, Köllner TG, Constabel CP. **2015**. Functional characterization of two acyltransferases from Populus trichocarpa capable of synthesizing benzyl benzoate and salicyl benzoate, potential intermediates in salicinoid phenolic glycoside biosynthesis. *Phytochemistry* **113**: 149–159.

Chen F, Tobimatsu Y, Havkin-Frenkel D, Dixon RA, Ralph J. **2012**. A polymer of caffeyl alcohol in plant seeds. *Proceedings of the National Academy of Sciences* **109**: 1772–1777.

Cheng AX, Gou JY, Yu XH, Yang H, Fang X, Chen XY, Liu CJ. **2013**. Characterization and ectopic expression of a populus hydroxyacid hydroxycinnamoyltransferase. *Molecular Plant* **6**: 1889–1903.

Curtis MD. **2003**. A Gateway Cloning Vector Set for High-Throughput Functional Analysis of Genes in Planta. *Plant Physiology* **133**: 462–469.

D'Auria JC. **2006**. Acyltransferases in plants: a good time to be BAHD. *Current Opinion in Plant Biology* **9**: 331–340.

Eigenbrode SD, Espelie KE. **1995**. Effects of Plant Epicuticular Lipids on Insect Herbivores. *Annual Review of Entomology* **40**: 171–194.

Fox J, Weisberg S. **2011**. *An R Companion to Applied Regression*. Thousand Oaks, CA: Sage.

Franke R, Hemm MR, Denault JW, Ruegger MO, Humphreys JM, Chapple C. **2002**. Changes in secondary metabolism and deposition of an unusual lignin in the ref8 mutant of Arabidopsis. *Plant Journal* **30**: 47–59.

Goodstein DM, Shu S, Howson R, Neupane R, Hayes RD, Fazo J, Mitros T, Dirks W, Hellsten U, Putnam N, *et al.* 2012. Phytozome: A comparative platform for green plant genomics. *Nucleic Acids Research* **40**: 1178–1186.

Greer S, Wen M, Bird D, Wu X, Samuels L, Kunst L, Jetter R. **2007**. The cytochrome P450 enzyme CYP96A15 is the midchain alkane hydroxylase responsible for formation of secondary alcohols and ketones in stem cuticular wax of Arabidopsis. *Plant physiology* **145**: 653–667.

Hartley RD. **1972**. p-Coumaric and ferulic acid components of cell walls of ryegrass and their relationships with lignin and digestibility. *Journal of the Science of Food and Agriculture* **23**: 1347–1354.

Haslam TM, Haslam R, Thoraval D, Pascal S, Delude C, Domergue F, Fernández AM, Beaudoin F, Napier JA, Kunst L, *et al.* 2015. ECERIFERUM2-LIKE Proteins Have Unique Biochemical and Physiological Functions in Very-Long-Chain Fatty Acid Elongation. *Plant physiology* **167**: 682–92.

Haslam TM, Kunst L. **2013a**. Extending The Story Of Very-Long-Chain Fatty Acid Elongation. *Plant Science* **210**: 93–107.

Haslam T, Kunst L. **2013b**. Wax Analysis of Stem and Rosette Leaves in Arabidopsis thaliana. *Bio-protocol* **3**: e782.

Haslam TM, Mañas-Fernández A, Zhao L, Kunst L. **2012**. Arabidopsis ECERIFERUM2 is a component of the fatty acid elongation machinery required for fatty acid extension to exceptional lengths. *Plant physiology* **160**: 1164–74.

Hefer CA, Mizrachi E, Myburg AA, Douglas CJ, Mansfield SD. **2015**. Comparative interrogation of the developing xylem transcriptomes of two wood-forming species: Populus trichocarpa and Eucalyptus grandis. *New Phytologist* **206**: 1391–1405.

Helliwell CA, Waterhouse PM. **2005**. Constructs and methods for hairpin RNA-mediated gene silencing in plants. *Methods in Enzymology* **392**: 24–35.

Hibino T, Shibata D, Ito T, Tsuchiya D, Higuchi T, Pollet B, Lapierre C. **1994**. Chemical Properties of Lignin from Aralia Cordata. *Phytochemistry* **37**: 445–448.

Hietala T, Laakso S, Rosenqvist H. **1995**. Epicuticular waxes of salix specied in relation to their overwintering survival and biomass productivity. *Phytochemistry* **40**: 23–27.

Hooker TS, Millar A a, Kunst L. **2002**. Significance of the expression of the CER6 condensing enzyme for cuticular wax production in Arabidopsis. *Plant physiology* **129**: 1568–80.

Jefferson RA, Kavanagh TA, Bevan MW. **1987**. GUS fusions: beta-glucuronidase as a sensitive and versatile gene fusion marker in higher plants. *The EMBO journal* **6**: 3901–3907.

Jenks MA, Tuttle HA, Eigenbrode SD, Feldmann KA. **1995**. Leaf Epicuticular Waxes of the Eceriferum Mutants in Arabidopsis. *Plant Physiology* **108**: 369–377.

Jetter R, Kunst L, Samuels AL. **2006**. Composition of Plant Cuticular Waxes. Biology of the Plant Cuticle. Oxford, UK: Blackwell Publishing Ltd, 145–181.

Johnson A. **2015**. The impact of endogenous acetylation on the deconstruction of Populus trichocarpa wood during pretreatment. : Master's thesis.

Joubès J, Raffaele S, Bourdenx B, Garcia C, Laroche-Traineau J, Moreau P, Domergue F, Lessire R. **2008**. The VLCFA elongase gene family in Arabidopsis thaliana: Phylogenetic analysis, 3D modelling and expression profiling. *Plant Molecular Biology* **67**: 547–566.

Karimi M, Inzé D, Depicker A. **2002**. GATEWAY^{TM} vectors for Agrobacterium-mediated plant transformation. *Trends in Plant Science* **7**: 193–195.

Karlen SD, Zhang C, Peck ML, Smith RA, Padmakshan D, Helmich KE, Free HCA, Lee S, Smith BG, Lu F, *et al.* 2016. Monolignol ferulate conjugates are naturally incorporated into plant lignins. *Science Advances* **2**: e1600393.

Kim J, Jung JH, Lee SB, Go YS, Kim HJ, Cahoon R, Markham JE, Cahoon EB, Suh MC. **2013**. Arabidopsis 3-ketoacyl-coenzyme a synthase9 is involved in the synthesis of tetracosanoic acids as precursors of cuticular waxes, suberins, sphingolipids, and phospholipids. *Plant physiology* **162**: 567–80.

Kunst L, Samuels LA. **2003**. Biosynthesis and secretion of plant cuticular wax. *Progress in Lipid Research* **42**: 51–80.

Landuccii L, Deka G, Roy D. **1992**. A 13C NMR study of milled wood lignins from hybrid Salix clones. *Holzforschung* **46**: 505–511.

Lee SB, Suh MC. **2015**. Advances in the understanding of cuticular waxes in Arabidopsis thaliana and crop species. *Plant Cell Reports* **34**: 557–572.

Lenth R V. **2016**. Least-Squares Means: The R Package lsmeans. *Journal of Statistical Software* **69**: 1–33.

Liu CJ. **2012**. Deciphering the enigma of lignification: Precursor transport, oxidation, and the topochemistry of lignin assembly. *Molecular Plant* **5**: 304–317.

Lu F, Karlen SD, Regner M, Kim H, Ralph S a., Sun R-C, Kuroda K, Augustin MA, Mawson R, Sabarez H, *et al.* 2015. Naturally p-Hydroxybenzoylated Lignins in Palms. *BioEnergy Research* **8**: 934–952.

Lu F, Ralph J, Morreel K, Messens E, Boerjan W. **2004**. Preparation and relevance of a cross-coupling product between sinapyl alcohol and sinapyl p-hydroxybenzoate. *Organic & Biomolecular Chemistry* **2**: 2888.

M. Marita J, Rancour D, Hatfield R, Weimer P. **2016**. Impact of Expressing p-Coumaryl Transferase in Medicago sativa L. on Cell Wall Chemistry and Digestibility. *American Journal of Plant Sciences* **7**: 2553–2569.

Maňkovská B, Percy KE, Karnosky DF. **2005**. Impacts of greenhouse gases on epicuticular waxes of Populus tremuloides Michx.: Results from an open-air exposure and a natural O3 gradient. *Environmental Pollution* **137**: 580–586.

Mansfield SD, Kang KY, Chapple C. **2012**. Designed for deconstruction - poplar trees altered in cell wall lignification improve the efficacy of bioethanol production. *New Phytologist* **194**: 91–101.

Marita JM, Hatfield RD, Rancour DM, Frost KE. **2014**. Identification and suppression of the p-coumaroyl CoA:Hydroxycinnamyl alcohol transferase in Zea mays L. *Plant Journal* **78**: 850–864.

Martínez ÁT, Rencoret J, Marques G, Gutiérrez A, Ibarra D, Jiménez-Barbero J, del Río JC. **2008**. Monolignol acylation and lignin structure in some nonwoody plants: A 2D NMR study. *Phytochemistry* **69**: 2831–2843.

McKown AD, Guy RD, Klápště J, Geraldes A, Friedmann M, Cronk QCB, El-Kassaby YA, Mansfield SD, Douglas CJ. **2014**. Geographical and environmental gradients shape phenotypic trait variation and genetic structure in Populus trichocarpa. *New Phytologist* **201**: 1263–1276.

Millar AA, Clemens S, Zachgo S, Giblin EM, Taylor DC, Kunst L. **1999**. CUT1, an Arabidopsis gene required for cuticular wax biosynthesis and pollen fertility, encodes a very-long-chain fatty acid condensing enzyme. *The Plant cell* **11**: 825–38.

Morreel K. **2004**. Profiling of Oligolignols Reveals Monolignol Coupling Conditions in Lignifying Poplar Xylem. *Plant Physiology* **136**: 3537–3549.

Mottiar Y, Vanholme R, Boerjan W, Ralph J, Mansfield SD. **2016**. Designer lignins: harnessing the plasticity of lignification. *Current Opinion in Biotechnology* **37**: 190–200.

Murashige T, Skoog F. **1962**. A Revised Medium for Rapid Growth and Bio Assays with Tobacco Tissue Cultures. *Physiologia Plantarum* **15**: 473–497.

Nakano J, Ishizu A, Migita N. **1961**. Studies on Lignin XXXII Ester Groups of Lignin. *Technical Association of the Pulp and Paper Industry* **44**: 30–32.

Nakayama T, Suzuki H, Nishino T. **2003**. Anthocyanin acyltransferases: Specificities, mechanism, phylogenetics, and applications. *Journal of Molecular Catalysis B: Enzymatic* **23**: 117–132.

Pascal S, Bernard A, Sorel M, Pervent M, Vile D, Haslam RP, Napier JA, Lessire R, Domergue F, Joubes J. **2013**. The Arabidopsis cer26 mutant, like the cer2 mutant, is specifically affected in the very long chain fatty acid elongation process. *Plant Journal* **73**: 733–746.

Petrik DL, Karlen SD, Cass CL, Padmakshan D, Lu F, Liu S, Le Bris P, Antelme S, Santoro N, Wilkerson CG, *et al.* 2014. p -Coumaroyl-CoA:monolignol transferase (PMT) acts specifically in the lignin biosynthetic pathway in Brachypodium distachyon. *The Plant Journal* **77**: 713–726.

Pichersky E, Noel P. J, Dudareva N. **2006**. Biosynthesis of Plant Volatiles; Nature's Diversity and Ingenuity. *American Association for the Advancement of Science* **311**: 808–811.

R Core Team. **2016**. R: A language and environment for statistical computing.

Ralph J. **1996**. Rapid communications. *Journal of Natural Products* **59**: 341–342.

Ralph J. **2010**. Hydroxycinnamates in lignification. *Phytochemistry Reviews* **9**: 65–83.

Ralph J, Hatfield RD, Quideau S, Helm RF, Grabber JH, Jung HG. **1994**. Pathway of p-Coumaric Acid Incorporation into Maize Lignin as Revealed by NMR. *Journal of the American Chemical Society* **116**: 9448–9456.

Ralph J, Lundquist K, Brunow PG, Lu F, Kim H, Schatz P, Marita J, Hatfield R, Ralph S, Christensen J, *et al.* 2004. Lignins: Natural polymer from oxidative coupling of 4-hydroxyphenylpropanoids. *Phytochemistry Review* **3**: 29–60.

Riederer M, Schreiber L. **2001**. Protecting against water loss: analysis of the barrier properties of plant cuticles. *Journal of Experimental Botany* **52**: 2023–2032.

Rowland O, Zheng H, Hepworth SR, Lam P, Jetter R, Kunst L. **2006**. CER4 Encodes an Alcohol-Forming Fatty Acyl-Coenzyme A Reductase Involved in Cuticular Wax Production in Arabidopsis. *Plant Physiology* **142**: 866–877.

Samuels L, Kunst L, Jetter R. **2008**. Sealing plant surfaces: cuticular wax formation by epidermal cells. *Annual review of plant biology* **59**: 683–707.

Schindelin J, Arganda-Carreras I, Frise E, Kaynig V, Longair M, Pietzsch T, Preibisch S, Rueden C, Saalfeld S, Schmid B, *et al.* 2012. Fiji: an open-source platform for biological-image analysis. *Nature Methods* **9**: 676–682.

Schindelin J, Rueden CT, Hiner MC, Eliceiri KW. **2015**. The ImageJ ecosystem: An open platform for biomedical image analysis. *Molecular Reproduction and Development* **82**: 518–529.

Shimada M, Fukuzuka T, Higuchi T. **1971**. Ester Linkages of Para Coumaric Acid in Bamboo and Grass Lignins. *Tappi* **54**: 72.

Sibout R, Le Bris P, Legee F, Cezard L, Renault H, Lapierre C. **2016**. Structural redesigning Arabidopsis lignins into alkali-soluble lignins through the expression of p-coumaroyl-CoA:monolignol transferase (PMT). *Plant Physiology*: pp.01877.2015.

Smirnova A, Leide J, Riederer M. **2013**. Deficiency in a very-long-chain fatty acid β-ketoacyl-coenzyme a synthase of tomato impairs microgametogenesis and causes floral organ fusion. *Plant physiology* **161**: 196–209.

Smith D. **1955**. p-hydroxybenzoate Groups in the Lignin of Aspen (Populus tremula). *Journal of the Chemical Society*: 2347–2351.

Smith RA, Gonzales-Vigil E, Karlen SD, Park J-Y, Lu F, Wilkerson C, Samuels AL, Ralph J, Mansfield SD. **2015**. Engineering monolignol p-coumarate conjugates into Poplar and Arabidopsis lignins. *Plant Physiology* **169**: 2992–3001.

St-Pierre B, De Luca V. **2000**. Evolution of Acyltransferase Genes: Origin and Diversification of the BAHD Superfamily of Acyltransferases Involved in Secondary Metabolism. Evolution of Metabolic Pathways. Oxford Elsevier Science Ltd., 285–315.

Stewart JJ, Akiyama T, Chapple C, Ralph J, Mansfield SD. **2009**. The effects on lignin structure of overexpression of ferulate 5-hydroxylase in hybrid poplar. *Plant physiology* **150**: 621–635.

Suh MC, Samuels AL, Jetter R, Kunst L, Pollard M, Ohlrogge J, Beisson F. **2005**. Cuticular lipid composition, surface structure, and gene expression in Arabidopsis stem epidermis. *Plant physiology* **139**: 1649–65.

Tamura K, Stecher G, Peterson D, Filipski A, Kumar S. **2013**. MEGA6: Molecular evolutionary genetics analysis version 6.0. *Molecular Biology and Evolution* **30**: 2725–2729.

Tuominen LK, Johnson VE, Tsai C-J. **2011**. Differential phylogenetic expansions in BAHD acyltransferases across five angiosperm taxa and evidence of divergent expression among Populus paralogues. *BMC genomics* **12**: 236.

Tuskan GA, DiFazio S, Faivre-Rampant P, Gaudet M, Harfouche A, Jorge V, Labbé JL, Ranjan P, Sabatti M, Slavov G, *et al.* 2012. The obscure events contributing to the evolution of an incipient sex chromosome in Populus: a retrospective working hypothesis. *Tree Genetics & Genomes* **8**: 559–571.

Unda F. **2012**. Evaluating the Role of the Raffinose Family of Oligosaccharides in Hybrid Poplar (Populus alba × grandidentata). : Doctoral dissertation.

Unda F, Kim H, Hefer C, Ralph J, Mansfield SD. **2016**. Altering carbon allocation in hybrid poplar (Populus alba × grandidentata) impacts cell wall growth and development. *Plant Biotechnology Journal* **38**: 42–49.

Unno H, Ichimaida F, Suzuki H, Takahashi S, Tanaka Y, Saito A, Nishino T, Kusunoki M, Nakayama T. **2007**. Structural and Mutational Studies of Anthocyanin Malonyltransferases Establish the Features of BAHD Enzyme Catalysis. *Journal of Biological Chemistry* **282**: 15812–15822.

Vanholme R, Demedts B, Morreel K, Ralph J, Boerjan W. **2010**. Lignin Biosynthesis and Structure. *Plant Physiology* **153**: 895–905.

Vitha S, Beneš K, Phillips JP, Gartland KMA. **1995**. Histochemical GUS Analysis. Agrobacterium Protocols. New Jersey: Humana Press, 185–194.

Wagner A, Tobimatsu Y, Phillips L, Flint H, Geddes B, Lu F, Ralph J. **2015**. Syringyl lignin production in conifers: Proof of concept in a Pine tracheary element system. *Proceedings of the National Academy of Sciences* **112**: 6218–6223.

Wang JP, Naik PP, Chen H-C, Shi R, Lin C-Y, Liu J, Shuford CM, Li Q, Sun Y-H, Tunlaya-Anukit S, *et al.* 2014. Complete Proteomic-Based Enzyme Reaction and Inhibition Kinetics Reveal How Monolignol Biosynthetic Enzyme Families Affect Metabolic Flux and Lignin in Populus trichocarpa. *The Plant Cell* **26**: 894–914.

Weng JK, Mo H, Chapple C. **2010**. Over-expression of F5H in COMT-deficient Arabidopsis leads to enrichment of an unusual lignin and disruption of pollen wall formation. *Plant Journal* **64**: 898–911.

Wilkerson CG, Mansfield SD, Lu F, Withers S, Park J-Y, Karlen SD, Gonzales-Vigil E, Padmakshan D, Unda F, Rencoret J, *et al.* 2014. Monolignol Ferulate Transferase Introduces Chemically Labile Linkages into the Lignin Backbone. *Science* **344**: 90–93.

Winter D, Vinegar B, Nahal H, Ammar R, Wilson G V, Provart NJ. **2007**. An 'Electronic Fluorescent Pictograph' Browser for Exploring and Analyzing Large-Scale Biological Data Sets (I Baxter, Ed.). *PLoS ONE* **2**: e718.

Withers S, Lu F, Kim H, Zhu Y, Ralph J, Wilkerson CG. **2012**. Identification of grass-specific enzyme that acylates monolignols with p-coumarate. *Journal of Biological Chemistry* **287**: 8347–8355.

Xia Y, Nikolau BJ, Schnable PS. **1996**. Cloning and characterization of CER2, an Arabidopsis gene that affects cuticular wax accumulation. *The Plant cell* **8**: 1291–1304.

Xu X, Xiao L, Feng J, Chen N, Chen Y, Song B, Xue K, Shi S, Zhou Y, Jenks MA. **2016**. Cuticle lipids on heteromorphic leaves of Populus euphratica Oliv. growing in riparian habitats differing in available soil moisture. *Physiologia Plantarum* **158**: 318–330.

Yeats TH, Rose JKC. **2013**. The formation and function of plant cuticles. *Plant physiology* **163**: 5–20.

Yu X-H, Gou J-Y, Liu C-J. **2009**. BAHD superfamily of acyl-CoA dependent acyltransferases in Populus and Arabidopsis: bioinformatics and gene expression. *Plant Molecular Biology* **70**: 421–442.

Zhang X, Henriques R, Lin S-S, Niu Q-W, Chua N-H. **2006**. Agrobacterium-mediated transformation of Arabidopsis thaliana using the floral dip method. *Nature protocols* **1**: 641–646.

Appendices

Appendix A : Materials and methods

Appendix Table A.1 FPKM expression levels of BAHD-ATs with putative pHBMT function, as selected from AtGolS3 RNA sequencing data. Differential gene expression was calculated by comparing transcript FPKM values of AtGolS3 transgenic and wild-type hybrid poplar (P39), and expressed as a log2fold value (Unda *et al.*, 2016).

		Xylem Tissue			Leaf Tissue			Cambium/Bark Tissue		
Uncharacterized BAHD	Clade	Wild-type Expression	Transgenic Expression	Log2fold change	Wild-type Expression	Transgenic Expression	Log2fold change	Wild-type Expression	Transgenic Expression	Log2fold change
Potri.005G052200	II	6.937	0.620	-3.484	6.989	11.838	0.760	0.150	1.063	2.827
Potri.001G152500	No HXXXD?	15.166	3.403	-2.156	11.602	21.110	0.864	5.182	5.778	0.157
Potri.010G054100	IIIa	8.619	2.571	-1.745	0.931	1.113	0.259	4.822	6.353	0.398
Potri.005G230900	Va	16.212	7.416	-1.128	0.551	0.798	0.534	19.099	13.662	-0.483


10 20 30 40 50
Potri.005g052200 P39 ATGGCGAACATAAACAGTCGGGTTAGTGTCCATTCAATGTTAACAGCAGT
Potri.005g052200 P.trichocapra ATGGCGAACATAAACAGTAGGGTTAGTGTCCATTCAATGTTAACAGCAGT
60 70 80 90 100
Potri.005g052200 P39 CTCCAGCAAGCCAGTCAGGCCGGGTCAGAACCATCCATTATCAGCGCTTG
Potri.005g052200 P.trichocapra CTCCAGCAAGCCAGTCGGGCCGGGTCAGACCCATCCATTATCAGCGCTTG
110 120 130 140 150
Potri.005g052200 P39 ACCATGCAATGGCTCTCCATACATTGCACTTAGTTTTTTACTACAAGAAA
Potri.005g052200 P.trichocapra ACCATGCAATGGCTCTCCATACATTACACTTAGTTTTTTACTACAAGAAA
160 170 180 190 200
Potri.005g052200 P39 AACCCATTTGGGATTTTTGACGTGGACCCTTTAAGGGTGTCTTTGTCGGA
Potri.005g052200 P.trichocapra AACCCATTTGGGATTTTTGACGTGGACCCTTTAAAGGTGTCTTTGTCGGA
210 220 230 240 250
Potri.005g052200 P39 GGCTCTTTCTTTGTATCCACAAGTTGCGGGTCGGTTGACCCGAGGGGAGT
Potri.005g052200 P.trichocapra GGTTCTTTCTTTGTATCCACAAGTTGCGGGTCGGTTGACCCGAGGGGAGT
260 270 280 290 300
Potri.005g052200 P39 CGGGTAATTGGGAAGTGAAGTGTAATGATGCTGGTGTTAGAATTTTGAGG
Potri.005g052200 P.trichocapra CGGGTAATTGGGAAGTGAAGTGTAATGATGCTGGTGTTAGAATTTTGAGG
310 320 330 340 350
Potri.005g052200 P39 GCAAATGTTGGAGTCACAATTGATGAATGGTTGAGATCAGCTGATGTCTC
Potri.005g052200 P.trichocapra GCAAATGTTGGAGTTACAATTGATGAATGGTTGAGATCAGCTGATGTCTC
360 370 380 390 400
Potri.005g052200 P39 GGAGGAGAAAGATCTCACGGTTTGGGAGGAAATGCCTGAGGATCCTAGTA
Potri.005g052200 P.trichocapra GGAGGAGAAAGATCTCACGGTTTGGGAGGAAATGCCTGAGGATCCTAGTA
410 420 430 440 450
Potri.005g052200 P39 CATGGTCACCCTTTCGTATCCAGGTAAATGAATTTGAAGGAGGAGGTGTA
Potri.005g052200 P.trichocapra CATGGTCACCCTTTCGTATCCAGGTAAATGAATTTGAAGGAGGAGGTGTA
460 470 480 490 500
Potri.005g052200 P39 GCCTTTGGACTAAGTTGTACACACATGAATGCAGACCCAACTTCAGTAAC
Potri.005g052200 P.trichocapra GCCTTTGGACTAAGTTGTACACACATGAATGCAGACCCAACTTCAGTAAC
510 520 530 540 550
Potri.005g052200 P39 TCTACTCTTCAAATCCTGGATTGAGAGTCACCGCCAGGAACCGATTGAGC
Potri.005g052200 P.trichocapra TCTGCTCTTCAAATCCTGGATTGAGAGTCACCGCCAGGAGCCGATTGAGC
560 570 580 590 600
Potri.005g052200 P39 ACCCACCCCTGTTCAACTCAACCCTGCTCCATCACCAACAAGTTCCTGAT
Potri.005g052200 P.trichocapra ACCCACCCCTGTTCAACTCAACCCCGCTCCATCACCAACAAGTTCCTGAT
610 620 630 640 650
Potri.005g052200 P39 ACTAGCGGTAAATCAACCAATTACTATGCAAATAAGGCCAATGCACGAAC
Potri.005g052200 P.trichocapra ACTAGCGGTAAATCAACCAATTACTATGCAAATAAGGCCAATGCACGAAC
660 670 680 690 700
Potri.005g052200 P39 TCCCTCGGTGAAAATGGTCACAGCTACGTTGAGGTTCTCTAATTCAGCGA
Potri.005g052200 P.trichocapra TCCCTCGGTGAAAATGGTCACCGCTACGTTCAGGTTTCTAATTCAGCGA
710 720 730 740 750
Potri.005g052200 P39 TCAATAAATGCCTTAATGAAGTGCATGATCAATGTCCTCAAGCCACCCCA
Potri.005g052200 P.trichocapra TCAATAAATGCCTTAATGAAGTGCATGATCAATGTCCTCAAGCCACCCCA

Appendix Figure A.1 Nucleotide coding sequence alignment showing differences between Potri.005g052200 in P39 and *P. trichocarpa*. Identical amino acids are shaded in black and similar residues in grey.

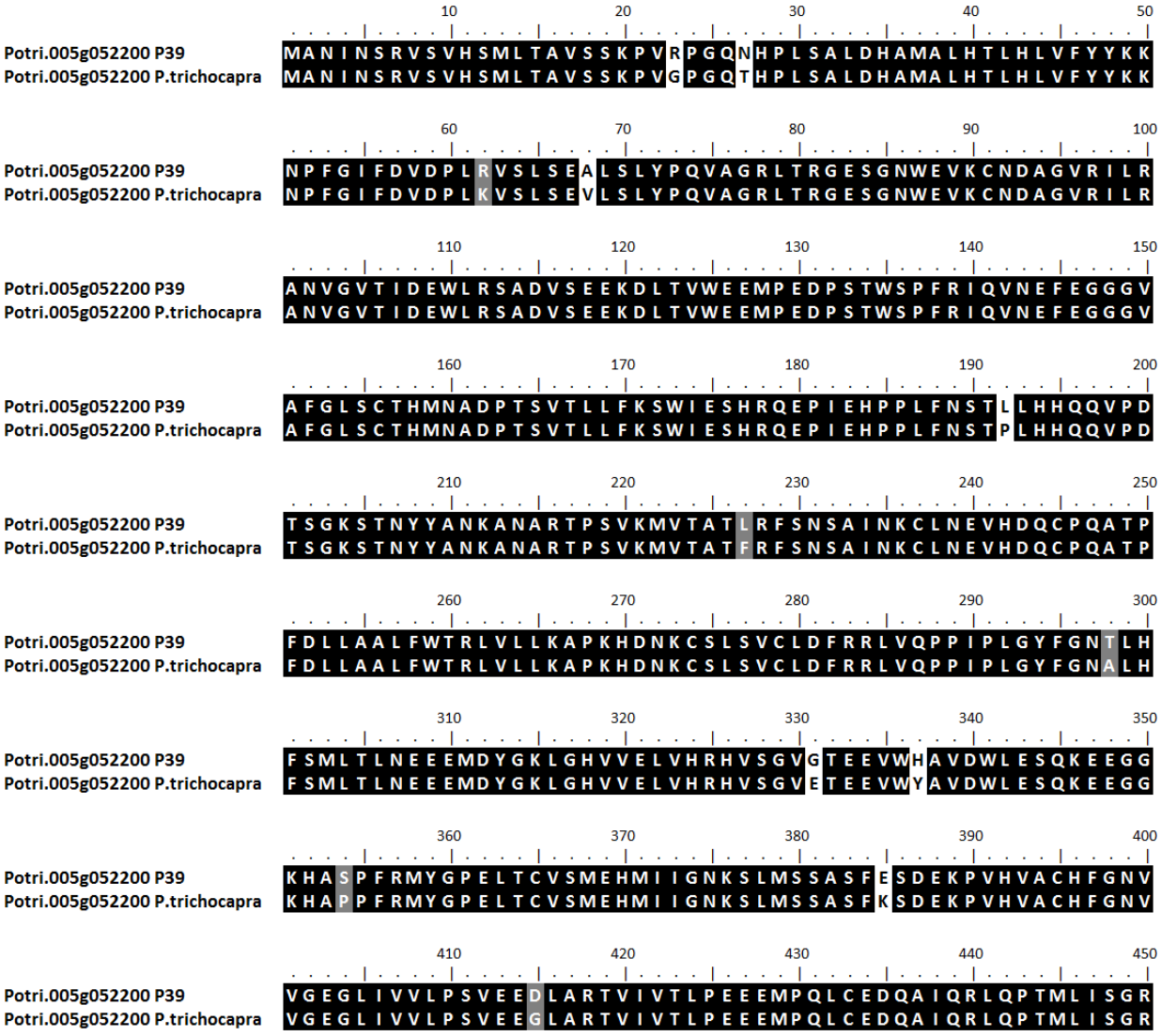

Appendix Figure A.2 Amino acid sequence alignment showing differences between Potri.005g052200 in P39 and *P. trichocarpa*. Identical amino acids are shaded in black and similar residues in grey.

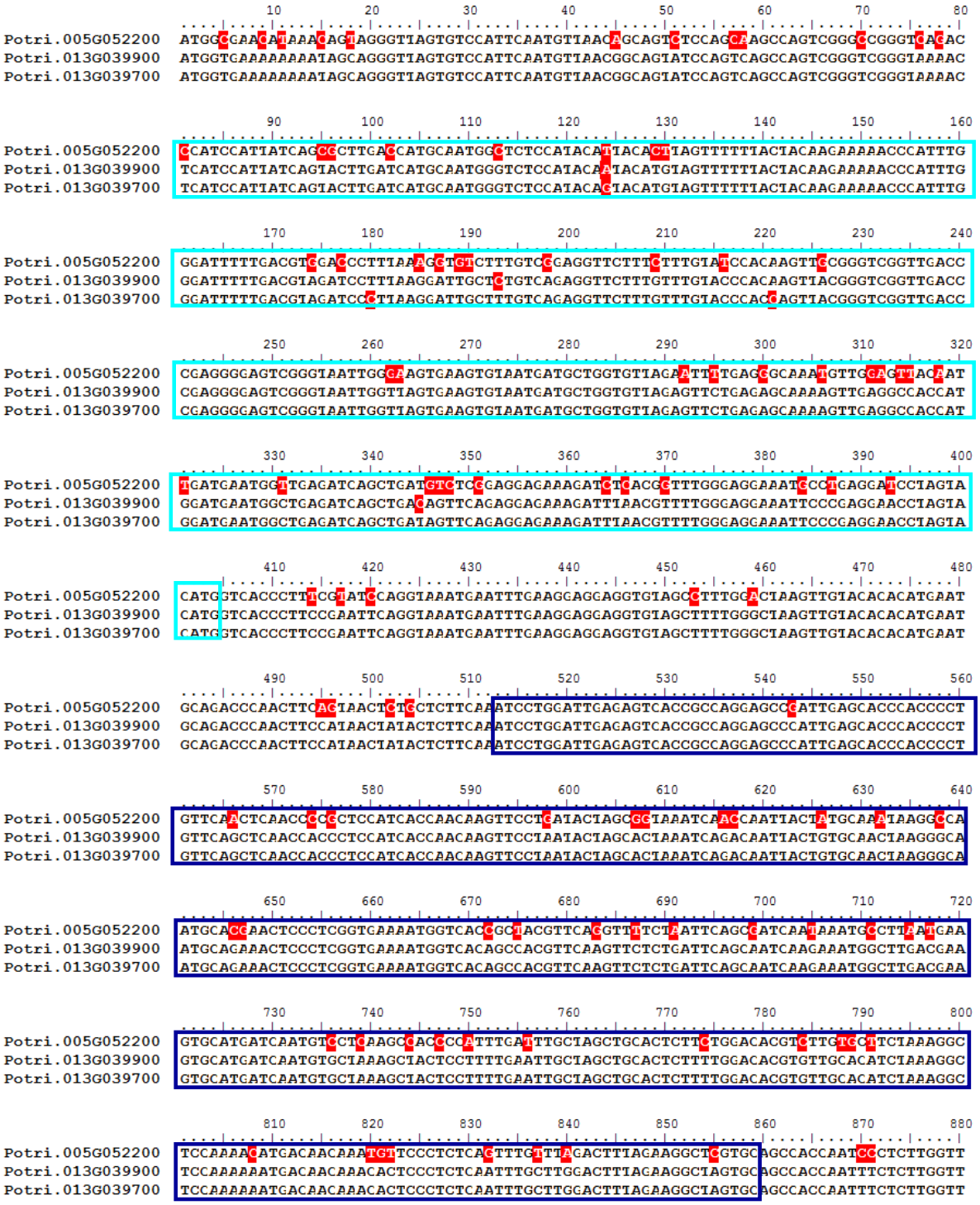

Appendix Figure A.3 Nucleotide coding sequence alignment showing differences between *Pa×gACT-like*, and close homologs Potri.013g039900 and Potri.013g039700, and the RNAi target regions. Light blue rectangles highlight *Pa×gACT-like-RNAi* S1 target region, and dark blue rectangles highlight *Pa×gACT-like-RNAi* S2 target region.

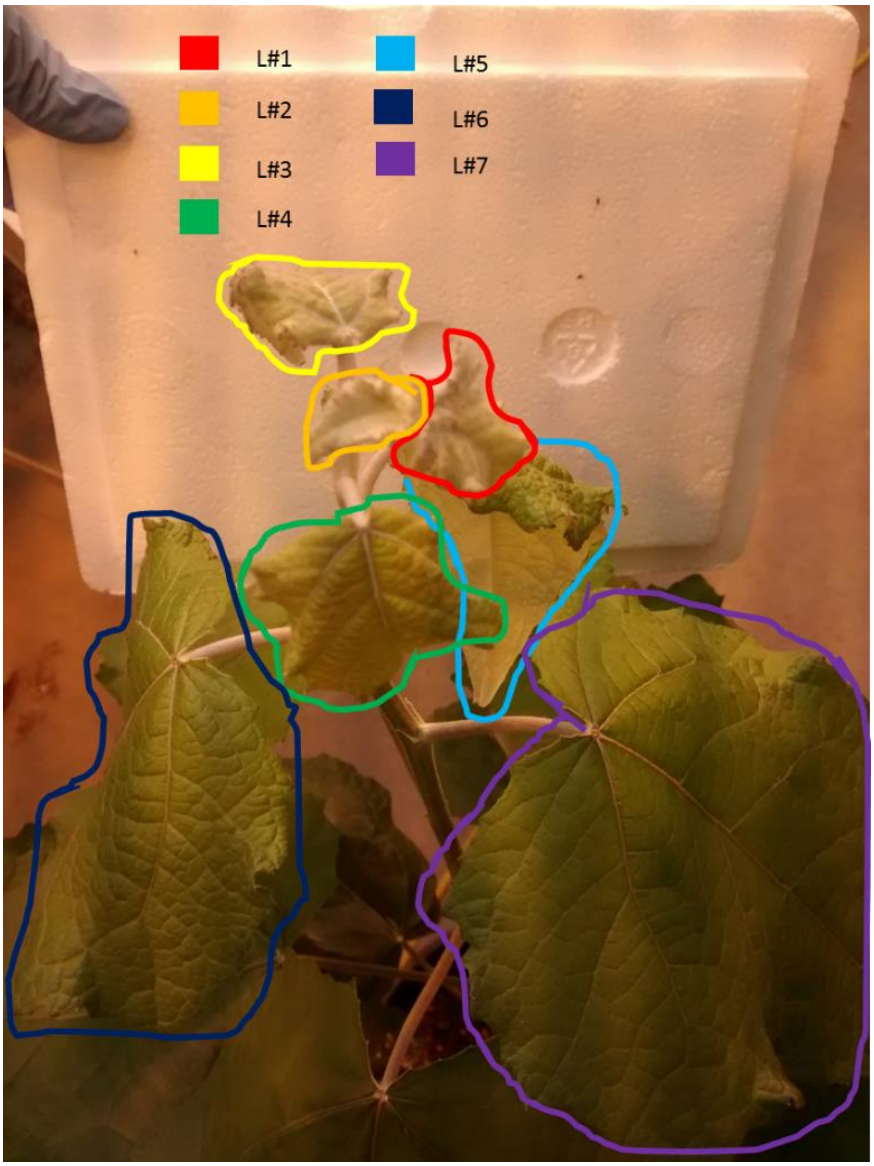

Appendix Figure A.4 Hybrid poplar leaves annotated with the leaf plastichron index to indicate leaf numbering system used in this study.

```
## Michelle's wax code for C30 wax compounds###
#libraries needed to run the following code##
library(ggplot2)
library(reshape2)
library(car)
library(lmerTest)
library(lsmeans)

##attach data sheet##
attach(AtStem_Wax_Dec)
detach(AtStem_Wax_Dec)

##boxplots##
qplot(Line, C30, data = AtStem_Wax_Dec, col= Line, geom= "boxplot")

##Model looking at combined C30 wax components pooling all trials##
C30.m1 <- glm(C30~ Line, data= AtStem_Wax_Dec)
C30.f1 <- fitted(C30.m1)
C30.r1 <- residuals(C30.m1)

##normality and variance test##
qplot(C30.f1,C30.r1) + geom_hline(yintercept = 0)
qqnorm(C30.r1)

##Anova and Least Square Means Plot##
Anova(C30.m1)
summary(C30.m1)
C30.ls.m1 <- lsmeans(C30.m1, ~Line)
plot(C30.ls.m1)

##Paired t-tests with adjusted alpha value##
(z1 <- lsmeans(C30.m1,~Line))
(z1.1 <- contrast(z1,"pairwise"))
```

Appendix Figure A.5 Example of R code run for statistical analysis of data.

Appendix B : GUS histochemical staining

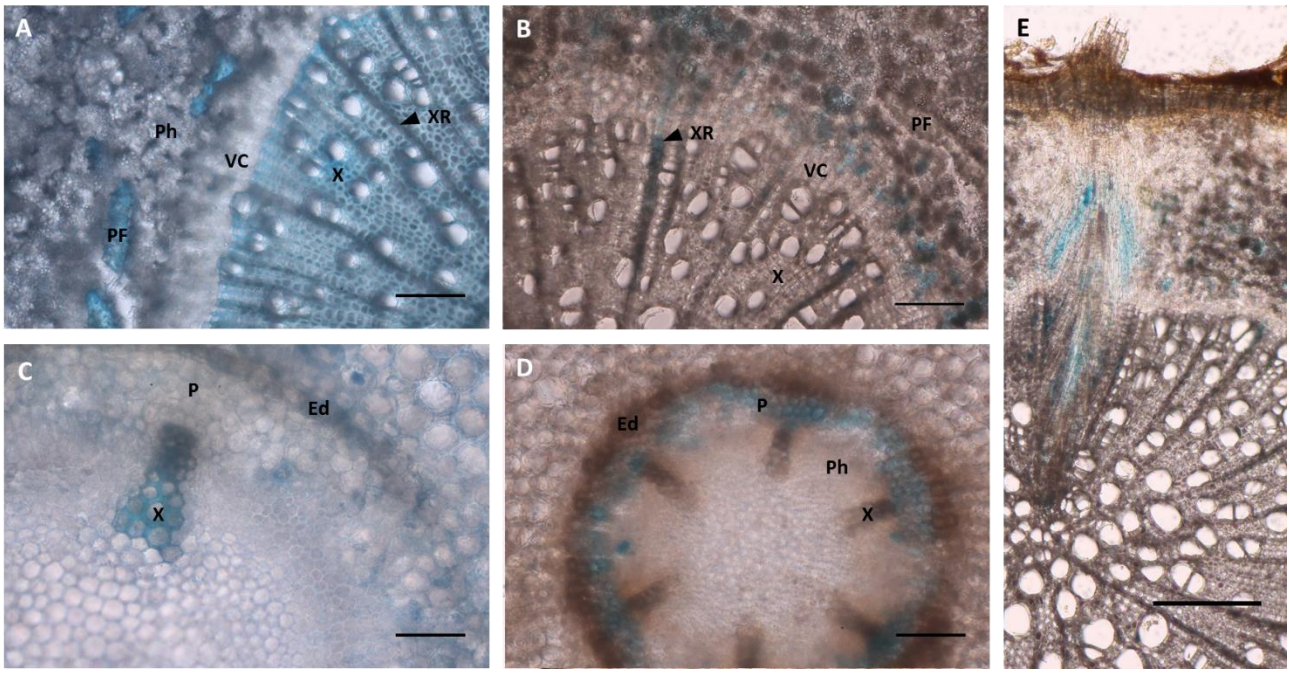

Appendix Figure B.1 Histochemical localization of GUS activity in Pa×gACT-like Prom::GUS line 2 transgenic hybrid poplar root tissues. (A, C) wild-type poplar stem cross-section stained with 0.05% Toluidine Blue, (B) mature root tissue, and (D) young root tissue. Ed = Endodermis, P = Pericycle, PF = Phloem Fibre, Ph = Phloem, VC = Vascular cambium, X = Xylem, XR = Xylem Ray. Scale bar: (A, B, D) 100 µm, (C) 50 µm and (E) 200 µm.

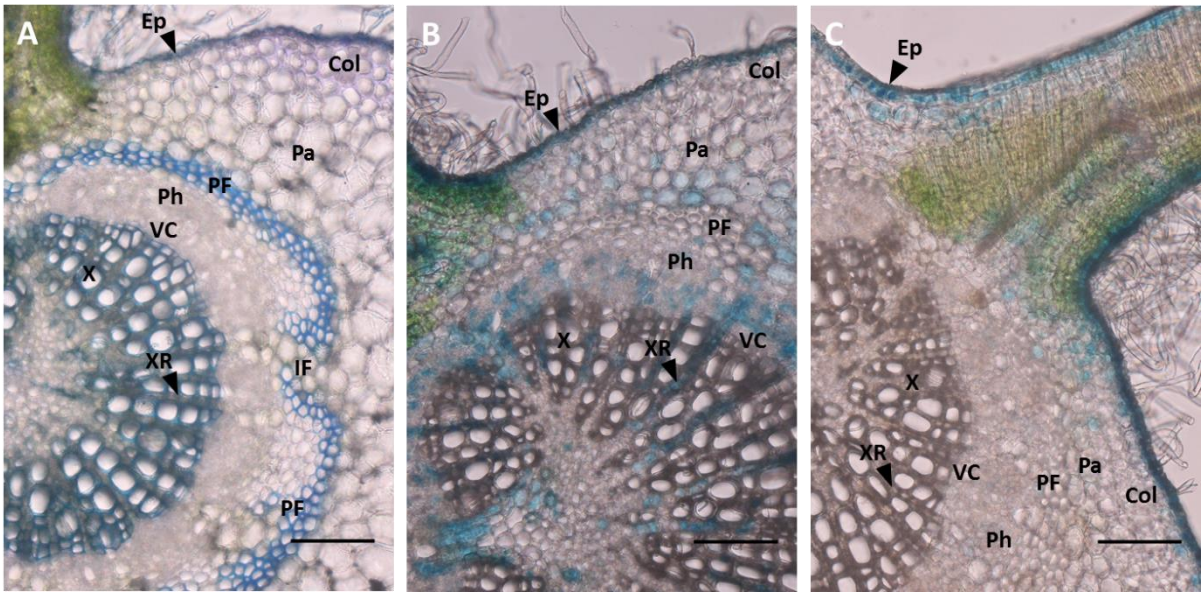

Appendix Figure B.2 Histochemical localization of GUS activity in *Pa×gACT-like Prom::GUS* transgenic hybrid poplar young leaf tissues. (A) wild-type poplar stem cross-section stained with 0.05% Toluidine Blue, (B) *Pa×gACT-like Prom::GUS* line 2 young stem tissue, and (C) *Pa×gACT-like Prom::GUS* line 3 young stem tissue. Ep = Epidermis, Col = Collenchyma, Pa = Parenchyma, PF = Phloem Fibre, IF = Interfascicular region, Ph = Phloem, VC = Vascular cambium, X = Xylem, XR = Xylem Ray. Scale bar: 100 µm.

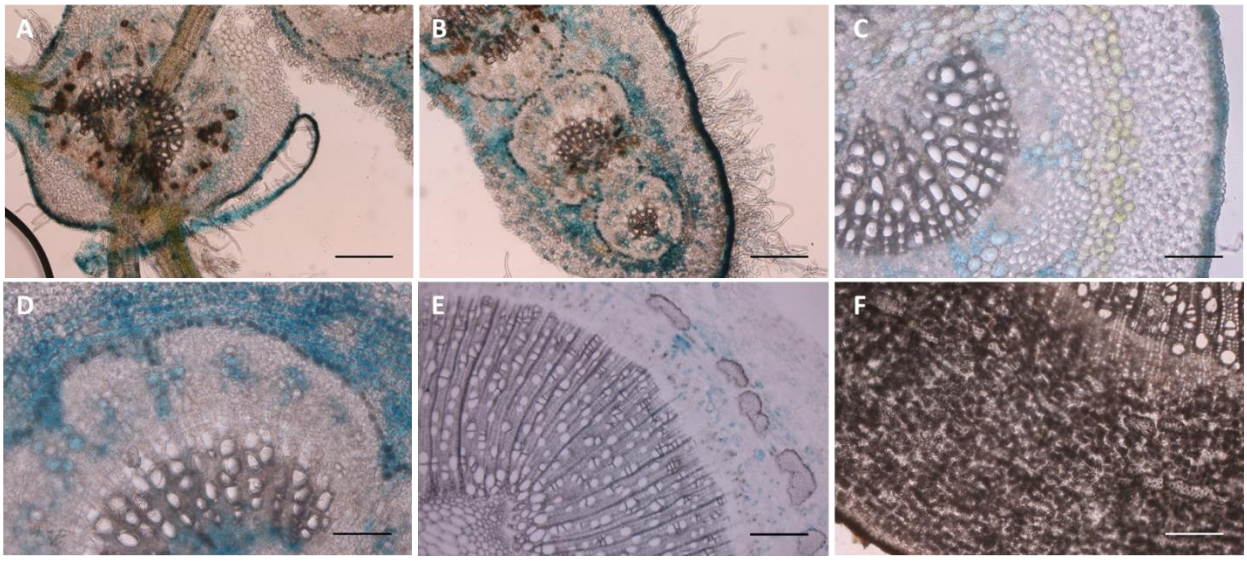

Appendix Figure B.3 *β-Glucuronidase* (GUS) staining of *Pa×gACT-like Prom::GUS* transgenic hybrid poplar line 19 tissues. Cross-sections of (A) mature leaf, (B) young petiole, (C) mature petiole, (D) young stem, (E) mature stem, and (F) mature root. Scale bar: 200 µm except for (C-D) where scale bar: 100 µm.

Appendix C : Wax profile data

Appendix Table C.1. Wax profile of *35S::Pa×gACT-like* Arabidopsis stem tissue relative to wild-type plants. Separated by individual chemical compound class, where numbers represent chain length. Values represent the mean relative abundance as a percentage of the total wax load as a function of area (µg/cm^2). Standard error of the mean in parenthesis. Bold values indicate a significant difference from wild-type following a one-way ANOVA and comparison of means by a student t-test where $p < 0.05$. (n=22-32).

Lines	Total wax	Alkanes		Alcohols			Aldehyde		Ketone	Sec. Alcohol
		29	*31*	*26*	*28*	*30*	*28*	*30*	*29*	*29*
L37	15.90 (0.72)	46.12 (0.35)	1.00 (0.03)	2.76 (0.07)	**5.11 (0.14)**	2.00 (0.05)	1.14 (0.05)	2.41 (0.13)	24.29 (0.27)	13.84 (0.09)
L38	15.84 (0.88)	46.92 (0.50)	0.91 (0.02)	2.84 (0.08)	**4.97 (0.14)**	1.95 (0.05)	**1.20 (0.03)**	2.49 (0.12)	24.06 (0.31)	13.47 (0.11)
WT	15.87 (0.63)	47.39 (0.45)	0.95 (0.03)	2.64 (0.08)	4.35 (0.15)	1.86 (0.06)	1.02 (0.08)	2.41 (0.14)	24.40 (0.32)	13.65 (0.17)

Appendix Table C.2 Carbon chain length distribution of cuticular wax compounds, and total wax amounts from *35S::Pa×gACT-like* Arabidopsis stem tissue. All wax components relative abundance pooled by chain length of precursors, where odd numbered compounds such as alkanes are derived from even numbered VLCFAs with an added carbon. Values represent the mean relative abundance as a percentage of the total wax load. Standard error of the mean in parenthesis. Bold values indicate a significant difference from wild-type following a one-way ANOVA and comparison of means by a student t-test where $p < 0.05$. (n=22-32).

Lines	C26	C28	C30	C32
L37	2.76 (0.07)	**6.26 (0.16)**	**88.66 (0.20)**	1.00 (0.03)
L38	2.84 (0.08)	**6.17 (0.15)**	**88.89 (0.20)**	0.91 (0.02)
WT	2.64 (0.08)	5.37 (0.20)	89.70 (0.26)	0.95 (0.03)

Appendix Table C.3 Wax profile of RNAi poplar leaf (PI-5, 7) tissue relative to wild-type trees. Separated by individual chemical compound class, where numbers represent chain length. Values represent the mean relative abundance as a percentage of the total wax load. Standard error of the mean in parenthesis. Bold values indicate a significant difference from wild-type following a one-way ANOVA and comparison of means by a student t-test where $p < 0.05$. (n = 5-6)

Lines	Alkanes				Alcohols			Aldehyde
	25	***27***	***29***	***31***	***26***	***28***	***30***	***28***
Leaf 5								
S1.10	3.45 (0.42)	49.80 (1.53)	7.60 (0.31)	1.05 (0.09)	0.67 (0.13)	2.42 (0.40)	1.96 (0.12)	1.51 (0.43)
S1.14	3.39 (0.36)	48.86 (1.27)	6.26 (0.45)	1.10 (0.22)	0.42 (0.05)	1.45 (0.14)	2.64 (0.20)	1.08 (0.18)
S1.15	2.93 (0.62)	46.01 (2.17)	7.63 (1.15)	0.76 (0.22)	0.65 (0.19)	2.51 (0.74)	3.17 (0.49)	1.05 (0.32)
WT	3.08 (0.20)	46.48 (0.16)	5.79 (0.46)	0.82 (0.10)	0.42 (0.05)	1.42 (0.05)	3.12 (0.28)	0.99 (0.23)
Leaf 7								
S1.10	3.86 (0.19)	46.65 (0.50)	6.43 (0.40)	1.15 (0.22)	1.81 (0.15)	5.19 (0.31)	2.08 (0.19)	2.24 (0.47)
S1.14	3.73 (0.24)	47.68 (0.85)	6.56 (0.39)	1.08 (0.18)	1.74 (0.13)	4.97 (0.44)	2.20 (0.19)	2.55 (0.44)
S1.15	5.02 (0.22)	47.17 (0.50)	5.77 (0.34)	1.13 (0.15)	1.82 (0.16)	4.04 (0.29)	2.41 (0.16)	1.36 (0.27)
WT	4.23 (0.22)	45.90 (0.58)	6.20 (0.47)	1.13 (0.10)	1.66 (0.13)	4.33 (0.33)	2.55 (0.17)	1.88 (0.30)

Appendix Table C.4 Carbon chain length distribution of cuticular wax compounds, and total wax amounts from RNAi poplar leaf (PI-5, 7) tissue. All wax components relative abundance pooled by length of VLCFA from which they were derived. Values represent the mean relative abundance as a percentage of the total wax load as a function of area (μg/cm^2). Standard error of the mean in parenthesis. Bold values indicate a significant difference from wild-type following a one-way ANOVA and comparison of means by a student t-test where $p < 0.05$. (n = 5-6)

Line	C26	C28	C30	C32	Total wax
Leaf 5					
S1.10	4.12 (0.46)	53.73 (1.06)	9.56 (0.32)	1.05 (0.09)	6.21 (0.31)
S1.14	3.81 (0.39)	51.39 (1.24)	8.90 (0.36)	1.10 (0.22)	7.00 (0.45)
S1.15	3.58 (0.67)	49.56 (2.38)	10.80 (0.76)	0.76 (0.22)	7.14 (0.63)
WT	3.50 (0.25)	48.89 (1.35)	8.91 (0.22)	0.82 (0.10)	6.53 (0.46)
Leaf 7					
S1.10	5.67 (0.32)	54.08 (0.69)	8.51 (0.28)	1.15 (0.22)	6.18 (0.19)
S1.14	5.47 (0.28)	55.20 (1.16)	8.75 (0.36)	1.08 (0.18)	5.96 (0.40)
S1.15	6.84 (0.33)	52.57 (0.45)	8.18 (0.20)	1.13 (0.15)	6.17 (0.23)
WT	5.89 (0.31)	52.11 (0.69)	8.75 (0.35)	1.13 (0.10)	6.80 (0.31)